

5-2011

ROLE OF VITAMIN-D3 AND RETINOIC ACID IN A HUMAN THP-1 MACROPHAGE MODEL OF MYCOBACTERIUM TUBERCULOSIS INFECTION

Jaymie L. Estrella

Follow this and additional works at: http://digitalcommons.library.tmc.edu/utgsbs_dissertations

 Part of the [Immunology of Infectious Disease Commons](#), [Immunopathology Commons](#), and the [Pathogenic Microbiology Commons](#)

Recommended Citation

Estrella, Jaymie L., "ROLE OF VITAMIN-D3 AND RETINOIC ACID IN A HUMAN THP-1 MACROPHAGE MODEL OF MYCOBACTERIUM TUBERCULOSIS INFECTION" (2011). *UT GSBS Dissertations and Theses (Open Access)*. Paper 129.

This Dissertation (PhD) is brought to you for free and open access by the Graduate School of Biomedical Sciences at DigitalCommons@The Texas Medical Center. It has been accepted for inclusion in UT GSBS Dissertations and Theses (Open Access) by an authorized administrator of DigitalCommons@The Texas Medical Center. For more information, please contact laurel.sanders@library.tmc.edu.

**ROLE OF VITAMIN-D₃ AND RETINOIC ACID IN A HUMAN THP-1 MACROPHAGE
MODEL OF *MYCOBACTERIUM TUBERCULOSIS* INFECTION**

By

Jaymie L. Estrella, B.S., B.A.

APPROVED:

Chinnaswamy Jagannath, Ph.D.

Robert Hunter, M.D., Ph.D.

David McMurray, Ph.D.

Audrey Wanger, Ph.D.

Bradley McIntyre, Ph.D.

APPROVED:

Dean, The University of Texas
Health Science Center at Houston
Graduate School of Biomedical Science

**ROLE OF VITAMIN-D₃ AND RETINOIC ACID IN A HUMAN THP-1 MACROPHAGE
MODEL OF *MYCOBACTERIUM TUBERCULOSIS* INFECTION**

A

DISSERTATION

Presented to the Faculty of
The University of Texas
Health Science Center at Houston
and
The University of Texas
M. D. Anderson Cancer Center
Graduate School of Biomedical Sciences
in Partial Fulfillment

of the Requirements

for the Degree of

DOCTOR OF PHILOSOPHY

by

Jaymie L. Estrella B.S., B.A.

Houston, TX

May 2011

"We need to teach our kids that it's not just the winner of the Super Bowl who deserves to be celebrated, but the winner of the science fair; that success is not a function of fame or PR, but of hard work and discipline." – 2011 State of the Union address, President Barack Obama

To my grandparents, who recognized early on that I had no athletic ability but instead encouraged my curiosity and interest to learn. Being immigrants who managed to thrive and succeed in a new country, America, they have always stood as my example of the merits of hard work and dedication. Thank you for always demanding the best from me and for your encouragements to dream big. I began this long journey to becoming a scientist under your proud gaze and I wish you could be here today, at the finish line, to share my success.

ACKNOWLEDGEMENTS

"Here is the basic rule for winning success. Let's mark it in the mind and remember it. The rule is: Success depends on the support of other people. The only hurdle between you and what you want to be is the support of other people." David Joseph Schwartz

There are many people who have supported and helped me attain this milestone in my life. I cannot name everyone but I would like to acknowledge a few key people, who I feel that without their help and guidance, I would have failed utterly in my endeavor.

First, I must thank my advisor, Dr. Chinnaswamy Jagannath. He accepted me into his lab during a critical time in my career and due to his own infectious curiosity and love of science, helped me regain my passion for the field of investigation. Dr. Jag is a true mentor and I count myself very lucky to have trained with him.

Second, my gratitude goes to Dr. David McMurray. He has been there since my first committee meeting and has seen me grow from a fledging student into a new scientist. He has provided me training at Texas A&M, tremendous support during my transition from Brownsville and has always given a critical eye to my efforts that has constantly challenged me to elevate my work.

Third, I must thank Dr. Robert L. Hunter, who along with providing me with financial support also shielded me from the chaos that resulted from my transition to Houston. He provided me with a safe haven in which I could flourish and I will always remember that.

Finally, I would like to thank my friends and family who truly own this achievement. Science is a hard field that, in my experience, brings success only at the cost of seemingly endless frustrations and disappointments. I would not have been able to continue during the darkest moments of this endeavor without the strong shoulders of my loved ones who's mixture of encouragement, sympathy, bullying, and humor, lifted me out of those dark pits and back into the light of the lab. Thank you to my family: Dad, Mom, my sisters (Lani, Peck, Gale & Norms), my Aunts (Terri & Joyce), my Uncle Norman and my cousins (Lani, Rhegs, Bran, TC, Drew & Loren). Thank you to my friends: Claudia & Shawn, Rudy & Christina, Alex & Jaclyn, Mikey & Josette, Rosa & Albert, Omar & Lien, Tes & Adam, Joey & Elisa, Hugo, Cameron, Brandon, Ronnie, Ray, Raquel, Ana, Chrissy, Pearl, Natalie, Janani, Sanchaika, Mike G., Letty, Celestine, Matt, Mary and Nick.

All of these people have contributed greatly to helping me achieve my life goal. They have made me a better scientist and provided me with great templates in which to model my career and life. Most importantly, thank you for making me a better person.

ABSTRACT

Mycobacterium tuberculosis (Mtb) replicates within the human macrophages and we investigated the activating effects of retinoic acid (RA) and vitamin D₃ (VD) on macrophages in relation to the viability of Mtb. A combination of these vitamins (RAVD) enhanced the receptors on THP-1 macrophage (Mannose receptor and DC-SIGN) that increased mycobacterial uptake but inhibited the subsequent intracellular growth of Mtb by inducing reactive oxygen species (ROS) and autophagy. RAVD also enhanced antigen presenting and homing receptors in THPs that suggested an activated phenotype for THPs following RAVD treatment. RAVD mediated activation was also associated with a marked phenotypic change in Mtb infected THPs that fused with adjacent cells to form multinucleate giant cells (MNGCs). Typically MNGCs occurred over 30 days of *in vitro* culture and contained non-replicating persisting Mtb for as long as 60 days in culture. We propose that the RAVD mediated inhibition of replicating Mtb leading to persistence of non-replicating Mtb within THPs may provide a novel human macrophage model simulating formation of MNGCs in human lungs.

TABLE OF CONTENTS

DEDICATION	iii
ACKNOWLEDGEMENTS	iv
ABSTRACT	v
TABLE OF CONTENTS	vi
LIST OF ILLUSTRATIONS	viii
LIST OF TABLES AND DIAGRAMS	xi
ABBREVIATIONS	xii
CHAPTER 1: Introduction	1
INTRODUCTION	1
CHAPTER 2: Treatment of THP-1 cells with retinoic acid and vitamin D leads to a phenotypic differentiation compared to phorbol myristate acetate mediated activation	7
INTRODUCTION	8
RESULTS	12
DISCUSSION	26
CHAPTER 3: Effects of retinoic acid and vitamin D on the ability of THP-1 cells to present antigen to humanized mouse T-cells	28
INTRODUCTION	29
RESULTS	33
DISCUSSION	37
CHAPTER 4: RAVD induces oxidants, autophagic pathways and cathelicidin to decrease viability of intracellular <i>Mycobacterium tuberculosis</i>	39
INTRODUCTION	40
RESULTS	44
DISCUSSION	58
CHAPTER 5: <i>Mycobacterium tuberculosis</i> infection followed by long term activation with RAVD leads to multinucleated giant cell (MNGC) formation in the THP-1 macrophages	60
INTRODUCTION	61
RESULTS	62
DISCUSSION	73
CHAPTER 6: Long term activation of <i>Mycobacterium tuberculosis</i> infected macrophages with RAVD leads to increased protease activity and lysosomal localization with bacteria in THP-1 macrophages	75

INTRODUCTION	76
RESULTS	77
DISCUSSION	85
CHAPTER 7: Overall general discussion and conclusions	86
CHAPTER 8: Materials and methods.....	90
REFERENCES.....	97
VITA.....	116

LIST OF ILLUSTRATIONS

Figure 1A. Flow cytometric analysis of receptors involved in the uptake of mycobacteria in human THP-1 macrophages activated with either phorbol myristate acetate (PMA) or retinoic acid and vitamin D (RAVD).....	14
Figure 1B. Flow cytometric analysis of chemokine receptors in human THP-1 macrophages activated with either PMA or RAVD.	16
Figure 1C. Flow cytometric analysis of antigen presenting receptors in human THP-1 macrophages activated with either PMA or RAVD.	18
Figure 1D. Flow cytometric analysis of DC-SIGN in human THP-1 macrophages activated with either RA alone, VD alone or their combination.....	21
Figure 2A. Flow cytometric analysis of mannosylated-BSA-FITC (mBSA-FITC) in human THP-1 macrophages activated with either PMA or RAVD before infection with H37Rv. ..	22
Figure 2B. Flow cytometric analysis of mannosylated-BSA-FITC (mBSA-FITC) in human THP-1 macrophages activated with either PMA or RAVD after infection with H37Rv.	23
Figure 3. PMA and RAVD have differential effects on the uptake of <i>Mycobacterium tuberculosis</i> (Mtb) within THP-1 macrophages.	25
Figure 4A. Evaluation of MHC-II dependent antigen 85B (Ag85B) presentation in BCG-14 or <i>M. tuberculosis</i> H37Rv infected THP-1 macrophages activated with IFN- γ using humanized mouse T-cells secreting IL-2.....	34
Figure 4B. Evaluation of MHC-II dependent Ag85B presentation in PMA or RAVD activated THP-1 macrophages using F9A6 cells specific for Ag85b.....	35
Figure 4C. Comparison of MHC-II dependent Ag85B presentation in THP-1 or MonoMac-6 activated macrophages using F9A6 cells.....	36
Figure 5. PMA and RAVD have differential effects on the survival of <i>Mycobacterium tuberculosis</i> (Mtb) within THP-1 macrophages.	47
Figure 6A. Enhanced co-localization of <i>gfp</i> H37Rv with components of the phagocyte (NADPH) oxidase in RAVD activated THP-1 macrophages.....	48
Figure 6B. Analysis of co-localization of <i>gfp</i> H37Rv with components of the phagocyte (NADPH) oxidase in PMA or RAVD activated THP-1 macrophages.....	49

Figure 6C. RAVD induce enhanced reactive oxygen species (ROS) response in THP-1 macrophages before infection with <i>M. tuberculosis</i> H37Rv.	50
Figure 6D. RAVD continue to induce enhanced reactive oxygen species (ROS) response in THP-1 macrophages after infection with H37Rv.	51
Figure 6E. Inhibition of ROS and RNS leads to increased intracellular survival of <i>M. tuberculosis</i> in RAVD-THPs.	52
Figure 7A. <i>M. tuberculosis</i> phagosomes purified from RAVD-THPs show greater amounts of beclin-1 during Western blot analysis.	53
Figure 7B. RAVD induces autophagy in THP-1 macrophages that leads to inhibition of intracellular <i>M. tuberculosis</i>	54
Figure 7C. siRNA inhibition of beclin-1 leads to reduced autophagosome formation in <i>gfpMtb</i> infected RAVD-THPs.	55
Figure 7D. <i>M. tuberculosis</i> phagosomes of RAVD-THPs recruit more autophagy proteins during Western Blot analysis.	56
Figure 8. RAVD induces cathelicidin expression in THPs infected with <i>M. tuberculosis</i> H37Rv.	57
Figure 9A. PMA-THPS are unable to control infection with <i>M. tuberculosis</i> H37Rv.	65
Figure 9B. Unlike PMA-THPs, RAVD-THPS are able to control short and long-term infection with <i>M. tuberculosis</i> H37Rv.	66
Figure 9C. RAVD induces MNGC formation in <i>M.tuberculosis</i> infected THPs.	67
Figure 9D. Electron microscopic (EM) analysis of multi-nucleated giant cell formation of THPs through treatment with RAVD.	68
Figure 10. Cell fusion in may involve ADAM-9 present between fusing RAVD-THPs. ...	69
Figure 11A. Activation with RAVD but not cell fusion-inducing cytokines leads to long lived MNGCs containing <i>M. tuberculosis</i>	71
Figure 11B. Cultured <i>M. tuberculosis</i> infected MNGCs exhibit biophasic cytokine and chemokine secretion.	72
Figure 12A. Sucrose–gradient purified phagosomes of <i>M. tuberculosis</i> H37Rv from RAVD-THP are enriched with cathepsin-D.	79
Figure 12B. RAVD induce co-localization of <i>M. tuberculosis gfpH37Rv</i> with Cathepsin-D and Cathepsin-G proteases in THP macrophages.	80

Figure 12C. RAVD induces co-localization of <i>M. tuberculosis</i> <i>gfpH37Rv</i> with lysosomal markers, CD63 and LAMP-1 within THP macrophages.....	81
Figure 12D. Some <i>M. tuberculosis</i> <i>gfpH37Rv</i> phagosomes avoid labeling with LAMP1, a known marker for Mtb phagosomes.....	82
Figure 13A. Mycobacterial growth cannot be consistently detected after 30 days in infected RAVD-THPs.....	83
Figure 13B. Mycobacterial growth cannot be consistently detected after 30 days in infected RAVD-THPs, but mRNA for Antigen 85B remain positive.....	84

LIST OF TABLES AND DIAGRAMS

Table 1A. Tabulated data of mean fluorescence intensity (MFIs) depicted in the flow cytometric analysis of uptake or binding receptors to mycobacteria on PMA or RAVD activated human THP-1 macrophages. **15**

Table 1B. Tabulated data of MFIs depicted in the flow cytometric analysis of chemokine receptors on PMA or RAVD activated human THP-1 macrophages. **17**

Table 1C. Tabulated data of MFIs depicted in the flow cytometric analysis of receptors involved in antigen presentation on PMA or RAVD activated human THP-1 macrophages. **20**

Table 2. Tabulated data of MFIs depicted in the flow cytometric analysis of mannosylated-BSA-FITC (mBSA-FITC) uptake in PMA or RAVD activated human THP-1 macrophages. **24**

Diagram 1. Mtb antigen processing in macrophages and the detection of presented peptides on MHC-II molecules by using F9A6 or 5MB humanized mouse cell lines specific for Antigen 85B and α -crystallin, respectively. **32**

Diagram 2. Vitamin A and D induce two anti-mycobacterial pathways, cathelicidin and autophagy to control intracellular *Mycobacterium tuberculosis* growth..... **42**

Table 3. Replicate experiments in which *M.tuberculosis* infected, PMA or RAVD treated MNGCs were maintained in culture **64**

ABBREVIATIONS

MNGC: Multi-nucleated Giant Cells

Mtb: *Mycobacterium tuberculosis*

PMA: Phorbol myristyl acetate

PMA-THPs: Phorbol myristyl acetate activated THP-1 monocytes

RA: Retinoic acid

RAVD: Retinoic Acid and Vitamin D₃

RAVD-THPs: Retinoic Acid and Vitamin D₃ activated THP-1 monocytes

THPs: THP-1 monocytic cell line

VD: Vitamin D₃

CHAPTER 1

INTRODUCTION

Mycobacterium tuberculosis

Tuberculosis (TB), a disease that has afflicted the human race for millennia, still causes 1.3 million deaths per year among HIV-negative patients(1). The etiologic agent, *Mycobacterium tuberculosis* (Mtb) is unique among bacterial pathogens in being able to survive *in vivo* for years before reactivation to cause disease. The clinical manifestations of TB represent a complex interaction between the bacteria, Mtb, and the human host immune response. Although, Mtb can parasitize, survive and grow within macrophages only a minority of people exposed to infection progress to disease. It is widely believed that protection against the disease requires immune-competent host reactions that activate T-helper 1-type (Th1) immune responses(2).

Inhalation of aerosol droplets containing Mtb is known to be the natural route for pulmonary TB infection. Following Mtb infection of alveolar macrophages, an intense local inflammatory response involving a series of innate immune and Th1 dominant adaptive pathways is induced. These responses lead to the recruitment of macrophages, lymphocytes and dendritic cells to the site of infection leading to the formation of a granuloma, the signature histopathological feature of tuberculosis(3). Granuloma formation is thought sufficient to contain the infection and prevent active disease in most healthy individuals, but is unable to completely eradicate the infection(4). Instead, the infection is kept at a latent state where the host is asymptomatic but still has Mtb within their lungs that can re-activate into active infection upon compromise of the host immune defense. One-third of the world's population is estimated to be currently infected with TB, where most those infected are in a latent state of infection(1), understanding the host and bacterial interactions during granuloma formation is necessary for disease management.

Vitamin D and Tuberculosis

For over a century, the administration of Vitamin D₃ (VD) has been considered beneficial for the treatment tuberculosis disease. Even before Robert Koch discovered the causative agent of TB as *Mycobacterium tuberculosis* (Mtb), foods high in this vitamin, such as Cod Liver Oil(5) and milk, along with exposure to sunlight was the recommended treatment course during the pre-chemotherapy era of tuberculosis disease. Current clinical studies show increasing roles for VD in tuberculosis; where lower serum VD levels(6, 7) and polymorphisms in the Vitamin D Receptor (VDR) gene were found associated with increased susceptibility.(8, 9)

In conjunction with these epidemiological studies, new roles for VD in immune responses have been discovered in recent years. VD, in the form of cholecalciferol, used in skeletal processes must travel to the liver to be converted into 25-dihydroxyvitamin D (25(OH)VD₃), then to the kidneys to be converted into its metabolically active form, 1,25-dihydroxyvitamin D₃ (1,25(OH)₂VD₃).(10) Unlike

the skeletal system that depends on shuttling VD metabolites around the body, immune cells have been found to express their own enzymes to metabolize VD (cholecalciferol) into $1,25(\text{OH})_2\text{VD}_3$. Macrophages and dendritic cells (DC) both express, CYP27A1, the enzyme needed to convert serum VD into $25(\text{OH})\text{VD}_3$, and CYP27B1, the enzyme that further converts it to active $1,25(\text{OH})_2\text{VD}_3$ (10, 11).

During Mtb infection, macrophages become a target for VD by increasing expression of VDR.(12) Expression of VDR promotes chemotaxis(13), phagocytosis(14), antigen processing(15), superoxide synthesis(14, 16) and production of pro-inflammatory cytokines, like interleukin 1-beta ($\text{IL-1}\beta$)(17)and tumor necrosis factor alpha ($\text{TNF-}\alpha$)(18), to eliminate the infection. Recently, VD has been shown to regulate the expression of LL-37(19), an antimicrobial peptide of the cathelicidin family with the dual ability of modulating the immune response by recruiting monocytes, T-lymphocytes and neutrophils to the site of infection(20).

Unlike macrophages and DCs, activated T-cells only express CYP27B1 and are therefore, more dependent on liver, macrophage or dendritic cell conversion of VD into $1,25(\text{OH})_2\text{VD}_3$ (21). The difference between VD metabolism in T-cells and macrophages also extends to their functional response to $1,25(\text{OH})_2\text{VD}_3$. While $1,25(\text{OH})_2\text{VD}_3$ initially stimulates a pro-inflammatory response in macrophages, the reverse is true for T-cells. The presence of $1,25(\text{OH})_2\text{VD}_3$ leads to inhibition of T-cell differentiation, proliferation, and Th1 cell immunoactivity(22). This inverse relation of VD function in macrophages and T-cells has led to the idea that VD is a “self-regulatory” molecule with essential roles in controlling the longevity of the inflammatory response.

Interestingly, $1,25(\text{OH})_2\text{VD}_3$ has been shown to have an autocrine effect on macrophages. Macrophages activated with interferon-gamma ($\text{IFN-}\gamma$) will secrete active $1,25(\text{OH})_2\text{VD}_3$ to negatively feedback onto itself and suppress the ongoing Th1 immune responses(23). To date, there are no studies conducted to determine if the THP-1 macrophage cell line exhibit VD metabolising enzymes, however, macrophages derived from human patients do express CYP27A1 and CYP27B1(11). Therefore, for our studies, we choose to use the more cost-effective and inactive form of VD (cholecalciferol) instead of $1,25(\text{OH})_2\text{VD}_3$ that would also allow us to lessen the effects of accidental suppression of the inflammatory response.

Retinoic Acid and Tuberculosis

Vitamin A is mostly associated with a role in vision, maintaining the integument and the reproductive system(24). However, its active metabolite, retinoic acid, has been found to affect multiple processes in the immune system. In the tissues, dietary vitamin A, in the form of β -carotene, *all-trans*-retinol or retinyl esters must be broken down by ubiquitously expressed enzymes such as, alcohol

dehydrogenases or short-chain dehydrogenase reductases, into *all-trans*-retinal(25, 26). Retinal dehydrogenases (RALDHs), the tightly controlled key enzymes in Vitamin A metabolism, converts *all-trans*-retinal into its active metabolite *all-trans*-retinoic acid (retinoic acid; RA)(25, 26). Excess RA is converted into retinyl esters and stored in the liver or excreted out of the urine or bile ducts(25, 26). Currently, the only immune cells to exhibit RALDHs are dendritic cells(27) that also have the ability to store and excrete RA to immunomodulate surrounding cells(28).

Prior to the discovery of antibiotics, the use of retinoic acid (RA) as an “anti-infective” agent was greatly debated for the treatment of infectious disease(29). During that period, as Vitamin D was being heralded as a treatment for tuberculosis, the role of RA was often overlooked even though it was usually found in equal or greater quantity in cod liver oil and milk(29). To date, there are no clinical trials on the sole effects of RA as a therapeutic or preventative therapy for tuberculosis. However, there is a correlation between RA serum levels and tuberculosis, where human studies have shown that tuberculosis patients exhibit decreased RA in their serum that return to normal once the infection has cleared(30). RA, given at a 10^{-5} M dose in cultured human macrophages immediately after infection, was shown to slow or stop intracellular Mtb growth(31). However, a lower, more physiologically relevant dose (10^{-7} M)(32) given before infection showed the same protective effect(31).

Although it is still unclear as to the role of RA in human tuberculosis, several studies have tried to elucidate its general effects on the immune system during infection. RA has been shown to have the ability to modulate lymphocyte and macrophage populations(33), increase mRNA transcription of TNF- α , IL-1 β , inducible nitric oxide synthetase and IFN- γ (33), which led to a decrease of TB severity and viable bacilli(33, 34). Interestingly, a study in viruses shows a link between autophagy and RA signaling pathways where the Atg12-Atg5 complex, a key regulator of autophagy, associates with the signaling molecules retinoic acid-inducible gene I (RIG-I) and interferon-beta promoter stimulator 1 (IPS-1)(35). Complexing of these molecules leads to a down-regulation of Type 1 interferons that are normally induced by viral infections and suppression of the innate anti-viral response(35). To date, no studies on the effects of RA inducing autophagy on anti-bacterial response in macrophages have been conducted, although it has been clearly demonstrated that autophagosome-lysosome pathway plays an essential role in eliminating Mtb infection(36).

Retinoic Acid and Vitamin D

In the early 1930s, clinical trials using cod liver oil(37), or combinations of Vitamin A & D(38) showed promise in reducing morbidity and mortality in tuberculosis in children. However, with the discovery of antibiotics, therapeutic studies on vitamins A & D waned(29). Presently, with the emergence of multi-drug resistant strains of tuberculosis on the rise, research into the effects of vitamin

A and D as therapeutic adjuvants has emerged. Unlike the pre-antibiotic era, most current clinical studies focus on the sole effects of one vitamin instead of combination therapy(39) that may be misleading since cross-talk between the two cell signaling pathways is likely(10, 40).

Both Vitamins A and D exert their cellular effects via nuclear receptors, which when activated, will bind to promoters of their response genes to facilitate transcription. Once VD is converted into its metabolite, $1,25(\text{OH})_2\text{VD}_3$, it will complex with the nuclear vitamin D receptor (VDR) that heterodimerizes with nuclear receptors of the retinoic X receptor (RXR) family(10). Retinoic acid, metabolized from Vitamin A, will also heterodimer with RXR via its retinoic acid receptor (RAR)(10). The common ability for RXR to bind to both VDR and RAR can lead to the possibility of cross-talk within their response elements(40) that may lead to a synergistic(41) or antagonistic(42) effect depending on the response element being evaluated.

In the case of tuberculosis, Vitamin A and D have shown to work synergistically to induce a decrease in tryptophan-aspartate-containing coat protein (TACO) gene transcription(43). Phagocytosis of Mtb leads to the recruitment of TACO onto the phagosomal membrane that prevents maturation and degradation of the pathogen. Therefore, a combined treatment of Vitamin A and D allowed greater phagosome maturation to occur in Mtb infected macrophages that, in turn, led to a decrease in pathogen viability(41).

Effects of Retinoic Acid and Vitamin D on THP-1 Macrophages

Given the importance of Vitamin A and D on the immune system, their classic role as preventive and therapeutic treatments in tuberculosis, and their common signaling systems, studies on the dual effects of Vitamin A and D are surprisingly lacking in tuberculosis. *Therefore, we initiated our study on the activating effects of retinoic acid (RA) and vitamin D₃ (VD) on macrophages in relation to Mtb infection.*

Due to the difficulty of obtaining alveolar macrophages we utilized a human monocytoid cell line, THP-1(44), which is commonly substituted for *in vitro* studies of macrophage responses to Mtb infection. THPs however need to be activated before they differentiate into a macrophage-like cells (45). Phorbol myristate acetate (PMA) is the most common chemical activator for THPs(46), inducing adherence, upregulation of phagocytic receptors and an overall macrophage-like state. However, PMA, *in vivo*, is toxic for humans and is not a substance endogenously produced in the host. Unlike PMA, all-trans retinoic acid (RA)(47) and Vitamin D₃ (VD)(48) are THP activating agents that are basic components of a healthy diet and have been shown to be linked to immune responses against Mtb infection(31, 34, 49). We therefore examined the effects of PMA and RA+VD on the phenotype and function of THP cells to develop an *in vitro* model that is closer to Mtb infected human alveolar

macrophages. During these studies, we observed differing effects of PMA and RAVD on THP cells. PMA activated THPs (PMA-THPs) allowed enhanced growth of Mtb as observed before. However, RAVD activated THPs (RAVD-THPs) inhibited Mtb and with the addition of physiologically relevant, increasing doses of RA and VD, sustained bacteriostasis occurred. Furthermore, only in RAVD-THPs, Mtb induced the generation and gradual evolution of various morphotypes of macrophages to represent epithelioid cells, binucleate and MNGCs, culminating in syncytia. Thus, for the first time, it appears possible to study a chronic interaction between a slowly replicating mycobacterium that also has the unique ability to remain in a persistent stage in macrophages.

CHAPTER 2

TREATMENT OF THP-1 CELLS WITH RETINOIC ACID AND VITAMIN D LEADS TO AN INCREASED PHENOTYPIC DIFFERENTIATION COMPARED TO PHORBOL MYRISTATE ACETATE MEDIATED ACTIVATION

INTRODUCTION

Activation of THP-1 cells

Macrophages have a wide range of plasma membrane receptors that allow them to sense pathogens and interact with their environment. THP-1 cells (THPs) are a monocytic cell line that has minimal receptor expression before activation that after exposure to PMA, a classic activator for THPs, will adhere and up-regulate phagocytic receptors to yield an overall macrophage-like state. However, PMA, *in vivo*, is toxic for humans while, all-trans retinoic acid (RA)(47) and Vitamin D₃ (VD)(48) are basic components of a healthy diet, endogenously metabolized by the host to affect immune response against Mtb infection(31, 34, 49). We therefore examined the effects of PMA and RAVD on the up-regulation of receptors important in tuberculosis.

Macrophage Receptors Involved in Tuberculosis Pathogenesis

Uptake or Binding to Mycobacteria (CD14, CD44, DC-SIGN, MMR)

Macrophages have the ability to recognize, respond and phagocytose Mtb they encounter in their environment. We focused on four receptors, CD14, CD44, Dendritic Cell-Specific Intercellular adhesion molecule-3-Grabbing Non-integrin (DC-SIGN), and Macrophage Mannose Receptor (MMR), which has been shown to be important in binding, signaling and uptake of Mtb during infection.

CD14, is a cell surface glycosylphosphatidyl-inositol anchored glycoprotein and has no transmembrane domain and therefore cannot induce signaling within the cell(50). However, it was found to induce signaling cascades during the detection of lipopolysaccharide (LPS) by acting as a co-receptor for Toll-like Receptor 4 (TLR-4)(50). In tuberculosis, CD14 can interact with several different Mtb surface components such as, lipoarabinomannan(51), trehalose 6,6'-dimycolate (TDM)(52), LprA(53), LprG(53), or LpqH(53), to mediate uptake of the bacilli and stimulate release of pro-inflammatory cytokines(51-53). Interestingly, several epidemiological studies show that polymorphism in the 159 amino acid sequence of CD14 is a risk factor for the development of tuberculosis (54, 55).

Similar to CD14, CD44 mediates mycobacterial phagocytosis and induces protective immunity against Mtb(56). CD44 is a transmembrane glycoprotein receptor for hyaluronic acid and is found on a plethora of immune cells where it is involved in lymphocyte activation, recirculation and homing, hematopoiesis, and tumor metastasis(57). CD44 has been shown to be important during granuloma formation in lungs infected with Mtb(56) and furthermore, CD44^{-/-} mice were more susceptible to TB infection and showed a decrease in macrophage and lymphocyte recruitment to the site of infection(56).

DC-SIGN is a transmembrane protein with a calcium dependent (C-type) lectin domain that is normally expressed on interstitial dendritic cells and tissue specific macrophages, including alveolar

macrophages, within the human body(58). In undifferentiated THP cells, it is usually found at low levels. However, THPs activated with PMA or other differentiating agents, can express high levels of DC-SIGN(58). This is in contrast to other *in vitro* monocytic cells lines such as, U937, HL-60, Mono-Mac6, and K562 cells, which do not express DC-SIGN regardless of activation(58). The lectin domain of DC-SIGN has been found to recognize a large array of sugar moieties on a number of pathogens, including *Mycobacterium tuberculosis*(59, 60), HIV(61), *Helicobacter pylori*(62), Candida(63), Ebola virus(64), *Schistosoma mansoni*(62) and Leishmania amastigotes(65). During Mtb infection, DC-SIGN is known to bind to mannosylated lipoarabinomannan (ManLAM), a lipoglycan component of the mycobacterial cell wall, which mediates bacterial recognition and uptake into the cell(66). Similar to CD44, DC-SIGN polymorphisms in the gene promoter region are associated with tuberculosis (67).

MMR is the major receptor involved in Mtb uptake for macrophages. Similar to DC-SIGN, MMR binds to the ManLAM component of the mycobacterial cell wall that initiates internalization of the pathogen(68). It has been theorized that phagocytosis facilitated by MMR can lead to targeting of Mtb to specific compartments. Thus, MMR mediated internalization of ManLAM leads to endocytic compartments tagged with CD1b, that may facilitate antigen presentation to T-cells(69). The beneficial role of MMR in control of tuberculosis is still debated since uptake of mycobacterial glycolipids by MMR has been shown to decrease phagosome maturation rate in macrophages(70). It is interesting to note that during multinucleated giant cell formation in macrophages, MMR expression levels are elevated indicating that it may be essential to cell fusion events(71). Alternatively, MMR may perform scavenging function(72).

Cross talk with T cells (HLA-DR, CD1d, CD80, CD86)

Along with phagocytosis and the degradation of internalized pathogens, macrophages have the ability to present processed antigens to T-cells to amplify immune responses in the host. Activation of T-cells is mediated by two signals that are provided by antigen presenting cells, such as macrophages, to generate adoptive immunity. The first signal requires the presentation of antigen by MHC molecules (such as HLA-DR or CD1d) on the macrophage cell surface that binds to the T-cell receptor (TCR)(73). The second signal requires no antigen presentation but involves the binding of co-stimulatory molecules (such as CD80 and CD86) to their respective T-cell ligands, such as CD28 and CTLA-4(73). We wished to determine if activation with RAVD would increase antigen presenting receptors, such as HLA-DR and CD1d along with co-receptors CD80 and CD86 that may allow better crosstalk between infected macrophages and T-cells.

HLA-DR (Human Leukocyte Antigens – DR) is a major histocompatibility complex class II (MHC-II) cell surface receptor, found on macrophages, which presents processed peptide antigens to

CD4⁺ T-cells. During infection, HLA-DR surface expression increases that elicit cytokine responses from activated T-cells. To combat this effect, Mtb has evolved mechanisms to reduce HLA-DR expression and thereby reduce inflammation that can eliminate the infection(74, 75). Although there are many subtypes of class II HLA molecules, such as HLA-DP,DM, DOA,DOB & DQ, only HLA-DR has been shown in epidemiological studies to be related to susceptibility to tuberculosis(76). Therefore, we were interested in determining if RAVD activation of macrophages would allow for a greater surface expression of HLA-DR.

CD1d (Cluster of Differentiation-1d) are class I antigen-presenting glycoproteins located on the surface of macrophages that present processed foreign lipid antigens to a unique subset of T-cells called Natural Killer T (NKT) cells(77). Once activated, NKT cells can rapidly produce cytokines that can activate innate and adaptive immune responses in the host(77). Mtb has been shown to subvert CD1d expression in dendritic cells by phosphorylating host cell p38 mitogen-activated protein kinase, thereby preventing mycobacterial lipids from being presented to T-cells(78).

CD80 and CD86 are two molecules that are located on the surface of monocytes and act together to stimulate T-cell responses to antigens. Accordingly, CD80 and CD86 have been shown to be important for the control of chronic Mtb infections. Thus, T-cell mediated granuloma formation was reduced in CD80/CD86 double knock-out mice(79). Both molecules have been shown to increase in surface expression during the maturation process of monocytes into dendritic cell and macrophages(80-82). Therefore, we tested PMA and RAVD treated cells to determine if surface expression of the two molecules differed depending on the activator used.

Homing and Migration Receptors (CD195 and CD184)

Trafficking of lymphocytes throughout the body allows for the presentation of antigens to immune cell rich organs such as the spleen and lymph nodes, which greatly facilitates immune responses against foreign invaders. For macrophages to be able to directly travel to specific organs in the host, they must express receptors that allow them to “home” to a specific location. These homing receptors are specific for addressins, which are extracellular proteins of the endothelium. The binding of these homing receptors to their specific addressin directs the macrophage to the infection or inflammation site.

CD195, also known as chemokine receptor type 5 (CCR5), is a G-linked integral protein that has been shown to bind a number of chemokines such as RANTES, MIP-1 α and MIP-1 β (83). Expression of CD195 is detected in monocytes and T lymphocytes where they participate in activation and migration of leukocytes(83). CD184, also known as CXCR4 chemokine receptor, binds stromal-derived factor-1 (SDF-1 or CXCL12) that allows it to home to the bone marrow. Along with their roles

in homing macrophages to specific sites inside the host body, both CD195 and CD184, are important co-receptors in mediating HIV entry into host cells(84). Since the synergistic interactions of TB and HIV-1 center on the role of macrophages in the disease process, we wished to evaluate macrophage receptor expression of CD195 and CD184, two cell surface receptors important to both Mtb and HIV infections(84).

RESULTS

Phorbol myristyl acetate (PMA) and a combination of Retinoic acid (RA) and Vitamin D3 (VD) induce a different surface receptor expression and bacterial uptake in THPs

Differential Receptor Expression in Activated Macrophages

Macrophages express several types of receptors with different functional consequences. Some mediate uptake of Mtb (CD44, DC-SIGN), while others help a cross talk with T cells (HLA-DR, CD1d, CD80, CD86). Others like chemokine receptors CD195 and CD184 enable homing to infected sites while some like CD14 bind mycobacterial cell wall components altering cytokine signaling. RA and PMA had differential effects on receptor expression analyzed using flow cytometry. Receptors were generally up regulated in THPs activated with RA and PMA compared to PMA. In an experiment repeated three times with similar results, THPs were tested naïve or treated with various concentrations of PMA or RA, infected with H37Rv, and then stained for CD11c after 24 hours (**Figure 1A-C; Tables 1A-C**). Expression of antigen presenting molecules HLA-DR, CD1d, CD80 and CD86 was increased. CD184 and CD195 were also increased in RA versus PMA activated THPs along with the TLR-4 co-receptor, CD14. Such receptors may make THPs more responsive to chemokines enabling homing, infiltration and bacterial detection. CD44 has been implicated as a receptor for Mtb but showed no difference between RA and PMA activated cells (56). However, DC-SIGN increased in RA-THPs that is important for capture of Mtb and antigen presentation to T cells (60).

We also evaluated receptor expression in THPs treated with RA alone, VD alone and in combination (RA and VD). We observed that RA and VD were separately able to activate THPs although, maximal differentiation occurred in the synergistic presence of the two vitamins. An example of the combined effect on DC-SIGN is shown in **Figure 1D**.

RA and PMA have differential effects on the uptake of *Mycobacterium tuberculosis* (Mtb) in THPs

Receptor expression in activated THPs suggested that the optimal dose of RA was 1 μ M (1000 nM) and PMA was 10ng/mL (16 nM) and the optimal activation time was 72 hrs. All further studies utilized this optimized dose and activation. RA-THPs showed enhanced uptake of mannosylated-BSA-FITC, a classic probe used to measure macrophage mannose receptor (MMR) function, before infection with Mtb (**Figure 2A**). Furthermore, only RA-THPs maintained mannose receptor expression even after Mtb infection (**Figure 2B**).

MMR was then evaluated to determine if the difference observed in receptor expression would lead to a functional disparity in PMA and RAVD treated THPs. Since MMR is a receptor for mycobacterial glycolipids that allows for Mtb uptake (85), we assessed whether activated THPs differed in their internalized Mtb populations. Activated THPs were infected with Mtb H37Rv (MOI of 10) and evaluated for uptake of mycobacteria. Microscopic analysis of Ziehl-Neelsen stained Mtb in fixed PMA and RAVD treated THPs demonstrated a differential uptake of Mtb (**Figure 3**). RAVD activated THPs were better able to engulf Mtb, where over 75% of the macrophage population had internalized at least one mycobacterium, while only 60% of the PMA activated THPs demonstrated internalized Mtb. This data correlated with the increased expression of mycobacterial up-take receptors (**Figure 1A, 2A-B**).

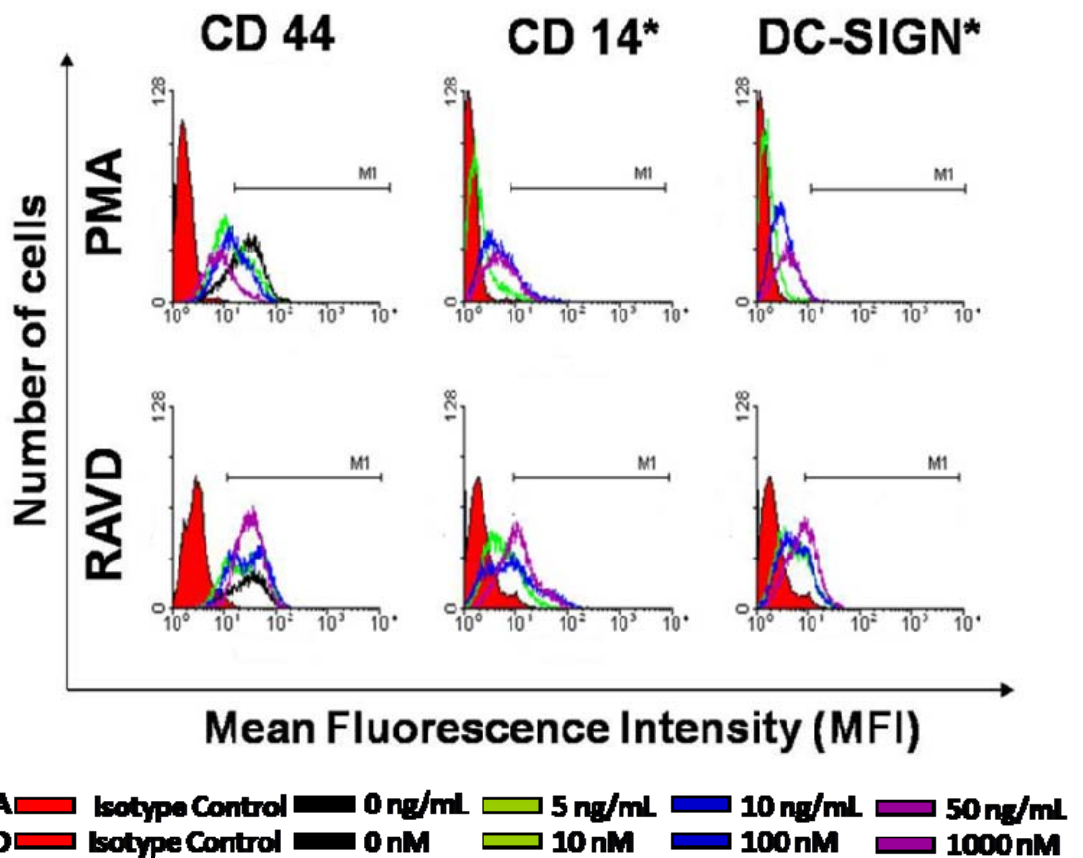


Figure 1A. Flow cytometric analysis of receptors involved in the uptake of mycobacteria in human THP-1 macrophages activated with either phorbol myristate acetate (PMA) or retinoic acid and vitamin D (RAVD).

THPs were activated with varying doses (as indicated) of PMA or a mix of RAVD for 72 hrs and were stained for surface receptors using fluorescent antibodies and analyzed in a BD FacsScan using Cellquest software. Mean Fluorescence Intensity (MFIs) from triplicate experiments were calculated to show significance as indicated (* indicates MFI significantly increased between PMA and RAVD activated THP-1 cells, paired t-test).

CD44	Low Dose			Mean +/- SEM
	Exp1 (Geo Mean)	Exp2 (Geo Mean)	Exp3 (Geo Mean)	
PMA (5ng/mL)	---	***	44.94	44.94±0
RAVD (10nM)	---	21.38	42.08	31.73±10.35
	Medium Dose			
PMA (10ng/mL)	---	27.48	35.31	31.40±3.92
RAVD (100nM)	---	***	44.23	44.23±0
	High Dose			
PMA (50ng/mL)	---	25.39	28.69	27.04±1.65
RAVD (1000nM)	---	20.48	36.90	28.69±8.20

Paired t-test $p = 0.5642$

CD14	Low Dose			Mean +/- SEM
	Exp1 (Geo Mean)	Exp2 (Geo Mean)	Exp3 (Geo Mean)	
PMA (5ng/mL)	41.08	21.48	38.69	33.75±6.17
RAVD (10nM)	38.01	31.15	39.61	36.26±2.60
	Medium Dose			
PMA (10ng/mL)	46.09	24.92	35.31	35.44±6.11
RAVD (100nM)	49.81	30.83	39.61	40.08±5.48
	High Dose			
PMA (50ng/mL)	40.15	26.43	33.80	33.46±3.96
RAVD (1000nM)	47.45	32.15	38.26	39.29±4.45

Paired t-test $p = 0.0078$

DC-SIGN	Low Dose			Mean +/- SEM
	Exp1 (Geo Mean)	Exp2 (Geo Mean)	Exp3 (Geo Mean)	
PMA (5ng/mL)	47.31	17.47	39.27	34.68±8.91
RAVD (10nM)	42.31	32.71	46.06	40.36±3.98
	Medium Dose			
PMA (10ng/mL)	39.58	24.98	39.82	34.79±4.91
RAVD (100nM)	46.17	33.94	44.82	41.64±3.87
	High Dose			
PMA (50ng/mL)	37.97	28.52	31.86	32.78±2.77
RAVD (1000nM)	46.47	32.64	45.03	41.38±4.39

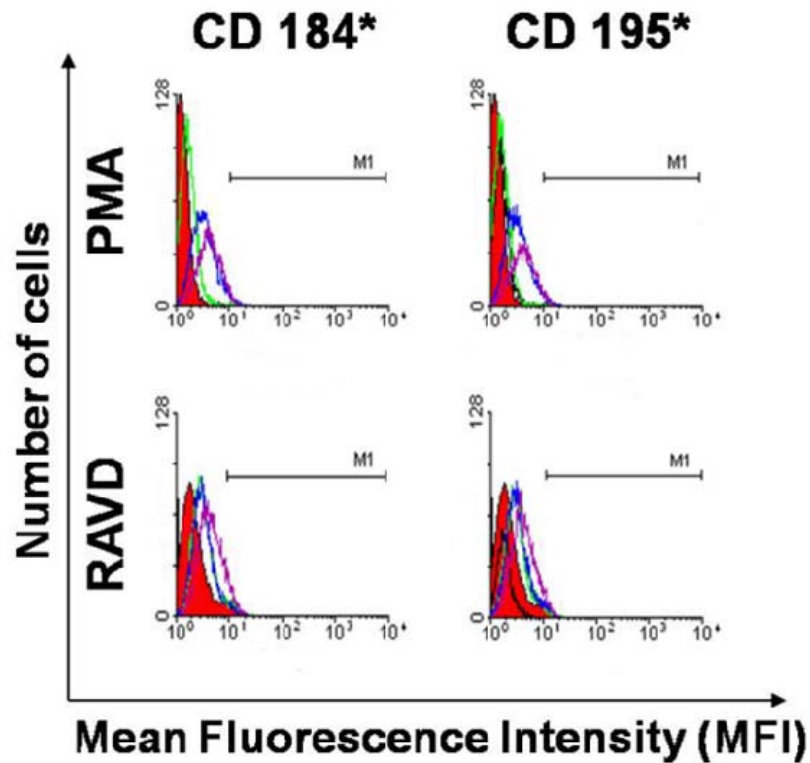
Paired t-test $p = 0.0065$

--- No data

***Incalculable data

Table 1A. Tabulated data of mean fluorescence intensity (MFIs) depicted in the flow cytometric analysis of uptake or binding receptors to mycobacteria on PMA or RAVD activated human THP-1 macrophages.

THPs were activated with varying doses (as indicated) of PMA or RAVD for 72 hrs and were stained for surface receptors using fluorescent antibodies and analyzed in a BD FacsScan using Cellquest software. MFIs from triplicate experiments were tabulated and analyzed using a paired t-test to show significance at $p < 0.05$ (***) indicates samples with no Geo Mean calculated during flow cytometry acquisition).



PMA ■ Isotype Control ■ 0 ng/mL ■ 5 ng/mL ■ 10 ng/mL ■ 50 ng/mL
RAVD ■ Isotype Control ■ 0 nM ■ 10 nM ■ 100 nM ■ 1000 nM

Figure 1B. Flow cytometric analysis of chemokine receptors in human THP-1 macrophages activated with either PMA or RAVD.

THPs were activated with varying doses (as indicated) of PMA or a mix of RAVD for 72 hrs and were stained for surface receptors using fluorescent antibodies and analyzed in a BD Facsan using Cellquest software. MFIs from triplicate experiments were calculated to show significance as indicated (* indicates MFI significantly increased between PMA and RAVD activated THP-1 cells, paired t-test).

CD184	Low Dose			Mean +/- SEM
	Exp1 (Geo Mean)	Exp2 (Geo Mean)	Exp3 (Geo Mean)	
PMA (5ng/mL)	---	***	41.02	41.02±0
RAVD (10nM)	---	34.74	46.81	40.78±6.04
Medium Dose				
PMA (10ng/mL)	---	25.40	37.60	31.50±6.10
RAVD (100nM)	---	36.97	49.40	43.19±6.22
High Dose				
PMA (50ng/mL)	---	27.95	31.15	29.55±1.60
RAVD (1000nM)	---	36.94	48.19	42.57±5.63

Paired t-test p = 0.0040

CD195	Low Dose			Mean +/- SEM
	Exp1 (Geo Mean)	Exp2 (Geo Mean)	Exp3 (Geo Mean)	
PMA (5ng/mL)	45.07	30.10	44.69	39.95±4.93
RAVD (10nM)	42.36	34.14	50.34	42.28±4.68
Medium Dose				
PMA (10ng/mL)	45.11	25.89	44.05	38.35±6.24
RAVD (100nM)	39.60	36.05	50.79	42.15±4.44
High Dose				
PMA (50ng/mL)	45.73	25.00	30.25	33.66±6.22
RAVD (1000nM)	51.11	36.36	51.38	46.28±4.96

Paired t-test p = 0.0431

--- No data

***Incalculable data

Table 1B. Tabulated data of MFIs depicted in the flow cytometric analysis of chemokine receptors on PMA or RAVD activated human THP-1 macrophages.

THPs were activated with varying doses (as indicated) of PMA or a mix of RA and VD for 72 hrs and were stained for surface receptors using fluorescent antibodies and analyzed in a BD FacsScan using Cellquest software. MFIs from triplicate experiments were tabulated and analyzed using a paired t-test to show significance at $p < 0.05$ (***) indicates samples with no Geo Mean calculated during flow cytometry acquisition).

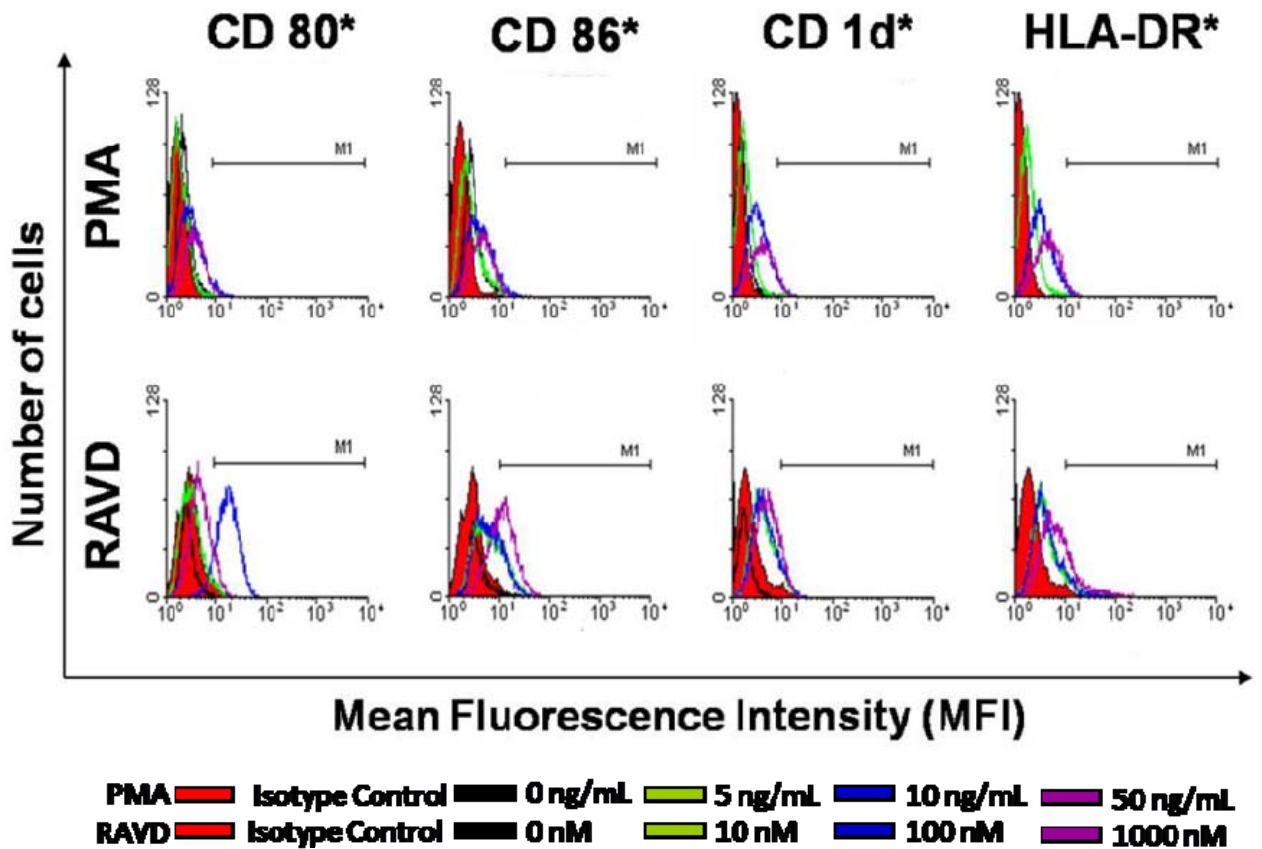


Figure 1C. Flow cytometric analysis of antigen presenting receptors in human THP-1 macrophages activated with either PMA or RAVD.

THPs were activated with varying doses (as indicated) of PMA or a mix of RAVD for 72 hrs and were stained for surface receptors using fluorescent antibodies and analyzed in a BD Facsan using Cellquest software. MFIs from triplicate experiments were calculated to show significance as indicated (* indicates MFI significantly increased between PMA and RAVD activated THP-1 cells, paired t-test).

CD80	Low Dose			Mean +/- SEM
	Exp1 (Geo Mean)	Exp2 (Geo Mean)	Exp3 (Geo Mean)	
PMA (5ng/mL)	34.73	13.26	13.63	20.54±7.10
RAVD (10nM)	35.02	14.34	14.98	21.45±6.79
	Medium Dose			
PMA (10ng/mL)	32.66	13.49	13.73	19.96±6.35
RAVD (100nM)	39.10	14.30	14.57	22.66±8.22
	High Dose			
PMA (50ng/mL)	30.37	13.66	14.13	19.39±5.49
RAVD (1000nM)	33.94	14.04	14.49	20.82±6.56

Paired t-test $p = 0.0392$

CD86	Low Dose			Mean +/- SEM
	Exp1 (Geo Mean)	Exp2 (Geo Mean)	Exp3 (Geo Mean)	
PMA (5ng/mL)	31.25	15.71	16.84	21.27±5.00
RAVD (10nM)	35.57	29.03	18.31	27.64±5.03
	Medium Dose			
PMA (10ng/mL)	33.98	15.95	17.80	22.58±5.73
RAVD (100nM)	34.16	17.56	18.21	23.31±5.43
	High Dose			
PMA (50ng/mL)	33.26	14.50	14.59	20.78±6.24
RAVD (1000nM)	35.46	15.63	18.42	23.17±6.20

Paired t-test $p = 0.0475$

CD1d	Low Dose			Mean +/- SEM
	Exp1 (Geo Mean)	Exp2 (Geo Mean)	Exp3 (Geo Mean)	
PMA (5ng/mL)	23.71	***	41.97	32.84±9.13
RAVD (10nM)	45.26	35.73	47.34	42.78±3.57
	Medium Dose			
PMA (10ng/mL)	39.88	26.95	39.96	35.60±4.32
RAVD (100nM)	42.46	34.73	47.80	41.66±3.79
	High Dose			
PMA (50ng/mL)	45.52	26.23	30.71	34.15±5.83
RAVD (1000nM)	49.29	32.51	40.76	40.85±4.84

Paired t-test $p = 0.0059$

HLA-DR	Low Dose			Mean +/- SEM
	Exp1 (Geo Mean)	Exp2 (Geo Mean)	Exp3 (Geo Mean)	
PMA (5ng/mL)	40.04	18.94	35.97	31.65±6.46
RAVD (10nM)	39.43	31.52	41.43	37.46±3.03
	Medium Dose			
PMA (10ng/mL)	37.37	23.90	38.71	33.33±4.73
RAVD (100nM)	40.10	29.89	39.87	36.62±3.37
	High Dose			
PMA (50ng/mL)	38.46	22.83	28.96	30.08±4.55
RAVD (1000nM)	41.13	29.11	39.38	36.54±3.75

Paired t-test $p = 0.0066$

--- No data

***Incalculable data

Table 1C. Tabulated data of MFIs depicted in the flow cytometric analysis of receptors involved in antigen presentation on PMA or RAVD activated human THP-1 macrophages.

THPs were activated with varying doses (as indicated) of PMA or a mix of RA and VD for 72 hrs and were stained for surface receptors using fluorescent antibodies and analyzed in a BD Facsan using Cellquest software. MFIs from triplicate experiments were tabulated and analyzed using a paired t-test to show significance at $p < 0.05$ (***) indicates samples with no Geo Mean calculated during flow cytometry acquisition).

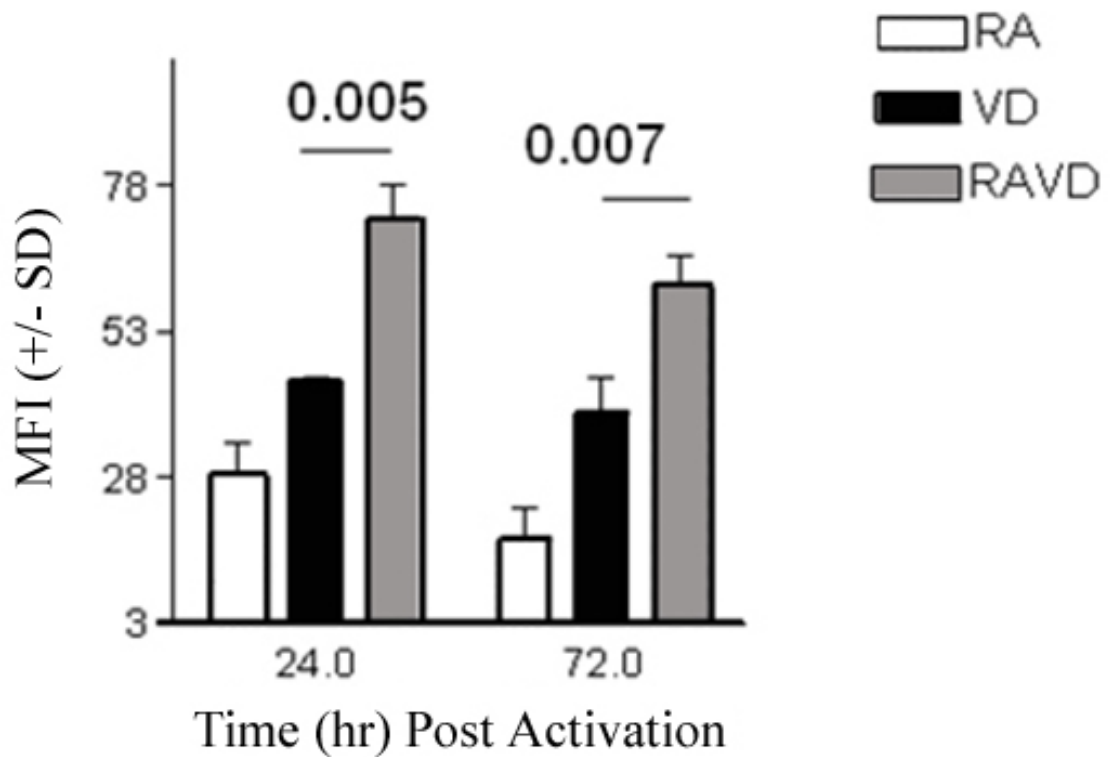


Figure 1D. Flow cytometric analysis of DC-SIGN in human THP-1 macrophages activated with either RA alone, VD alone or their combination.

THPs were treated with RA alone (1 μ M), VD alone (1 μ M) or their combination (1 μ M each), stained for DC-SIGN using fluorescent antibodies and analyzed in a BD Facsan using Cellquest software at 24 hrs and 72 hrs after activation. Data show that RAVD combination induces the best expression of DC-SIGN in THPs (p values shown above bars for groups compared, t test; MFI \pm SD of 2 experiments).

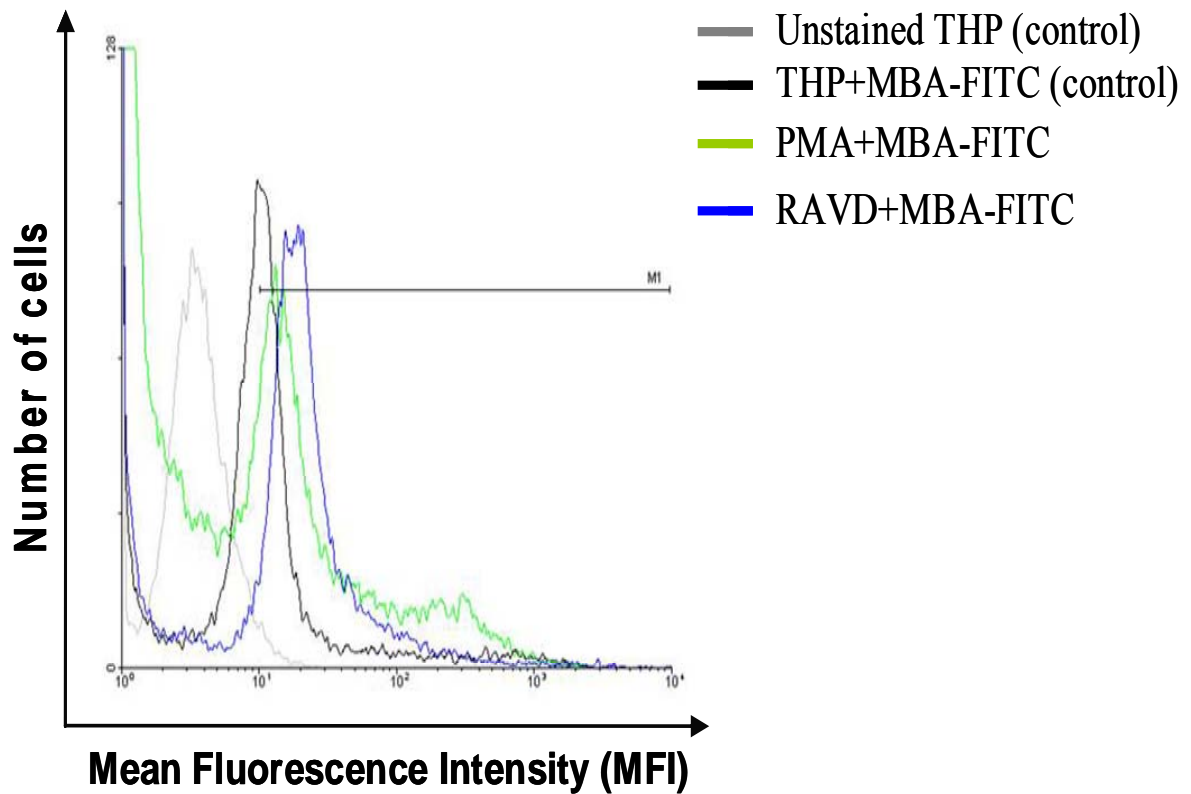


Figure 2A. Flow cytometric analysis of mannosylated-BSA-FITC (mBSA-FITC) in human THP-1 macrophages activated with either PMA or RAVD before infection with H37Rv.

THPs were activated for 3 days with either PMA or RAVD, treated with mBSA-FITC at 37°C and analyzed for uptake via macrophage-mannose receptor. RAVD enhanced the expression of macrophage-mannose receptor compared to PMA activated or naïve cells (one of three similar experiments shown for histograms).

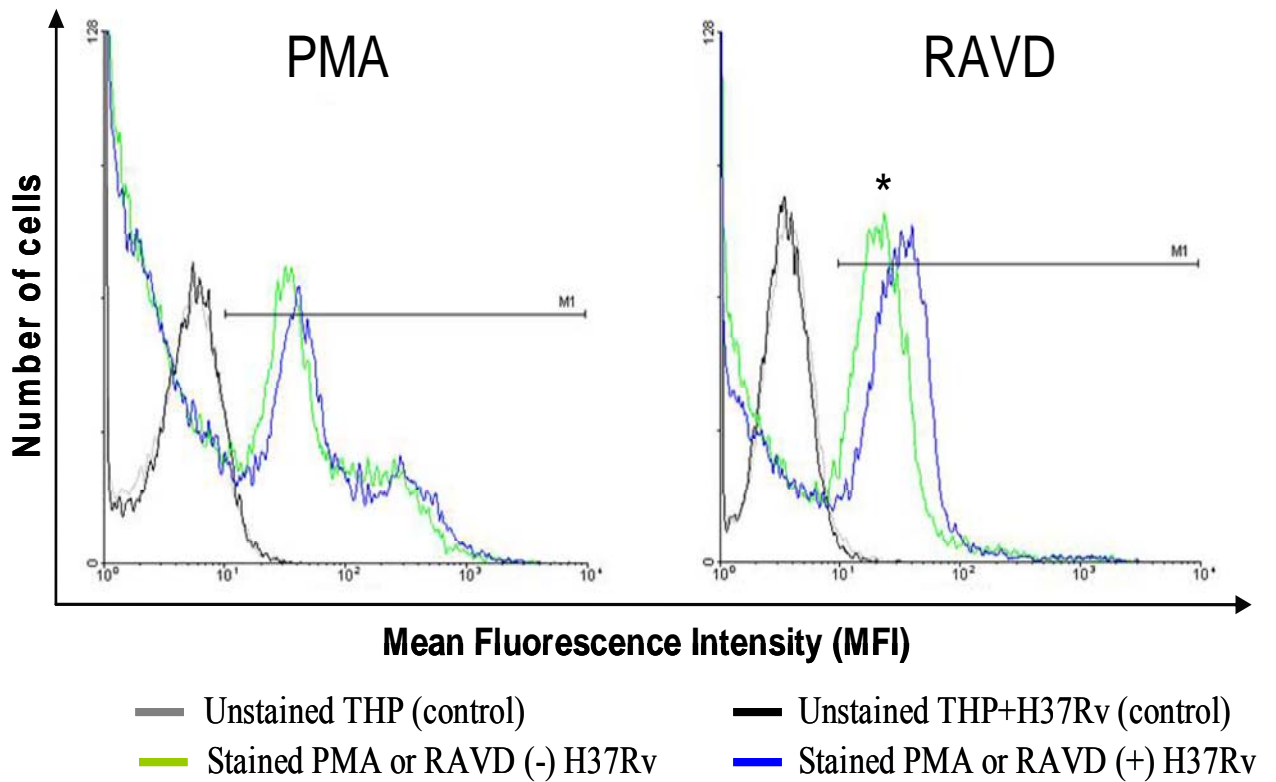


Figure 2B. Flow cytometric analysis of mannosylated-BSA-FITC (mBSA-FITC) in human THP-1 macrophages activated with either PMA or RAVD after infection with H37Rv.

THPs were activated for 3 days with either PMA or RAVD, infected with H37Rv for 24 hrs, treated with mBSA-FITC at 37 °C and uptake was analyzed by flow cytometry. After infection, RAVD-THPs increased their uptake of mBSA-FITC compared to PMA activated cells (one of three similar experiments shown for histograms).

	(-) H37Rv		(+) H37Rv	
	PMA (Geo Mean)	RAVD (Geo Mean)	PMA (Geo Mean)	RAVD (Geo Mean)
Exp1	35.51	66.09	26.82	86.76
Exp2	96.16	154.27	88.14	173.14
Exp3	52.17	72.55	50.76	93.24
Mean +/- SEM	61.28±18.09	97.64±28.38	55.24±17.84	117.7±27.78

Paired t-test p = 0.0009 between RAVD groups before and after infection

Table 2. Tabulated data of MFIs depicted in the flow cytometric analysis of mannosylated-BSA-FITC (mBSA-FITC) uptake in PMA or RAVD activated human THP-1 macrophages.

THPs were activated for 3 days with either PMA or RAVD, infected with or without Mtb H37Rv for 24 hrs, then treated with mBSA-FITC at 37°C and uptake was analyzed by flow cytometry. Tabulated data is graphically represented in Figure 2A and 2B. Paired t-test analysis between RAVD groups (-/+ H37Rv) shows an increase in mBSA-FITC uptake (p=0.0009).

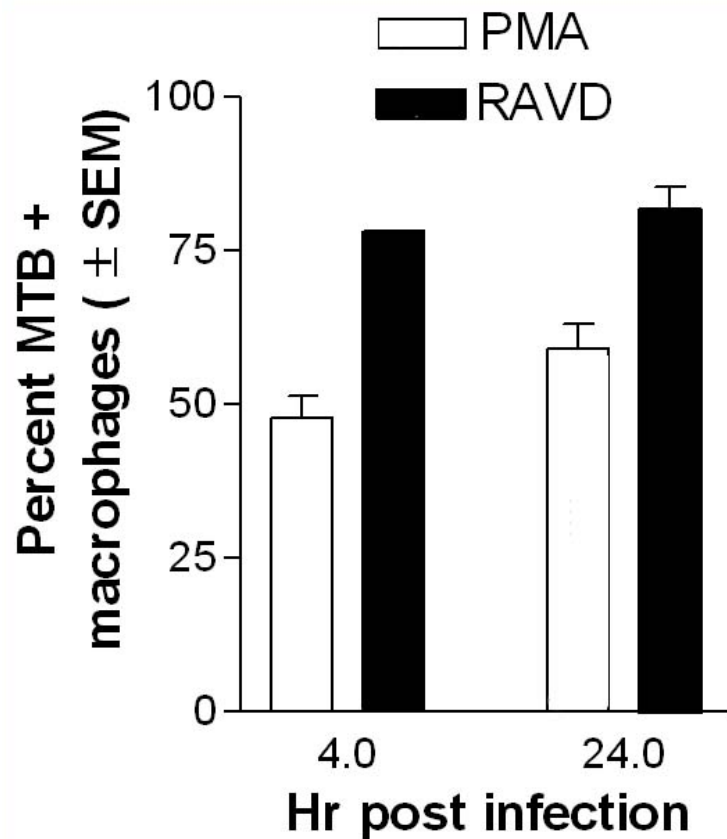


Figure 3. PMA and RAVD have differential effects on the uptake of *Mycobacterium tuberculosis* (Mtb) within THP-1 macrophages.

THPs were activated with either 10 ng/mL of PMA or 1 μ M each of RA and VD for 72 hrs and infected with Mtb H37Rv for 4 and 24 hrs. Bacteria internalized in cultures of washed monolayers were visually scored by microscopy using acid fast stain. Mtb uptake by THPs is significantly increased after RAVD treatment (* $p < 0.009$, t-test, mean \pm SEM of 3 experiments).

DISCUSSION

Monocytes and monocytoid cell lines generally express reduced numbers of receptors and are less efficient in phagocytosing pathogens(86). However, differentiated macrophages express abundant receptors and are more phagocytic. Monocyte to macrophage differentiation occurs after binding of pathogens to monocytes via their receptors in combination with the release of self-activating cytokines such as TNF- α , G-CSF and GM-CSF. Differentiation can be induced *in vitro* by phorbol esters(46), VD₃(47) and RA(48). Although RA and VD have been shown to separately activate THPs, limited studies have looked into the synergistic effects of the two vitamins to induce a mature macrophage phenotype.

As Mtb is an intracellular parasite, it is phagocytosed by the macrophage where it can survive and multiply. RAVD-THPs expressed higher levels of uptake and binding receptors (CD14, DC-SIGN, MMR) along with a corresponding increase in internalized Mtb during bacterial infection. VD₃ was found to enhance DC-SIGN levels in THPs earlier and the well documented role of DC-SIGN in mycobacterial recognition confirmed the increased efficacy of RAVD-THPs during phagocytosis. It is interesting to note that before and after infection, RAVD-THPs expressed higher levels of MMR than PMA-THPs. Mtb phagocytosis facilitated by MMR has been suggested as an advantageous route of entry for the pathogen since internalization of this receptor is not directly linked to the activation of cytotoxic reactive oxygen intermediates(70). Furthermore, uptake of mycobacterial glycolipids by MMR leads to decreased phagosome maturation rates in macrophages thus allowing greater bacterial survival(70). It would be exciting if future studies could determine if binding of Mtb to specific receptors influences the response produced by the host cell. These findings could help elucidate the mechanism by which Mtb is able to enter into a latent phase inside the host.

Following the uptake of Mtb into the phagosome, a step-wise process begins where phagosome-lysosome fusion occurs. This leads to the degradation of the pathogen and allows processed bacterial peptides to be loaded onto antigen presentation molecules for recognition by T-cells to induce a Th1 immune response. Since RAVD-THPs, compared to PMA-THPs, expressed higher levels of HLA-DR, CD1d, CD80, CD86, we speculated that antigen presentation and cross-talk with T-cells would be better observed in these cells. However, Mtb is also known to down-regulate antigen presentation receptors during infection(87). Therefore, further evaluation of antigen presentation and cross-talk receptor expression during Mtb infection appeared to be necessary and are elaborated next.

Along with evaluating uptake and antigen presentation receptors, we were interested in the possibility of using RAVD-THPs as a model for TB/HIV-1 co-infections. Both CD195 and CD184, up-regulated in RAVD-THPs, are important co-receptors in mediating HIV-1 entry into host cells(84). DC-

SIGN, another receptor shown to facilitate HIV-1 entry into immune cells, is also up-regulated in RAVD-THPs. We speculated that RAVD-THPs may allow us to study Mtb/HIV-1 coinfections.

In conclusion, our studies show that RAVD transformed THPs to a more efficient macrophage phenotype than PMA. The observation that PMA-THPs were less able to phagocytose Mtb correlated well with their reduced expression of uptake receptors.

CHAPTER 3

EFFECTS OF RETINOIC ACID AND VITAMIN D ON THE ABILITY OF THP-1 CELLS TO PRESENT ANTIGEN TO HUMANIZED MOUSE T-CELLS

INTRODUCTION

Once we found Mtb internalized into THPs, we investigated the fate of ingested organisms. Usually the ingested Mtb are enclosed in a phagosome that fuses with lysosome in a process called maturation. During maturation, Mtb is delivered to lysosomes for degradation and mycobacterial peptides are sorted to be eventually presented via MHC-II on the cell surface to T-cells.

MHC-II Maturation

An important function of macrophages is their ability to present foreign antigens to T-cells, which release cytokines, such as IL-2, upon antigen recognition. Unlike major histocompatibility complex class I (MHC-I) that presents peptides from cytosolic proteins, MHC class II (MHC-II) antigen presentation originates primarily from phagocytosed extracellular proteins or pathogens. Therefore, as mentioned above, MHC-II antigen presentation is highly dependent on maturation of the phagosome into a phagolysosome.

Processing and loading of peptides to MHC-II molecules has been studied broadly although not as extensively in tuberculosis(88). During synthesis in the endoplasmic reticulum (ER), MHC-II is a trimer composed of a dimer of α and β chain along with an invariant chain. The invariant chain blocks the peptide-binding site while the MHC-II molecule is being processed in the ER to prevent cellular peptides from binding and being presented. It also targets the MHC-II molecule for export via budding of the ER in a vesicle. During acidification of the vesicle or endosome, the invariant chain is degraded but the peptide-binding site remains blocked by a residual peptide called Class II-associated invariant chain peptide (CLIP). CLIP remains in place even when the MHC-II containing endosome merges with the matured phagosome containing endocytosed antigens. Only when an MHC-II like structure, such as HLA-DR, binds to MHC-II does CLIP get released and peptides allowed binding. Once peptides are bound, MHC-II can travel to the cell surface and present the antigen exclusively to CD4⁺ T-cells. The latter have specific T-cell Receptors (TCR) that can bind MHC-II-peptide complex.

MHC-II Molecules and Tuberculosis

Mtb has developed several strategies to inhibit macrophages without being detected and thus degraded. One major mechanism is that it inhibits phagosome-lysosome fusion that enables it to avoid lysosome-mediated degradation. This mechanism has been discussed in Chapter 6. A second mechanism is to manipulate the antigen presentation pathway in MHC-II molecules. The secreted bacterial lipoprotein, LpqH (also known as 19kDa) has been shown to down-regulate MHC-II surface expression by excessive signaling through Toll-Like Receptor 2 (TLR-2)(89-91). Extended exposure of

LpqH to TLR-2 receptor decreases the activity of MHC-II transcriptional activator (CIITA) that hinders gene expression of the MHC-II molecule(90, 91). Paradoxically, TLR-2 signaling is more important during *in vitro* MHC-II presentation, since, chimeric animal studies have demonstrated that TLR-2 deficient macrophages show no difference in the surface expression of MHC-II than wild-type(92). However, this observation can also be explained by the finding that LpqH-mediated down-regulation of MHC-II expression occurs exclusively in macrophages infected with Mtb(93). Thus, even Bacillus Calmette-Guérin (BCG) vaccine, that also contains LpqH, when given to mice eventually causes decreased expression of MHC-II *in vivo*(93).

Additionally, Mtb can manipulate MHC-II intracellular trafficking to prevent antigen presentation from occurring. Since Mtb phagosomes already have MHC-II peptide, loading can occur *in situ*(94). However, for MHC-II to be loaded properly with peptide, the compartment must be acidified to activate cathepsin proteases to cleave Mtb peptides along with the invariant chain of MHC-II. Two important enzymes that are involved in MHC-II peptide loading are Cathepsin D (CatD), a protease that can cleave Mtb peptides(95) and Cathepsin S (CatS), a lysosomal cysteine protease that is responsible for cleaving the invariant chain of MHC-II(96).

To interfere with peptide presentation, Mtb has evolved several mechanisms to modulate the immune response. First, Mtb decreases MHC-II expression by inducing IL-10, an anti-inflammatory cytokine, which leads to the inhibition of CatS function(97, 98). Second, Mtb intra-phagosomally expresses a urease, encoded by the *ureC* gene, which catalyzes the hydrolysis of urea into carbon dioxide and ammonia(99). The excess ammonia produced by the urease alkalizes the phagosomal compartment preventing it from acidifying thus inhibiting cathepsin activity critical for MHC-II peptide loading and maturation.

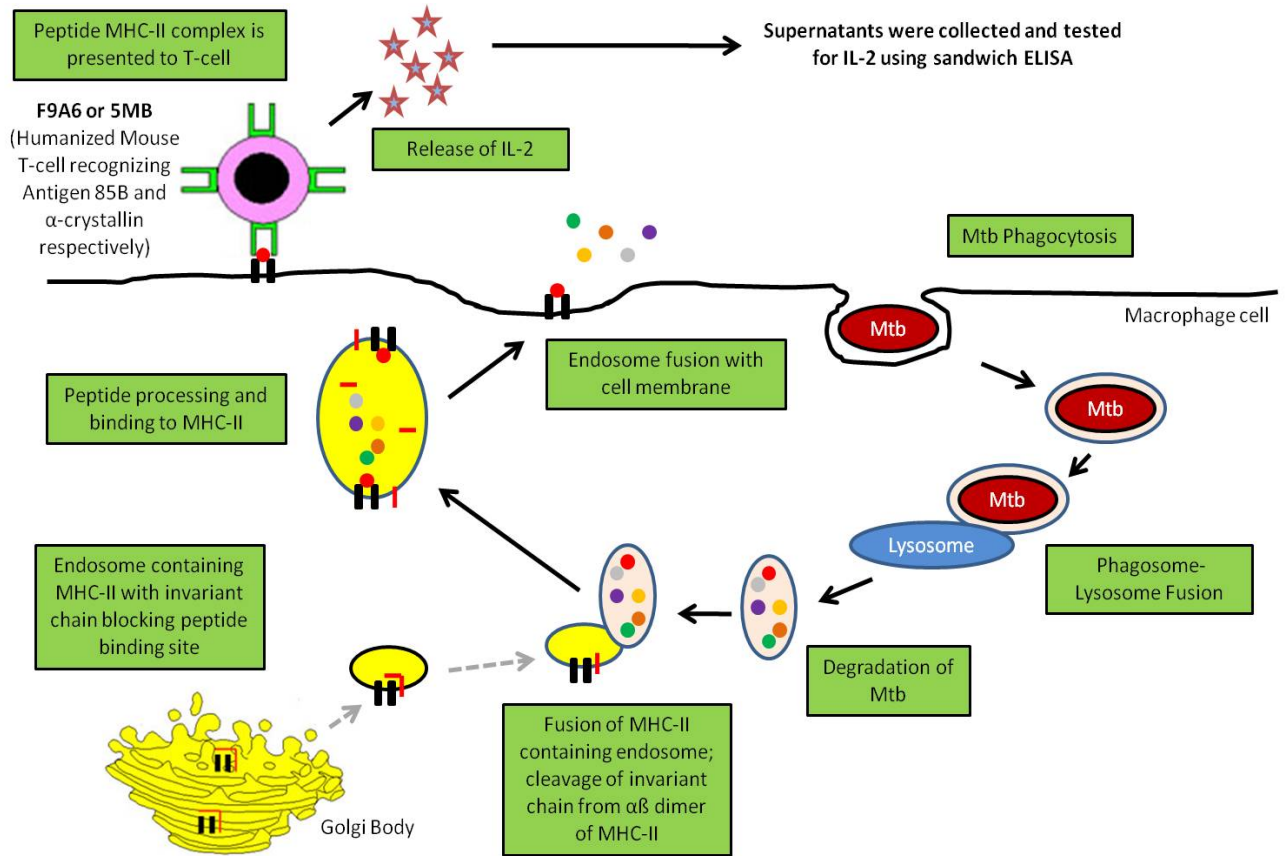
Mtb has also been shown to exclude vacuolar proton-ATPase (v-ATPase) from the phagosomal compartments (100). Bacterial v-ATPase phagosome exclusion prevents protons from being pumped into the compartment to keep it acidified. In one study, v-ATPase phagosome exclusion was linked to the decrease in presentation of Antigen 85b(95), an important mycobacterial protein vaccine candidate eliciting T cell response to Mtb(101).

MHC-II Antigen Presentation to Hybridoma CD4⁺ T-cell

We previously determined that activation of THP cells with RAVD led to an increase in antigen presenting receptors, HLA-DR, CD1d, CD80 and CD86 (**Figure 1C; Table 1C**) compared to PMA-THPs (Chapter 2). Using two humanized mouse T-cell lines (kind gift of Dr. David Canaday)(91) that recognize peptides specific for Antigen 85B (F9A6 cells) and α -crystallin (5MB cells), we attempted to determine if the increase in surface expression of antigen presenting receptors led to an increase in T-

cell priming resulting in IL-2 secretion. Quantitation of IL-2 release by these T-cell hybridoma cell lines allowed us to evaluate the processing and presentation of mycobacterial antigens in activated THP macrophages. A diagram of *in vitro* antigen presentation appears below.

Diagram 1: Mtb antigen processing in macrophages and the detection of presented peptides on MHC-II molecules by using F9A6 or 5MB humanized mouse cell lines specific for Antigen 85B and α -crystallin, respectively.



RESULTS

PMA and RAVD activated Mtb infected THP cells do not induce IL-2 secretion from T-cell hybridomas specific for Antigen 85B or α -crystallin

We previously determined that activation of THP cells with RAVD led to an increase in antigen processing and presenting receptors, HLA-DR, CD1d, CD80 and CD86 (**Figure 1C and Table 1C**) compared to PMA-THPs. Using F9A6 cells, which recognize Antigen 85b (Ag85b) and 5MB cells, which recognize α -crystallin (acr), we attempted to determine if mycobacterial antigen presentation was occurring in RAVD-THPs. Unfortunately, our attempts to elicit an IL-2 T-cell response from activated and infected THPs were unsuccessful. In an experiment repeated several times, THPs were tested naïve or treated with IFN- γ , PMA or RAVD, followed by infection with Mtb H37Rv or BCG-14, a mutant strain of BCG vaccine that hyper-expresses Antigen 85B. After infection, the cells were washed and overlaid with either F9A6 or 5MB T-cells. The supernatants were collected and tested for IL-2 using sandwich ELISA.

Earlier studies by Dr. Canaday's laboratory demonstrated that Mtb infected THP cells activated with IFN- γ and overlaid with the hybridoma T-cells produced the most IL-2 secretion. Following his suggested protocol, we attempted to determine the time course that would yield optimal IL-2 production (**Figure 4A**). Unfortunately, after several attempts to find the most favorable infection time point, using either BCG-14 or Mtb H37Rv strains to infect IFN- γ activated THPs, we were unable to detect IL-2 levels above control groups (no overlay with T-cells).

Although IFN- γ activated THPs did not facilitate high levels of IL-2 secretion from F9A6 or 5MB cells, we were curious to determine the effects of PMA and RAVD (**Figure 4B**). BCG-14 was used to infect PMA-THPs and RAVD-THPs at various infection times (4 hrs and 24 hrs), the cells washed, then overlaid with F9A6 for 4 hrs or 24 hrs. The supernatants were collected and tested for IL-2 using sandwich ELISA. Again, the levels of IL-2 detected did not rise above the controls groups (no overlay with T-cells).

Since we did not detect any increase in supernatant IL-2 levels using varying conditions of activated and infected THPs, we decided to evaluate the effects of another cell line, MonoMac-6, an antigen presenting macrophage (**Figure 4C**). THP-1 and MonoMac-6 cells were treated with either IFN- γ or RAVD and infected with either BCG-14 or Mtb H37Rv for 4 hrs. The infected macrophages were washed and overlaid with F9A6 cells for an additional 4 hrs. The supernatants were collected and evaluated for IL-2 using sandwich ELISA. Unfortunately, the change of macrophage cell lines also did not lead to an increase in IL-2 levels above background (normally considered over 250 pg/mL).

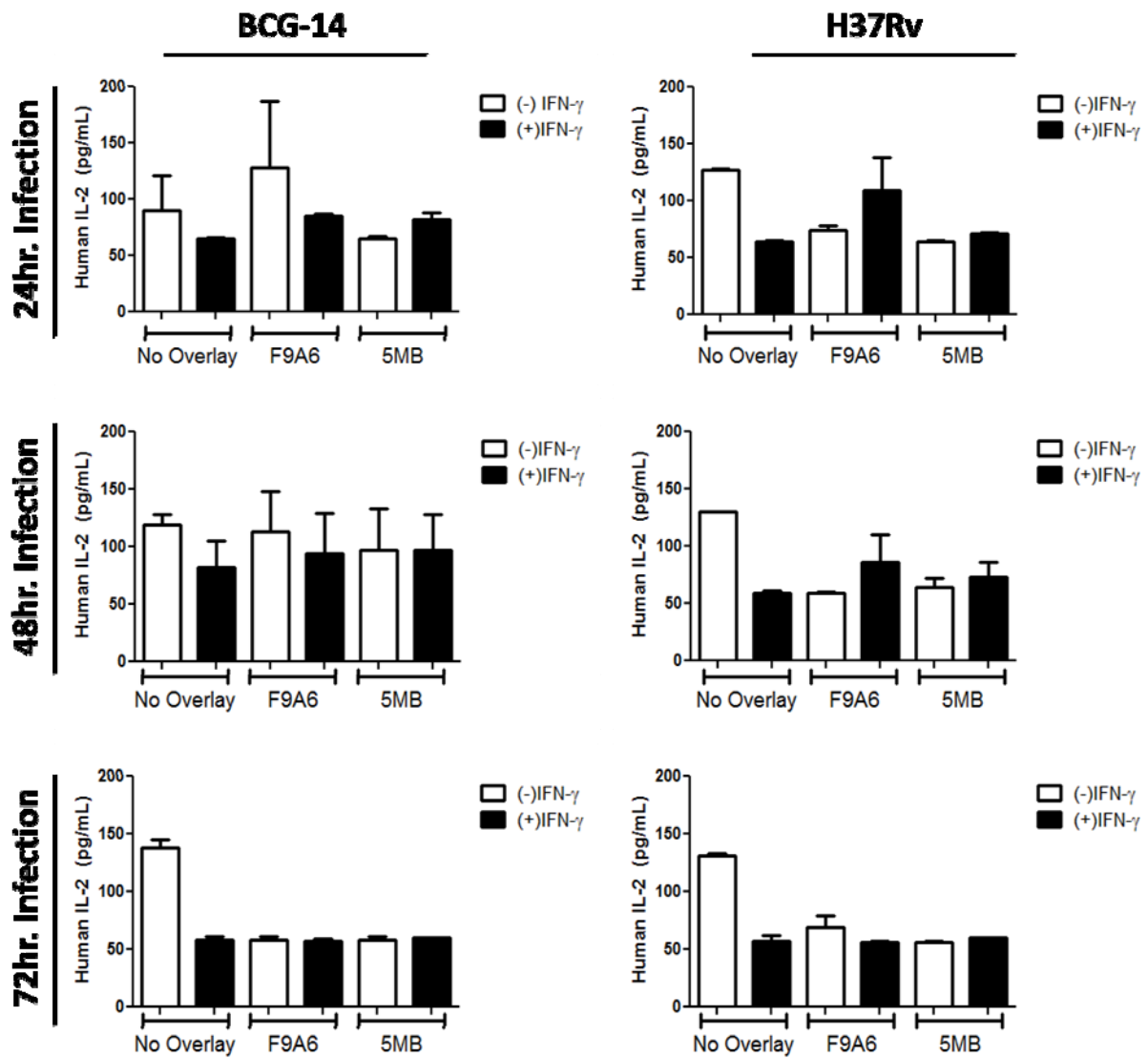


Figure 4A. Evaluation of MHC-II dependent antigen 85B (Ag85B) presentation in BCG-14 or *M. tuberculosis* H37Rv infected THP-1 macrophages activated with IFN- γ using humanized mouse T-cells secreting IL-2.

Macrophages were activated with IFN- γ and infected with either BCG-14 (mutant BCG strain hyper-expressing Ag85B) or H37Rv. After infection, the cells were washed and overlaid for 4 hrs. with either F9A6, a T-cell specific for Ag85B, or 5MB, a T-cell specific for α -crystalline (acr). Supernatants were collected and tested for IL-2 using sandwich ELISA. Supernatants collected from overlaying with either F9A6 or 5MB did not show IL-2 levels above control groups (no overlay with T-cells).

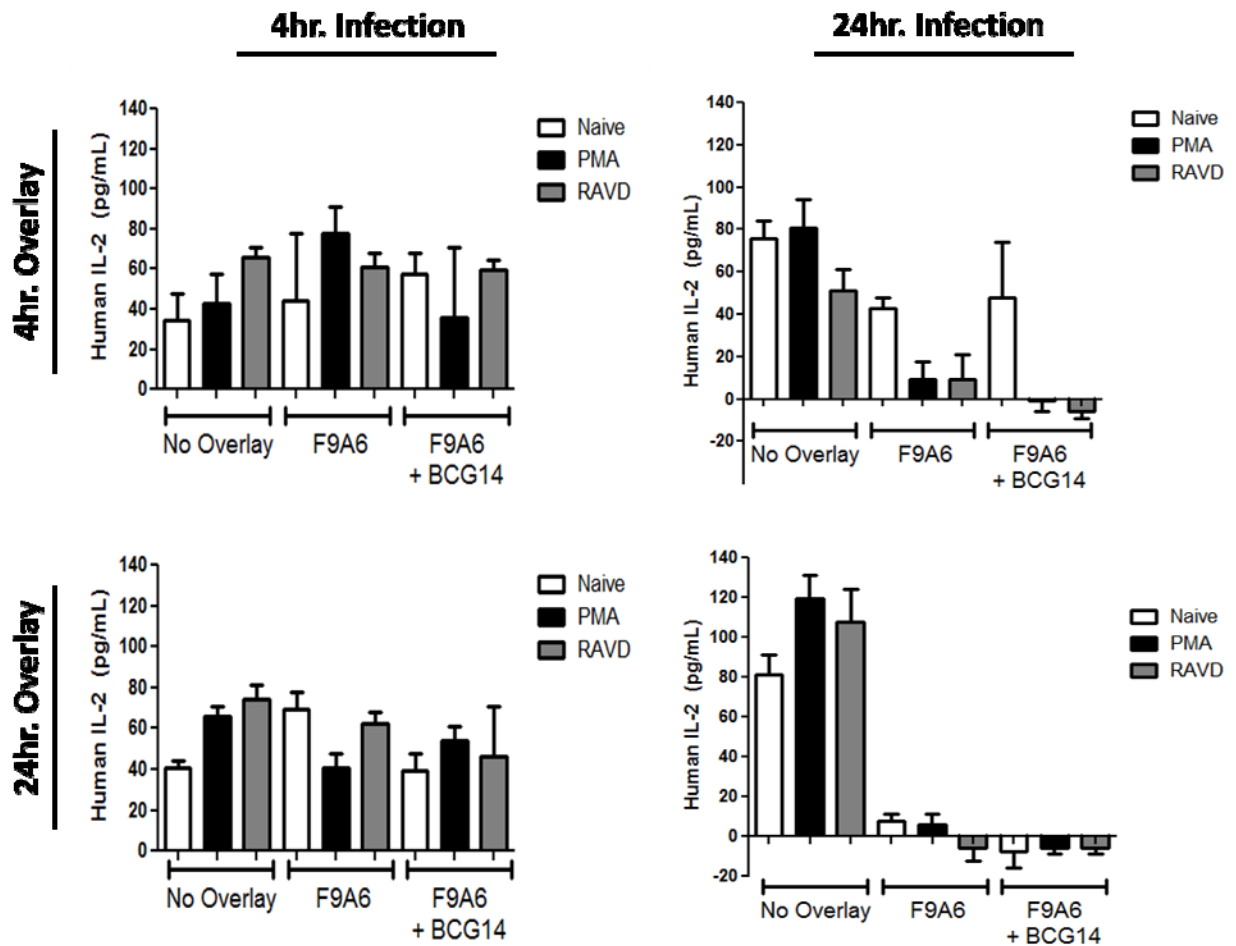


Figure 4B. Evaluation of MHC-II dependent Ag85B presentation in PMA or RAVD activated THP-1 macrophages using F9A6 cells specific for Ag85b.

Macrophages were activated with PMA or RAVD and infected with BCG-14 (mutant BCG strain hyper-expressing Ag85B). After infection, the cells were washed and overlaid for either 4 hrs or 24 hrs with F9A6, a humanized mouse T-cell specific for Ag85B. Supernatants were collected and tested for IL-2 using sandwich ELISA. Supernatants collected from overlaying with F9A6 did not show IL-2 levels above control groups (no overlay with T-cells).

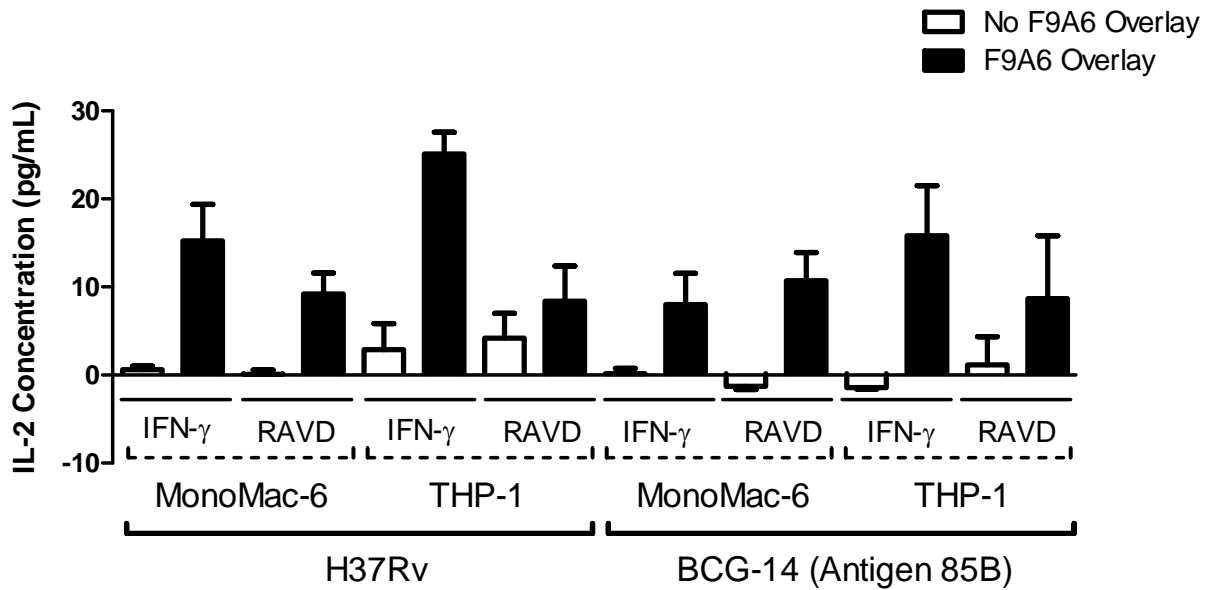


Figure 4C. Comparison of MHC-II dependent Ag85B presentation in THP-1 or MonoMac-6 activated macrophages using F9A6 cells.

Macrophages were activated with IFN- γ or RAVD and infected with BCG-14 (mutant BCG strain hyper-expressing Ag85B) or *M. tuberculosis* H37Rv. After 4 hr infection, the cells were washed and overlaid for 4 hrs with F9A6, a T-cell specific for Ag85B. Supernatants were collected and tested for IL-2 using sandwich ELISA. Supernatants collected from overlaying with F9A6 did not show IL-2 levels above control groups (no overlay with T-cells).

DISCUSSION

IL-2 production by antigen specific hybridoma T-cells is a well established technique used to demonstrate MHC-II presentation by antigen presenting cells (APCs)(102). We examined the ability of two humanized T-cell hybridoma cell lines, F9A6 and 5MB, to detect antigen presentation in RAVD and PMA activated THPs infected with mycobacteria. Although the hybridoma cell lines grew in culture and remained viable during co-culture with infected macrophages, IL-2 release could not be detected above the baseline level.

Initial consultation with Dr. Canaday, the donator of the F9A6 and 5MB cell lines, led us to initiate our antigen presentation studies using IFN- γ activated THPs. Since previous studies determined that there is a difference in antigen presentation between macrophages infected with virulent and avirulent mycobacteria strains(89, 103), we infected our THPs with either Mtb H37Rv (virulent) or BCG-14 (avirulent vaccine candidate). Phagosomes containing either H37Rv or BCG-14 have been shown to process and present Ag85b, a mycobacterial protein important in human T cell response to Mtb(101). Given assurances by Dr. Canaday that IFN- γ activated THPs would be the best presenters of antigen to the hybridoma cell lines, we were disappointed to discover that no IL-2 production was detected in our ELISA assays (**Figure 4A**). Variations in the IFN- γ dose, MOI infection rates and macrophage:T-cell ratio during overlay, all yielded similar negative results (data not shown).

Published work demonstrating that F9A6 could recognize antigen presentation by PMA-THPs(91) led us to our next endeavor (**Figure 4B**). We opted to focus strictly on F9A6 since Dr. Canaday communicated it was a more reliable cell line than 5MB, which on occasion gave inconsistent results. Since F9A6 recognizes peptides processed from Ag85b, we infected our macrophage with BCG-14, a mutant BCG strain that super-secretes Ag85B, with the hope of increasing antigen presentation. Our previous work in antigen presentation using mouse macrophages overlaid with mouse T-cell hybridomas demonstrated that the optimal incubation time for macrophage:T-cell co-culture was 4 hrs. This differed from the published work(91) that used an incubation overlay time of 24 hrs. Therefore, we opted to vary the overlay and infection times to increase the chance of positive results. Regrettably, IL-2 levels detection did not exceed baseline (250 pg/mL). Several repeated experiments were conducted using varying doses of BCG-14 resulting in similar negative results (data not shown).

Our final attempt at determining antigen recognition by our T-cells was to use another monocytic cell line, MonoMac-6 (kindly donated by Dr. Andrew Rice, Baylor Collge of Medicine, Houston, Texas). Similar to THP-1 cells, MonoMac-6 is a monocytic cell line that upon activation with IFN- γ , exhibits a mature macrophage phenotype(104). Once more, we were unable to detect IL-2 levels above background. Several experiments were attempted using MonoMac-6 and various conditions, all of

which presented negative results (data not shown). Also, a single experiment using human peripheral blood monocyctic cells (PBMCs) donated by Dr. Rice was conducted with similar negative results (data not shown).

Since we were unable to confirm the correlation between the increase in antigen presentation molecules (HLA-DR, CD1d, CD80 and CD86) in RAVD-THPs with an increase in T-cell recognition and IL-2 secretion, we tentatively propose that either Mtb resides in an inactive state in THPs or interferes with antigen presentation by unknown mechanisms. Additional studies are needed in this direction.

CHAPTER 4

RAVD INDUCES OXIDANTS, AUTOPHAGIC PATHWAYS AND CATELICIDIN TO DECREASE VIABILITY OF INTRACELLULAR *MYCOBACTERIUM TUBERCULOSIS*

INTRODUCTION

Macrophage Mycobactericidal Mechanisms

Although, Mtb infects approximately one-third of the human population each year only a about 10% of those infected develop active tuberculosis(1). In most infected individuals, a healthy immune response eliminates the pathogen or keeps it “walled off” in a latent state where no disease manifests(1). Therefore, it appears that macrophages, the primary target of Mtb infection, have developed several mechanisms to control or eliminate the bacteria. Since RAVD are routinely ingested by humans, we hypothesized that they could potentially trigger four mechanisms that could control Mtb infection.

Reactive Oxygen Species (ROS)

A powerful macrophage defense mechanism to combat bacterial infections is to induce a process called “oxidative burst” or “respiratory burst”(105). This process produces large quantities of reactive oxygen species (ROS) by activating phagocyte oxidase (phox), also known as nicotinamide adenine dinucleotide phosphate-oxidase (NADPH-oxidase). Phagocyte oxidase is composed of six protein subunits that assemble on phagosomes during macrophage activation. The activated phagocyte oxidase complex, which contains the p47^{phox} and p67^{phox} subunits, catalyzes the transfer of electrons from cytosolic NADPH to superoxide anions inside the phagosome(105).

The importance of ROS in controlling bacterial infections can be seen in patients with chronic granulomatous disease (CGD), a congenital disorder where a mutation occurs in any of the four phox subunit proteins, resulting in a failure to produce a proper ROS response(106). Thus, patients with CGD have a higher susceptibility to pyogenic infections, such as *Staphylococcus aureas*, *Aspergillus* species, and *Nocardia* species(106). CGD is also implicated in higher susceptibility to TB infection, where some estimates calculate CGD patients to be 170 times more likely to contract the disease than the general immunocompetent population(107, 108).

Reactive Nitrogen Species (RNS)

A potent antimycobacterial mechanism, in macrophages, is the induction of a family of isoenzymes called nitric oxide synthases (NOSs). During infection, IFN- γ signaling recruits inducible NOS (iNOS) to Mtb-containing phagosomes. iNOS oxidizes guanidino nitrogen of L-arginine to produce nitric oxide (NO) and citrulline. Then, NO rapidly reacts with molecular oxygen and water to eventually generate reactive nitrogen species (RNS)(109). In addition, highly reactive peroxynitrite (ONOO⁻) is formed by the combination of NO and superoxide produced by phagocyte oxidase leading

to bacterial death(110). NO itself is a very potent antimycobacterial agent that kills 99% of cultured Mtb at low concentrations of <100 ppm (111).

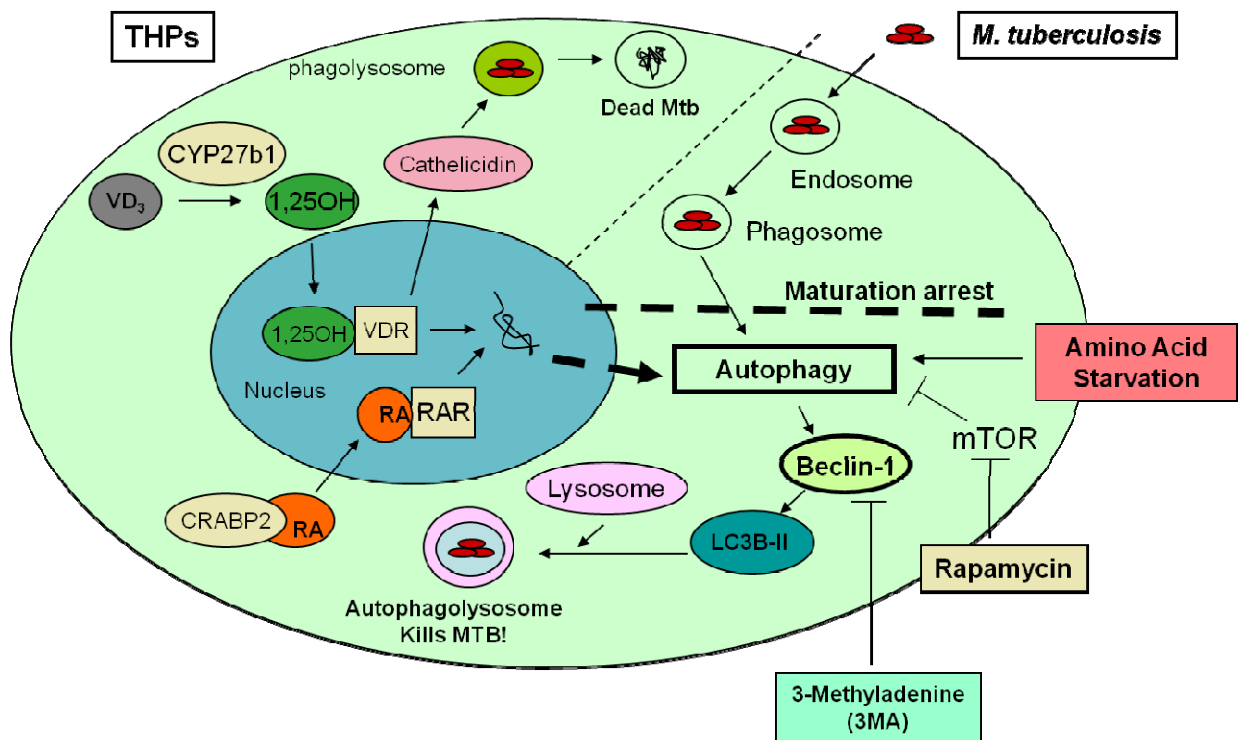
The role of RNS in human tuberculosis is controversial. In murine TB studies, iNOS activation and NO production has been shown to be a major pathway in controlling the disease(112). However, in early human TB studies, RNS was difficult to detect leading most researchers to discount its importance in disease control(109). Initial human studies of RNS relied on the use of Griess reagent, a chemical used to determine the presence of nitrites in samples. This posed a problem since NO production leads to both nitrate (NO_3^-) and nitrite (NO_2^-) metabolites with levels below the sensitivity range of Griess reagent(113). Current studies that utilize more sensitive probes, such as diaminonaphthalene (DAN), and NOS inhibitors, such as L-NG-monomethylarginine (L-NMMA), have demonstrated the ability of human macrophages to produce NO in response to Mtb infections (112, 114).

Autophagy

A newly discovered pathway to control TB invasion of the host cell is through autophagy(36). Autophagy was initially discovered as a pathway for the cell to catabolize damaged cytosolic components as well as a means to produce metabolites and energy under starvation conditions(115). In TB infections, autophagy functions to enhance host resistance by circumventing MTB-induced phagosome maturation arrest(36, 116). During autophagy, immature phagosomes containing Mtb, are tagged with a succession of autophagy related genes (Atg) proteins, starting with Atg6 (Beclin-1). The attachment of beclin-1 to the membrane initiates the recruitment of other Atg proteins that complex onto the phagosome to form the distinctive double membrane feature of autophagy, the autophagosome. Ultimately, the autophagosome complex of proteins initiates the cleavage of cytosolic microtubule-associated protein 1 light chain 3 (LC3-I; also known as Atg8) into its active form LC3-II. LC3-II integrates into the autophagosomal membrane allowing fusion with lysosomes to form the antimycobacterial autophagolysosome(115).

Interestingly, Vitamin D has been shown to play a role in autophagic processes. A recent study of 1,25-dihydroxyvitamin D3 (1,25(OH)₂D₃) and an analog, EB1089, has revealed the induction of autophagy to promote cell death in human breast adenocarcinoma cell line(117). Another significant study demonstrated that binding of TLR-1/2 and its co-receptor, CD14, to Mtb lipoprotein LpqH, activated Vitamin D-dependent antimycobacterial mechanisms to initiate autophagic processes and cathelicidin recruitment to the MTB-phagosomes(118).

Diagram 2: Vitamin A and D induce two anti-mycobacterial pathways, cathelicidin and autophagy to control intracellular *Mycobacterium tuberculosis* growth.



Cathelicidin

Although there are a number of studies into the antimicrobial mechanisms controlling TB infection, there is scant information on anti-microbial peptides. One such important peptide, cathelicidin (hCAP-18/LL-37), has been shown to be regulated by either Toll-like receptor (TLR-1/2(119), TLR-4(119) and TLR-9(119)) activation, $1,25(\text{OH})_2\text{D}_3$ (120) (a metabolite of Vitamin D₃) or retinoic acid(121, 122), and contribute to the control of tuberculosis. Cathelicidin is a family of lysosomal peptides that have direct mycobactericidal properties and cause lysis upon direct contact with bacterial surfaces(119). In addition, cathelicidin has recently been shown to be an important immunoregulator of autophagy. siRNA knock-down studies of cathelicidin demonstrated that it was required to induce autophagy in $1,25(\text{OH})_2\text{D}_3$ treated cells by activating transcription of the autophagy-related genes Beclin-1 and Atg5(123).

RESULTS

PMA and RAVD have differential effects on the survival of *Mycobacterium tuberculosis* (Mtb) in THPs

One of the most important functions of mature and fully activated macrophages is to control and eliminate bacterial infections. Activated THPs were infected with Mtb H37Rv (MOI of 10) and evaluated for control of intracellular bacterial growth. Subsequent to increased uptake (**Figure 3**), RAVD-THPs controlled the infection with Mtb better than PMA-THPs (**Figure 5**). Mtb grew 10-fold in 10 days within PMA-THP macrophages while RAVD decreased Mtb numbers by one log₁₀ in 10 days of infection. Thus, RAVD exerted anti-tuberculosis effects.

RAVD induce enhanced levels of reactive oxygen species (ROS) and reactive nitrogen species (RNS) response in THPs that leads to the inhibition of intracellular Mtb.

In order to determine the basis for the anti-tuberculosis effects of RAVD, ROS and iNOS production was evaluated during Mtb infection of THPs. When Mtb is internalized by macrophages, it is sequestered within a phagosome that triggers the acquisition of the multimeric components of the NADPH oxidase (phagocyte oxidase; ^{phox}). In our earlier study(124), we demonstrated that NADPH oxidase colocalizes with Mtb phagosomes in macrophages. The colocalization, evidence of targeting of the ROS complex to Mtb phagosomes, is detectable using antibody stain against p47/67^{phox} components (124). Accordingly, RAVD or PMA treated THPs were infected with Mtb *gfp*H37Rv and immunostained and scored microscopically for colocalization (124). PMA-THPs showed a reduced colocalization of the NADPH oxidase proteins with Mtb phagosomes while RAVD-THPs showed an enhanced colocalization (**Figure 6A-B**).

These microscopic studies correlated with intracellular levels of ROS in PMA and RAVD activated THPs, which was determined using a ROS specific probe, 2',7'-dichlorodihydrofluorescein diacetate (H₂DCFDA). Non-fluorescent H₂DCFDA is cleaved by intracellular esterases to yield the dichlorofluorescein (DCF) that is then oxidized by ROS to yield a fluorescent hydrophobic product trapped within the cell. **Figure 6C** shows the flow cytometric analysis of fluorescent ROS positive cells after activation and before infection as analyzed by flow cytometry. PMA-THPs showed an increased shift due to ROS induced fluorescence on day 1 that returned to background levels by day 3. On the other hand, RAVD-THPs showed a shift on day 1 that was sustained until day 3 when the cells were infected with Mtb. The specificity of ROS mediated conversion of DCF was confirmed by using the ROS inhibitor, diphenyleneiodonium (DPI) (data not shown). Intracellular ROS was also quantitated following activation and Mtb infection using an Ascent-Fluorocan fluorometer, as Mtb infected THPs

could not be loaded to the flow cytometer for safety reasons. RAVD-THPs with internalized Mtb showed increasing ROS levels over 5 days while PMA-THPs showed a spike that declined by day 5 (**Figure 6D**). Together, these studies indicate that both before and after infection, RAVD-THPs had stronger ROS response than PMA-THPs.

Finally, ROS specific effects were correlated to bactericidal killing. THPs were activated in the presence or absence of 10 mM each of diphenyleneiodonium chloride (DPI), an inhibitor of ROS response or 10 μ M N-methyl-monoarginine (NMMA), an inhibitor of nitric oxide response. After inhibition, cell lysates of infected RAVD-THPs were plated for viable colony counts (CFU) at the end of 24 and 72 hrs infection. At both time points, inhibition of ROS response with DPI increased viability of intracellular Mtb compared to inhibition of NO response (**Figure 6E**).

RAVD induced autophagy in THPs leads to inhibition of Mtb growth.

A recent study demonstrated that Vitamin D₃ can induce autophagosome formation to kill internalized Mtb(123). Since autophagy could be another antimicrobial pathway that can control Mtb infection, we investigated the ability of RAVD to induce autophagy. We addressed this issue in three experiments.

First, RAVD or PMA activated THPs were infected with Mtb H37Rv and their phagosomes were purified using a sucrose gradient. Western blot analysis demonstrated that Mtb phagosomes from RAVD-THPs recruited more beclin-1, an initiator molecule of autophagy, than those from PMA-THPs (**Figure 7A**).

Second, we blocked autophagy in THPs to determine effects of siRNA knock-down of beclin-1 expression. RAVD-THPs were treated or untreated with siRNA vs. beclin-1, to abolish autophagy and then were infected with Mtb. **Figure 7B** shows that knock-down of autophagy led to an increase in intracellular survival of Mtb and thus RAVD induced killing of Mtb was inhibited by siRNA vs. beclin-1. Furthermore, when Mtb phagosomes of such macrophages were stained using an autophagosome marker, phagosomes colocalized with monodansylcadaverine (MDC) in RAVD-THPs while MDC uptake was absent in siRNA knockdown THPs (**Figure 7C**). Indeed, the THPs here needed to be stained with a nuclear DAPI stain to visualize macrophages. These data suggested that the bactericidal activity of RAVD was also attributable in part to the induction of autophagy.

Finally, we performed an additional analysis of purified phagosomes using Western blot for a panel of autophagic molecules and this panel showed differential recruitment of proteins to Mtb-containing phagosomes (**Figure 7D**). Mtb phagosomes of RAVD-THPs recruited increased amounts of autophagy proteins (Atg16L, Atg4b, Atg7, Beclin-1 and LC3) to its phagosomes in comparison to those from PMA-THPs. Positive control groups where serum starvation (SS) was used to induce autophagy

showed similar or lower levels of proteins in comparison with RAVD-THPs. The addition of 3-methyladenine (3-MA) to THP cultures was intended to inhibit autophagy but showed higher levels of proteins after treatment than before (naïve). It is however known that 3-MA besides inhibiting autophagy also has other non-specific effects on endosome traffic.

RAVD increases levels of cathelicidin in THPs infected with Mtb.

Cathelicidin is a potent bactericidal peptide that has been shown to be important in controlling Mtb infection. We were interested to know if the combined effects of RAVD could induce cathelicidin expression. Western blot analysis of Mtb H37Rv infected PMA-THPs and RAVD-THPs demonstrate that high levels of cathelicidin is expressed in the latter versus former cells (**Figure 8**).

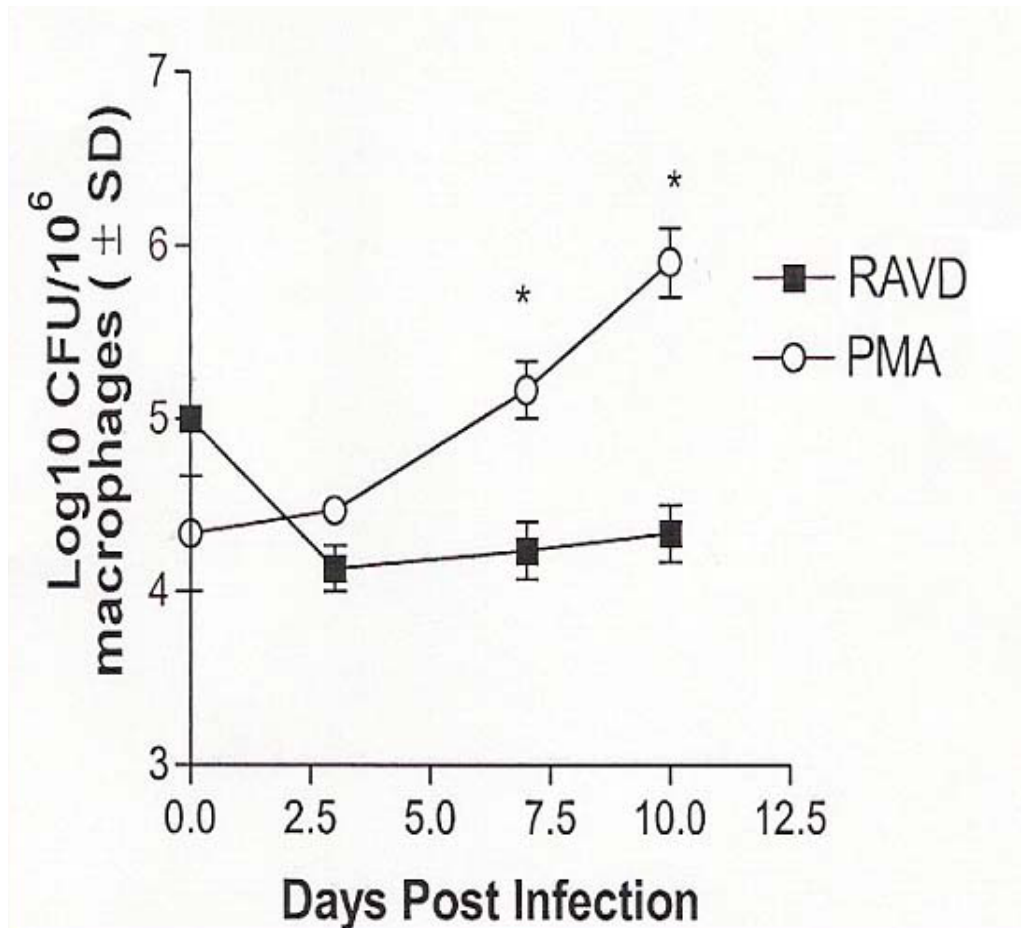


Figure 5. PMA and RAVD have differential effects on the survival of *Mycobacterium tuberculosis* (Mtb) within THP-1 macrophages.

THPs were activated with either 10 ng/mL of PMA or 1 μ M each of RA and VD for 72 hrs and infected with Mtb for 24 hrs. The cells were washed three times to remove non-phagocytosed bacteria, incubated for 10 days with media, aspirated, pelleted, and lysed in 0.05% SDS within the same well thus accounting for adherent as well as some floating macrophages, and plated for colony (CFU) counts. RAVD treatment inhibited bacterial replication while Mtb showed an increase in colony counts in PMA treated macrophages (* $p < 0.009$, t test, mean \pm SD of 3 experiments).

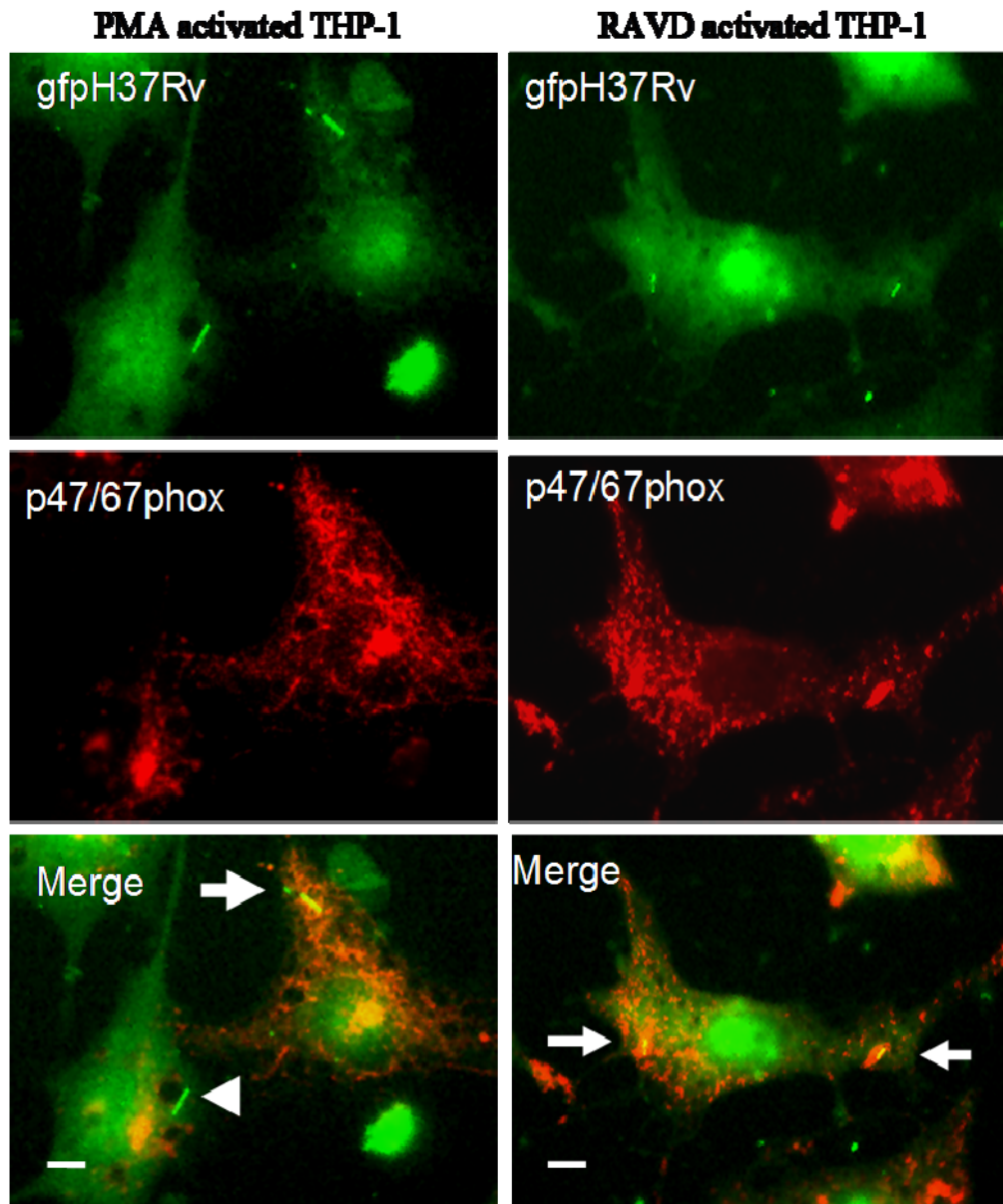


Figure 6A. Enhanced co-localization of *gfpH37Rv* with components of the phagocyte (NADPH) oxidase in RAVD activated THP-1 macrophages.

THPs were activated with either PMA or RAVD and phagocytosed with *gfp*-expressing strain of Mtb (*gfpH37Rv*) for 4 hrs followed by fixation and staining with primary Texas Red fluorescent antibodies against p47/p67^{phox} components of the phagocyte (NADPH) oxidase followed by Texas-Red conjugate. Arrow in bottom panels shows a co-localizing *gfpH37Rv*, while the arrowhead shows a non-colocalizing *gfpH37Rv*.

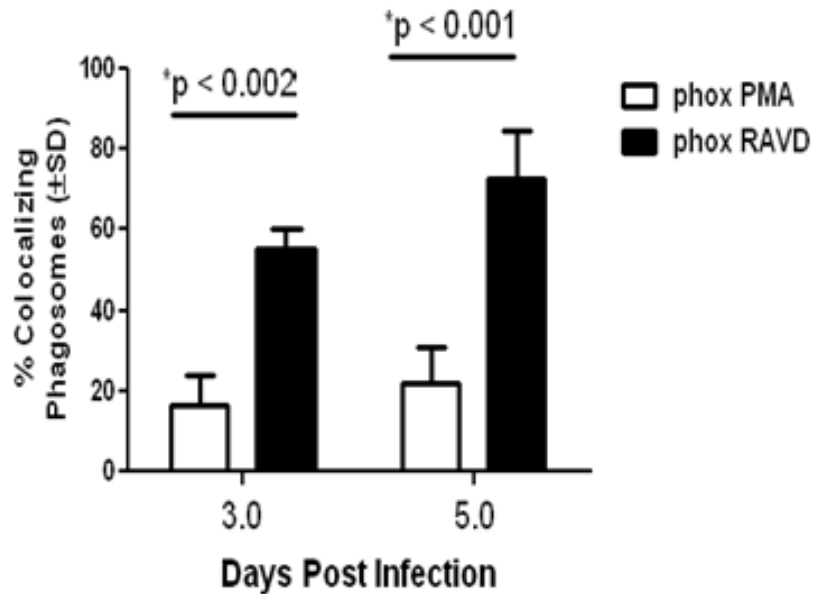


Figure 6B. Analysis of co-localization of *gfpH37Rv* with components of the phagocyte (NADPH) oxidase in PMA or RAVD activated THP-1 macrophages.

Percentage of positive *gfpH37Rv* phagosomes were scored for colocalization with p47/p67^{phox} in activated and infected THPs. RAVD-THPs recruited more phox proteins to the Mtb-containing phagosomes than PMA-THPs. Bacteria of over 100 macrophages in each chamber of triplicate well slides were counted and averaged from three separate experiments. (p values shown above bars for groups compared, t test; mean±SD of 3 experiments).

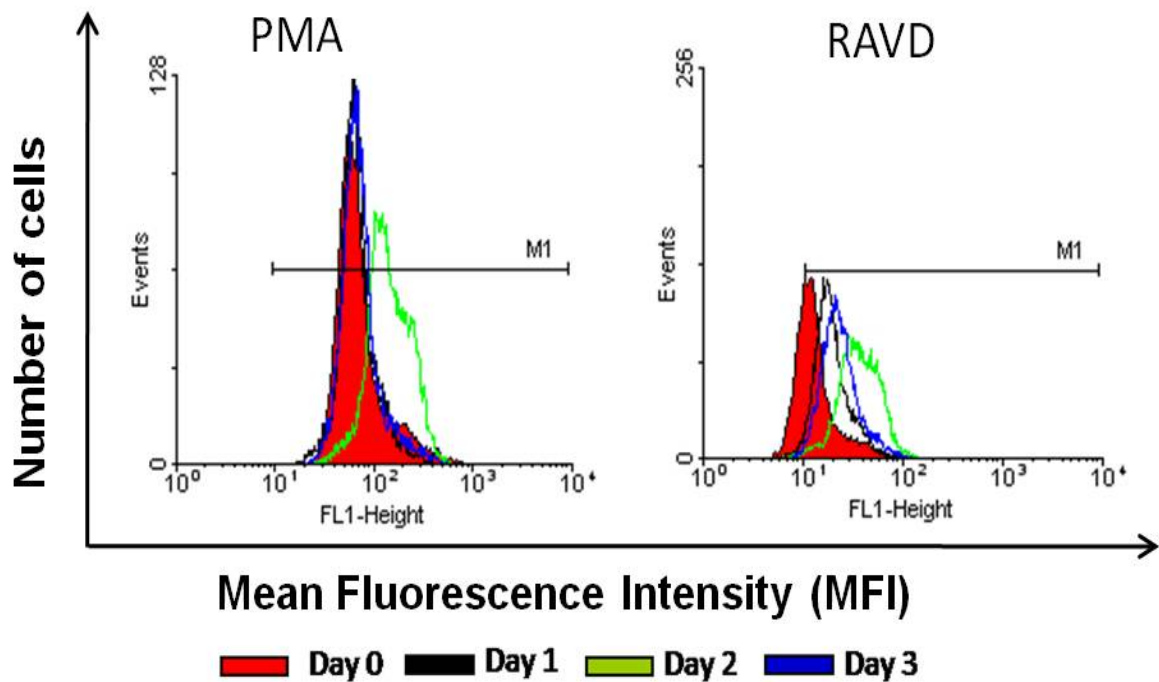


Figure 6C. RAVD induce enhanced reactive oxygen species (ROS) response in THP-1 macrophages before infection with *M. tuberculosis* H37Rv.

THPs activated with PMA or RAVD were labeled with 2',7'-dichlorodihydrofluorescein diacetate (H₂DCFDA), a probe for intracellular ROS and quantitated using flow cytometry on day 1 (black), day 2 (green) and day 3 (blue). RAVD-THPs maintained ROS production over 3 days, whereas ROS response declined in PMA-THPs after day 2 (one of three similar experiments shown). Red fill shows basal levels of ROS production in naïve (unactivated) THPs.

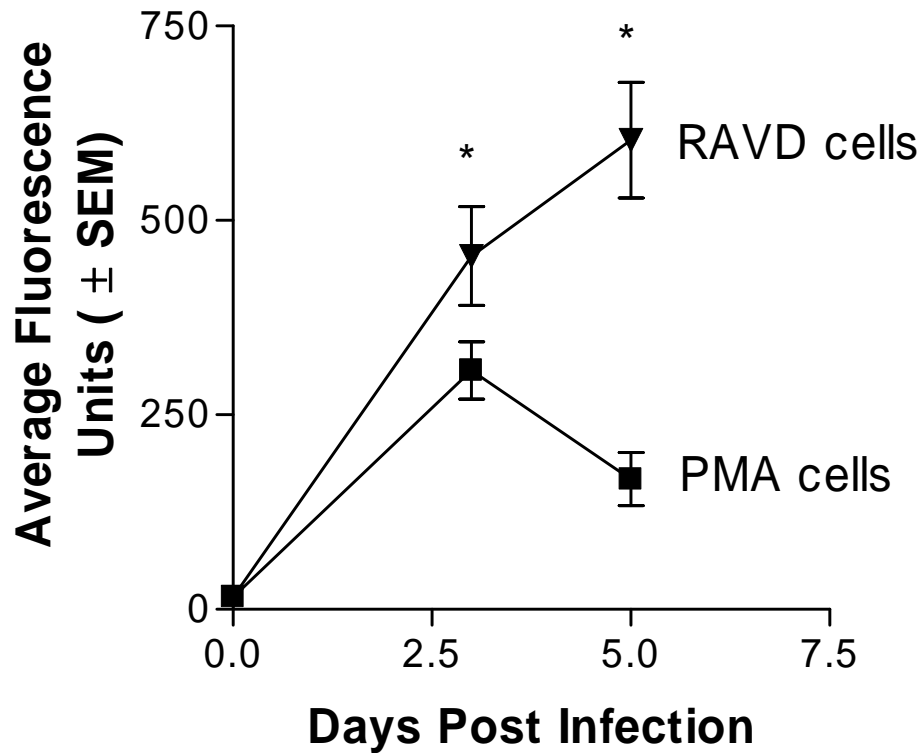


Figure 6D. RAVD continue to induce enhanced reactive oxygen species (ROS) response in THP-1 macrophages after infection with H37Rv.

THPs activated with PMA or RAVD were labeled with H₂DCFDA, a probe for intracellular ROS, and using an Ascent-Fluorocan, ROS production was quantitated and expressed as in average fluorescence units (AFU). Data show that ROS increased in RAVD-THPs over three days of activation but decreased by day 3 in PMA-THPs (t test; mean±SEM of 3 experiments).

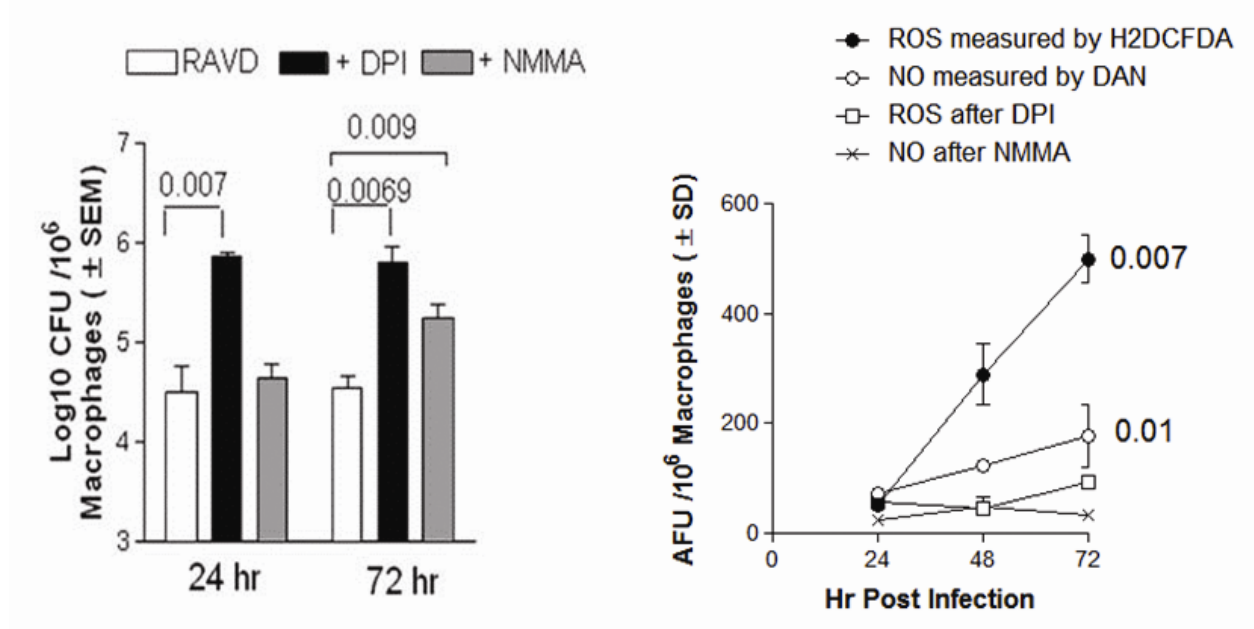


Figure 6E. Inhibition of ROS and RNS leads to increased intracellular survival of *M. tuberculosis* in RAVD-THPs.

ROS and RNS inhibitors (left panel): THPs were activated with RAVD, infected with Mtb and then incubated in the presence or absence of 10 mM of diphenyleneiodonium chloride (DPI), an inhibitor of ROS response, or 10 μ M of N -monomethyl-L-arginine (L-NMMA), an inhibitor of nitric oxide response. Macrophage lysates were then plated for CFU counts at the end of 24 and 72 hrs of infection. Inhibition of ROS response with DPI increased the viability of intracellular Mtb compared with inhibition of NO response (p values shown above bars for groups compared, *t* test; 3 experiments). *ROS and RNS levels after inhibition (right panel):* Supernatants of macrophage cultures of macrophage cultures were tested with H₂DCFDA or diaminonaphthalene (DAN) respectively for ROS or NO induced average fluorescence units (AFU) using an Ascent fluoroscan.

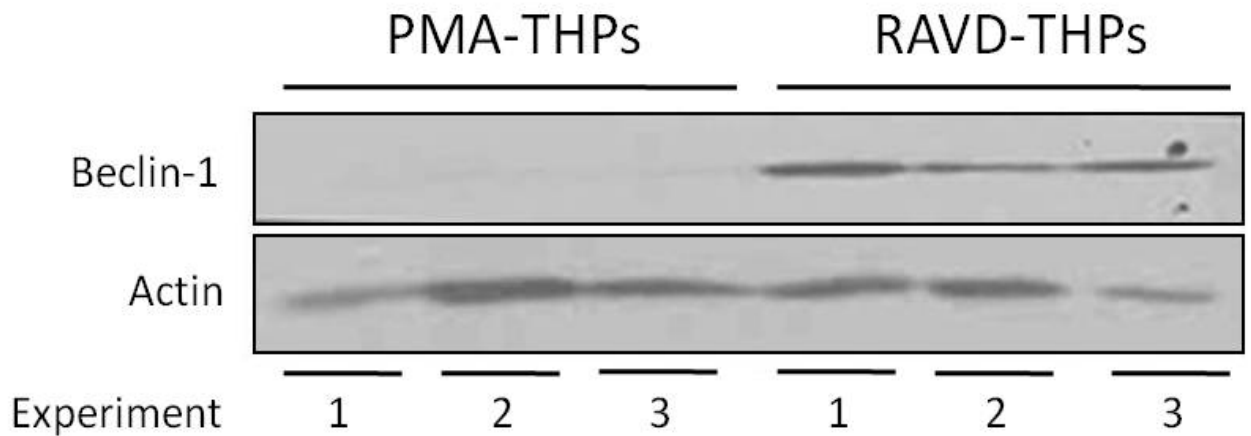


Figure 7A. *M. tuberculosis* phagosomes purified from RAVD-THPs show greater amounts of beclin-1 during Western blot analysis.

PMA and RAVD activated THPs were infected for 4 hrs with Mtb H37Rv (MOI of 10) and the phagosomes purified using sucrose gradients. Isolated phagosomes were analyzed by Western blot using antibodies specific to beclin-1. Phagosomes of RAVD-THPs have an increased level of beclin-1 than those from PMA-THPs. One of three independent experiments with similar results is shown.

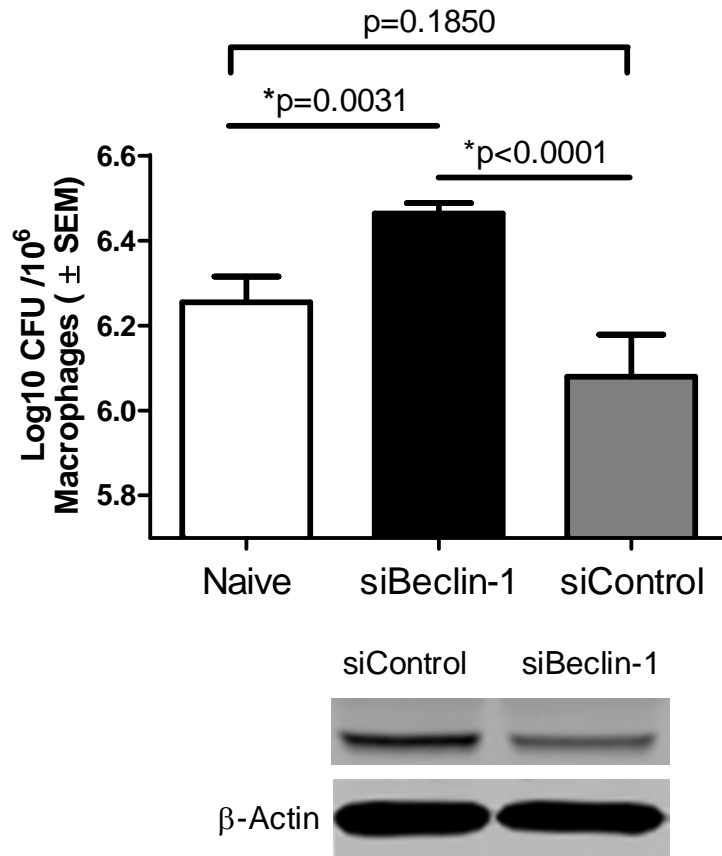


Figure 7B. RAVD induces autophagy in THP-1 macrophages that leads to inhibition of intracellular *M. tuberculosis*.

RAVD activated THPs were treated or untreated with siRNA vs. beclin-1, to abolish autophagy, and were infected with Mtb (MOI of 10). Lysates were then plated for CFU counts at the end of 24 hrs infection. Inhibition of autophagy with siRNA beclin-1 increased the viability of intracellular Mtb compared to siRNA Control (p values shown above bars for groups compared, t test; ±SEM of 3 experiments).

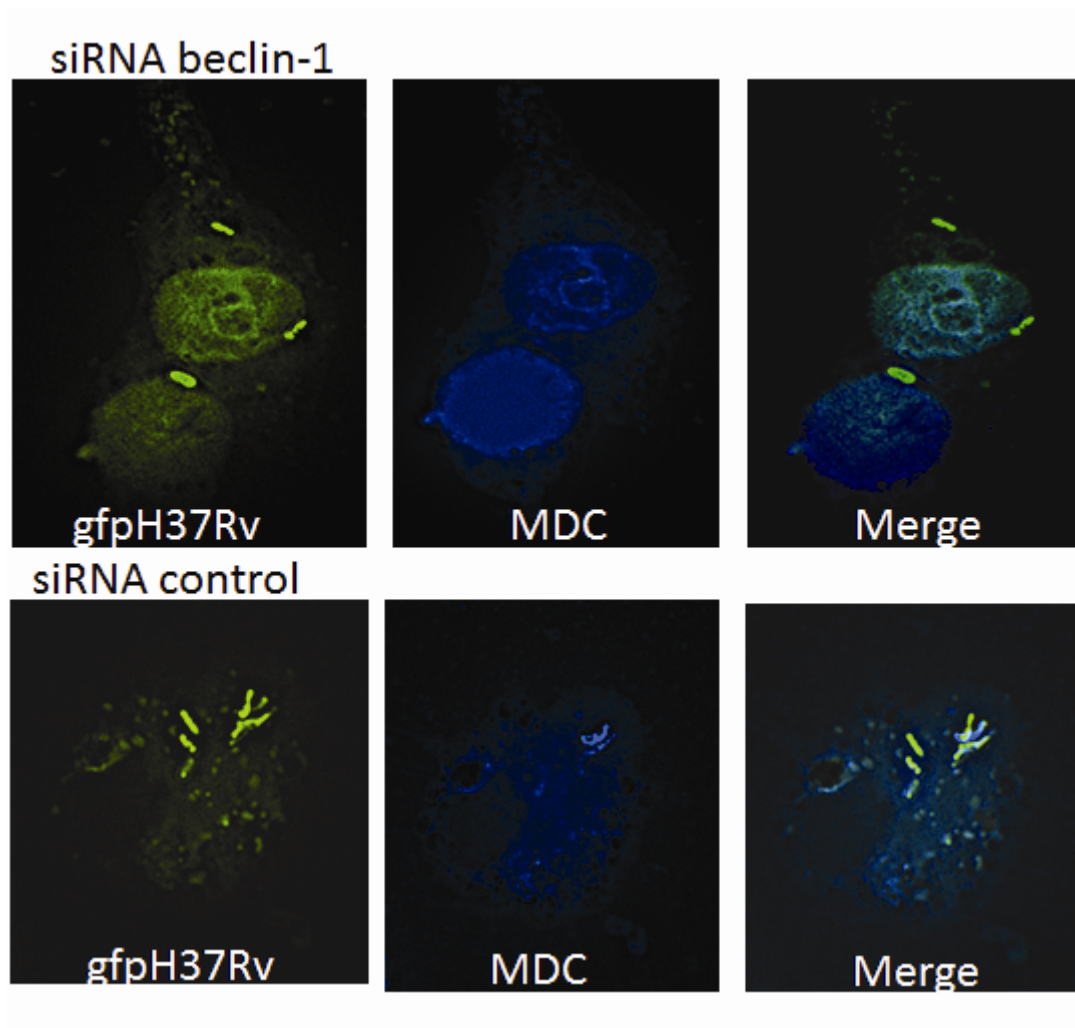


Figure 7C. siRNA inhibition of beclin-1 leads to reduced autophagosome formation in *gfpMtb* infected RAVD-THPs.

RAVD activated THPs were treated or untreated with siRNA vs. beclin-1 to abolish autophagy, and were infected with *Mtb* *gfpH37Rv* (MOI of 10). Monodansyl cadaverine (MDC) was used to label autophagosomes in infected RAVD-THPs. *gfpH37Rv* colocalizes with MDC in RAVD treated macrophages. MDC uptake was poor in siRNA vs.beclin-1 macrophages so that the nuclei were labeled with DAPI to visualize macrophages and *gfpH37Rv*.

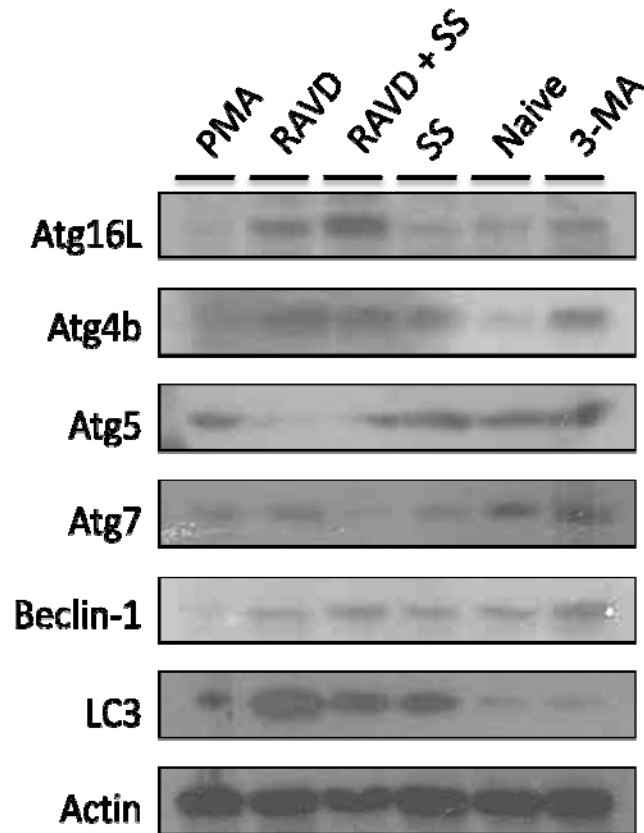


Figure 7D. *M. tuberculosis* phagosomes of RAVD-THPs recruit more autophagy proteins during Western Blot analysis.

THPs were left untreated (naïve), activated with PMA or RAVD, serum starved (SS) to induce autophagy or treated with 3-methyladenine (3-MA) to inhibit autophagy. Macrophages were infected for 4 hrs with Mtb H37Rv (MOI of 10) and the phagosomes purified using sucrose gradients. Isolated phagosomes were analyzed by Western blot using antibodies specific to various autophagy related proteins. RAVD-THP derived phagosomes had an increased presence of autophagic proteins than those from PMA-THPs. One of three independent experiments with similar results is shown above.

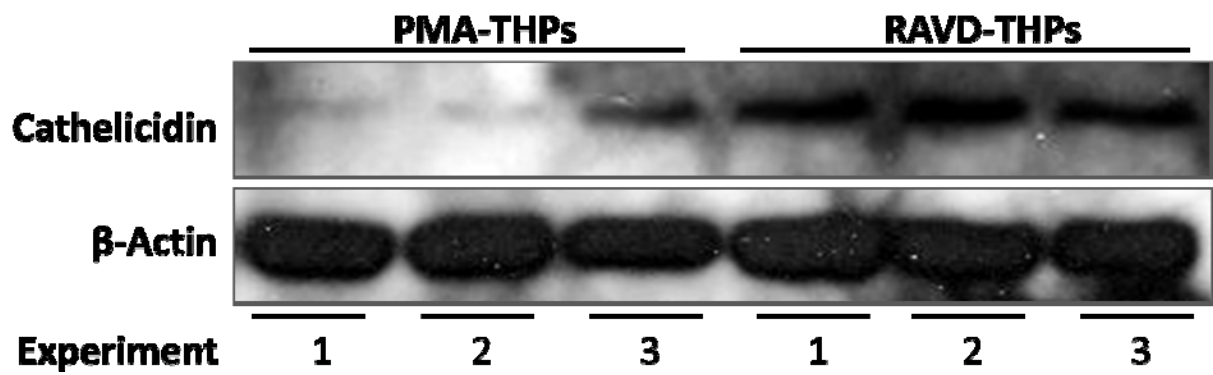


Figure 8. RAVD induces cathelicidin expression in THPs infected with *M. tuberculosis* H37Rv. PMA and RAVD activated THPs were infected for 4 hrs with Mtb H37Rv (MOI of 10) and the cells cultured for 24 hrs. Whole cell lysates were analyzed by Western blot using antibodies specific to cathelicidin. RAVD-THP lysates showed an increased presence of cathelicidin than PMA-THPs. One of three independent experiments with similar results is shown above.

DISCUSSION

Monocyte to macrophage maturation leads to increased receptor expression, phagocytosis and enhanced mechanisms of bactericidal activity. We have previously demonstrated that RAVD-THPs had increased receptor expression and phagocytic ability than PMA-THPs. In this study, we show that even though RAVD-THPs are more phagocytic and carry a heavier internal Mtb burden (**Figure 3**), they are better able to control bacterial growth than PMA-THPs (**Figure 5**). This observation led us to investigate the antimicrobial activities that RAVD could generate in terms of the induction of reactive oxygen species (ROS), reactive nitrogen species (RNS), cathelicidin and autophagy.

Our initial studies indicated that inhibition of iNOS with NMMA enhanced the survival of intracellular Mtb in RAVD-THPs although, curiously, we did not find significant levels of nitrate, an indicator of NO synthesis in the medium. It is possible that NO is induced but at such low levels that are not detectable by the Greiss reagent. RA(125) and VD₃(126) has been reported to induce iNOS in murine and human macrophages and it remains to be determined whether their combination induces sustained iNOS in THPs. Given that inhibition of iNOS led to increased bacterial survival only after 72 hrs, it is tempting to speculate that RNS response may be time dependent and could contribute more in long term control of bacterial infection than acute disease.

The bactericidal function of RAVD-THPs was partly due to the induction of ROS since the ROS inhibitor, DPI, significantly enhanced Mtb survival (**Figure 6E**). In a recent study, phagocyte (NADPH) oxidase was shown to be critical for 1,25(OH)₂D₃-mediated mycobactericidal response by activating cathelicidin expression via TLR-2 signaling of ROS responses(127). Our model confirms this finding along with several other separate studies that demonstrate RA and VD separately induce ROS response(122, 128) and cathelicidin(121, 122). However, unlike previous studies, our model demonstrates a strong induction of ROS even without internalized pathogen, where TLR signaling does not occur. It would be interesting to determine if the combination of RA and VD led to a synergistic interaction greater than if the vitamins are given separately.

Recently, a study showed that Vitamin D₃ alone can induce autophagosome formation to kill internalized Mtb(123). Knock-down of beclin-1, a key protein involved in targeting vesicles for autophagy, demonstrated that RAVD can also activate autophagy to keep intracellular Mtb growth in check. PMA-THPs consistently showed little to no beclin-1 present on their Mtb-containing phagosomes. However, after 24hrs of Mtb infection, Atg5 was found on PMA-THPs while not being present on RAVD-THPs. This result is interesting since it suggests that RAVD-THPs may be undergoing an alternative autophagy pathway that is Atg5-independent(129) or that PMA-THPs are inducing autophagy but at a much slower rate than RAVD-THPs. Since the role of cathelicidin in

inducing alternative autophagy is still unstudied, our model may be a good method to investigating this pathway. That RAVD induces four major antimycobacterial mechanisms suggests that they act as basic regulators of innate host defense.

CHAPTER 5

***MYCOBACTERIUM TUBERCULOSIS* INFECTION FOLLOWED BY LONG TERM ACTIVATION WITH RAVD LEADS TO MULTINUCLEATED GIANT CELL (MNGC) FORMATION IN THP-1 MACROPHAGES**

INTRODUCTION

Granulomas and Tuberculosis

A signature feature of tuberculosis is the granuloma formation histologically evident in the infected lungs and other organs. The major function of granulomas in tuberculosis is the containment of Mtb to a localized area that prevents the spread of disease to other healthy regions of tissue. The structure, function and evolution of granulomas have been studied using various animal models(130-132), within lungs of tuberculous humans(133-135), explant(3, 136-138) and cell cultures *in vitro*(139). These studies have identified that monocytes infected with Mtb differentiate into macrophages, epithelioid cells and several types of multinucleate giant cells (MNGCs). Many of these studies emphasize the critical role of MNGCs in bacterial containment and clearance within the granuloma.

Multi-nucleated Giant Cells and Tuberculosis

Although the presence of MNGCs was described early in TB research(3), their precise formation and their contribution in TB pathogenesis is only recently being elucidated. Cultured monocytes and macrophages have been induced to differentiate into MNGCs by exposure to various stimulants, such as cytokines(71, 140-143), lectins(144, 145), monoclonal antibodies(146-148) and conditioned media(149-152). However, Mtb is a slow growing organism with a doubling time of about 18 hours and the interaction of Mtb and macrophages is a chronic process *in vivo*, while, the available models are limited by their short lived macrophages.

In this study, we discovered that human THP-1 cells treated with physiologically compatible vitamins like RA and VD and infected with live Mtb induce a differentiation process that result in the generation of MNGCs. We have studied these MNGCs for their phenotypic properties and to determine their possible functionality during tuberculosis.

RESULTS

Activation of THP-1 macrophages with RAVD leads macrophage to differentiate into giant cells

A striking change observed during *in vivo* tuberculosis is the morphological transformation of macrophages that yield various morphotypes in guinea pigs, rats, rabbits and humans (153-155). They include giant cells, spindle cells, fibroblast like cells and epithelioid cells. This suggested that macrophage activation may lead to differentiation and giant cells. However, we noted that, PMA-THPs with phagocytosed Mtb progressively led to a loss of viability of macrophages after seven days due to uncontrolled growth of mycobacteria (**Figure 9A**). On the other hand, RAVD-THPs were able to control Mtb infection and prevent loss of viability in macrophages. In our studies, viability was constantly monitored using Alamar blue vital dye. Furthermore, RAVD induced cell fusion to form giant cells. **Figure 9B** illustrates the growth curve of intracellular Mtb recovered from RAVD treated, adherent macrophages between days 1-10 and then from adherent multinucleate giant cells (MNGCs) between days 10-35. **Figure 9C** illustrates the nuclear morphology of DAPI stained MNGCs that contain *gfpH37Rv* observed over a period of 30 days *in vitro* culture. Finally, when MNGCs fuse with additional macrophages, the zone of fusion is delineated by characteristic ‘inter-digitating septae’ observable only through electron-microscopy (EM). For example, **Figure 9D** illustrates an EM image of MNGC fusing with individual THP.

We also sought to determine the mechanism of cell fusion. It has been reported that ‘a disintegrin and metalloproteinase’ (ADAM) family of proteins mediate cell fusion that occurs during osteoclast formation as when mycobacteria induce cell fusion (156). We therefore stained RAVD-THPs for several ADAMs and found that RAVD induced only a transient staining for ADAM-9 between THPs undergoing cell fusion early after infection (**Figure 10**).

Long-term activation of THP-1 macrophages with RAVD leads to long living MNGCs that contain persistent *M. tuberculosis*

Since RAVD-THPs remained viable even after several weeks and such macrophages contained *gfpH37Rv*, although in low numbers (**Figure 9C**), we sought to determine if long term activation with RAVD led to a long-living ‘macrophage reservoir’ that contained persistent Mtb. Since PMA-THPs die by 7-10 days in Mtb infection and other *in vitro* macrophage models do not permit long term cultures of Mtb, it appears that there are no *in vitro* cell culture models to study long term persistence of Mtb. Most reports of macrophages in culture show loss of viable cultures by day 28 or less. We therefore optimized a protocol of activation of THPs that included repeated pulsing of RAVD to MNGCs through a supply of freshly activated THPs to expand adherent Mtb infected MNGCs *in vitro*. We hypothesized that

adherent, pre-formed MNGCs would fuse with incoming, freshly activated THPs leading to larger MNGCs, which contained non-replicating Mtb and survived longer. **Figure 11A** shows adherent, well differentiated MNGC that have *gfpH37Rv* and overlaid with single THPs that are strongly stained with carboxyfluorescein diacetate (CFSE). The MNGCs were found to fuse with freshly added THPs. Such fused MNGCs with intact *gfpH37Rv* could be maintained in culture for as long as 60 days (phase contrast image of day 60 MNGC, **Figure 11A**). Our cultures remain the longest period for which Mtb infected macrophages have been maintained viable in culture to date (**Table 2**).

In order for MNGCs to survive and differentiate, an optimal growth environment is necessary where cytokine signalling may be required, both for self-activation and to recruit mononuclear cells *in vivo*. Furthermore, it is well established that cytokine treatment of human peripheral blood derived monocytes or rat macrophages can lead to the formation of short lived MNGCs(157, 158). To determine whether cytokines could regulate the survival of MNGCs in culture, THPs were activated with either IL-4 or GM-CSF or their combination followed by infection with Mtb. The key issue we wished to determine was whether cytokines such as IL-4 and GM-CSF were enough to create MNGCs or was RAVD required for long living MNGCs. **Figure 11A** (bar graph) illustrates the survival of MNGCs after cytokine alone or RAVD activation. IL-4 and GM-CSF tested alone or in combination did result in MNGCs, although they did not prevent the growth of Mtb and as a consequence, Mtb ultimately destroyed the MNGCs between days 12-14. Thus, only RAVD treatment was found to induce long lasting MNGCs and addition of either IL-4 or GM-CSF was not beneficial.

While cytokines were not required for MNGC formation using RAVD-THPs followed by Mtb infection, we determined that cytokine and chemokine secretion occurred from MNGCs. Interestingly, after an initial burst of cytokines (TNF- α , IL-6 and IL-10), RAVD-THPs showed a decline in the level of cytokines after Day 21 but switched to higher levels of chemokine secretion. **Figure 11B** illustrates that the altered secretion of cytokine-chemokines over 30 days of *in vitro* culture of MNGCs.

Table 3. Replicate experiments in which *M.tuberculosis* infected, PMA or RAVD treated MNGCs were maintained in culture

Experiments	Duration for which MNGCs were maintained in vitro	Studies performed
1-5	45 days	Microscopy, CFU counts and cytokine-chemokine analysis
6-10	47 days	CFU counts only
11-15	60 days	Microscopy, CFU counts and cytokine-chemokine analysis

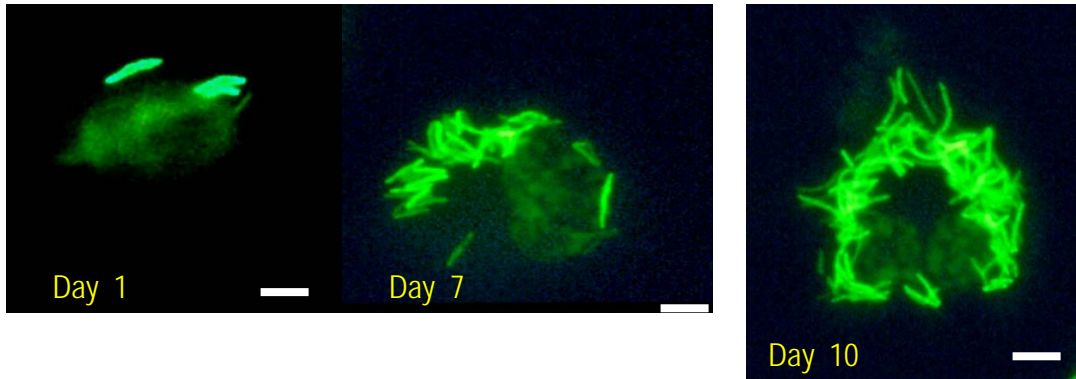


Figure 9A. PMA-THPS are unable to control infection with *M. tuberculosis* H37Rv.

THPs activated with PMA were infected for 4 hrs with *gfp*H37Rv (MOI of 5), washed 3X then incubated for 10 days. By Day 7, PMA-THPs showed robust intracellular growth of Mtb and by Day 10, most of the macrophages died of uncontrolled bacterial growth. Viability was measured by using both trypan blue as well semi quantitative conversion of alamar blue vital dye in culture (data not shown).

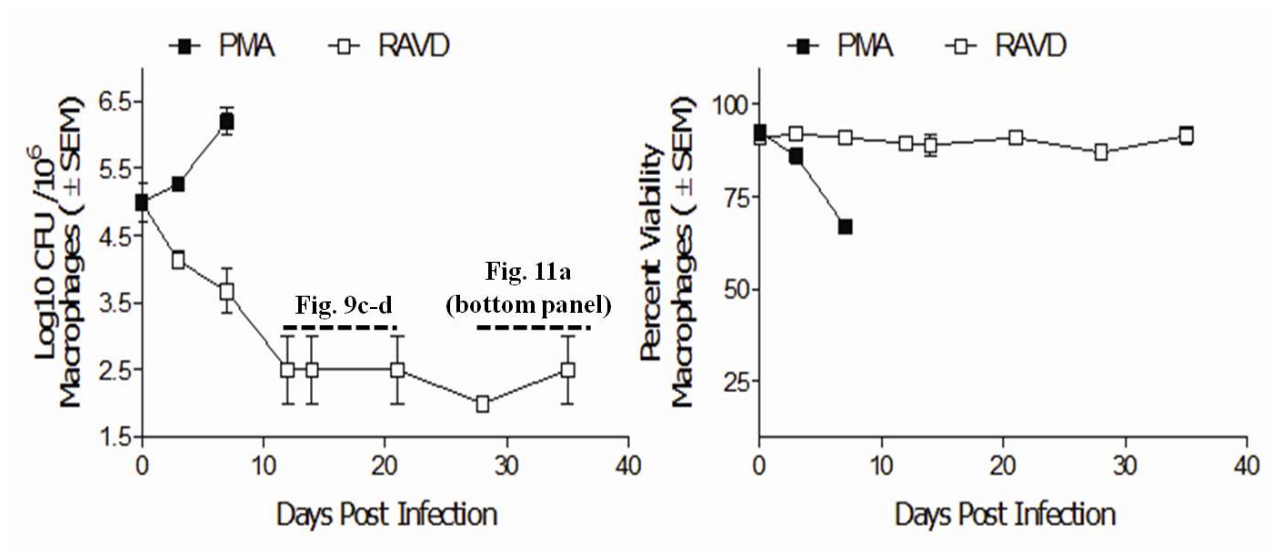


Figure 9B. Unlike PMA-THPs, RAVD-THPS are able to control short and long-term infection with *M. tuberculosis* H37Rv.

THPs were activated with either PMA (■) or RAVD (□), infected for 4 hrs (MOI of 1), washed three times to remove non-phagocytosed bacteria, incubated, then were lysed at intervals and plated for colony (CFU) counts (left panel) or treated with Alamar blue (right panel) to determine cell viability. Cell viability was measured in supernatants of replicate cultures containing alamar blue that was quantitated using emission at 590 nm in a fluorometer and expressed as AFUs (100 AFU=100% viability; 10⁶ THPs well; dye conversion in 4 hrs). Every week, from day 10, cultures were spiked with fresh, uninfected RAVD-THPs that eventually fused to the monolayer. By Day 10, most PMA-THPs died of uncontrolled bacterial growth and CFU counts were discontinued. However, replenishment of cells prolonged the survival of adherent Mtb infected RAVD-THPs, progressively showing morphology typical of multinucleated giant cells. Microscopic images of morphological changes that correlated with CFU counts are indicated next (Data representative of 5 separate experiments).

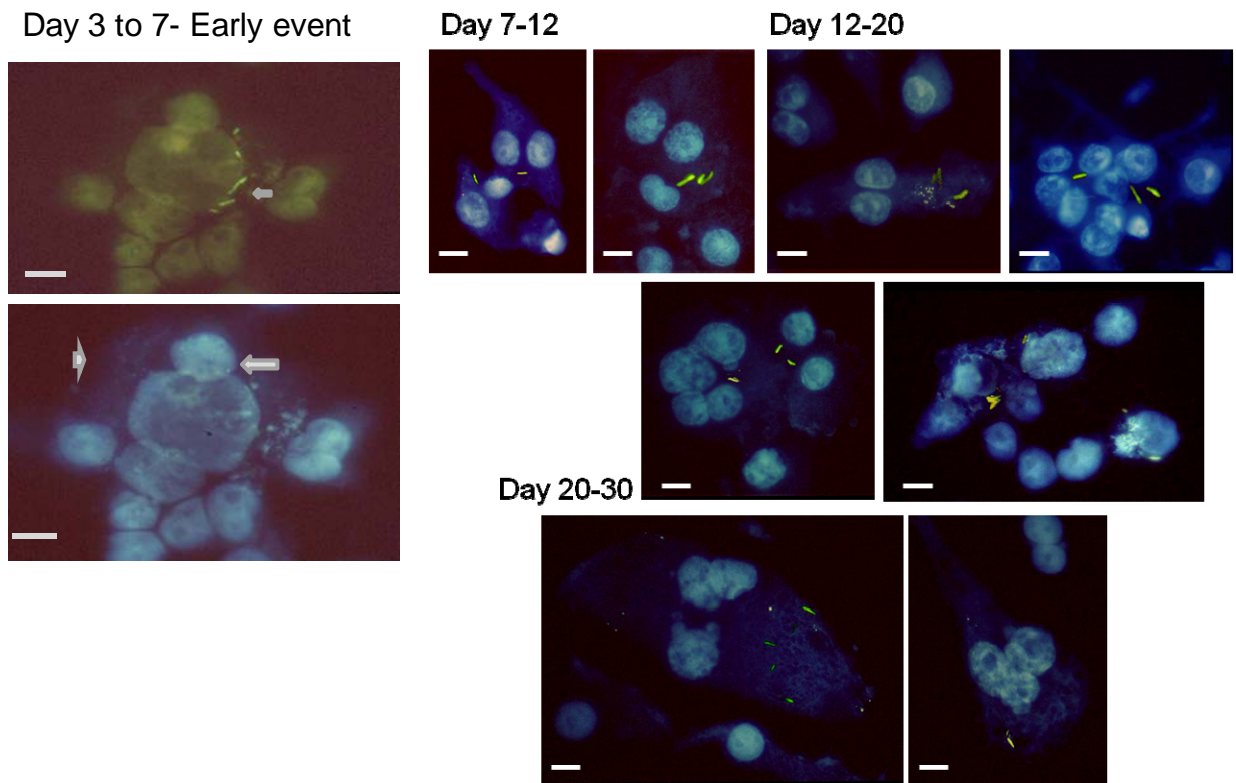


Figure 9C. RAVD induces MNGC formation in *M.tuberculosis* infected THPs.

RAVD-THPs were infected for 4 hrs (MOI of 1), washed to remove non-phagocytosed bacteria, and allowed to incubate. Replenishment of RAVD, fresh medium and uninfected THPs every seven days to the cell culture was performed, then at intervals the cells observed under fluorescent microscopy. a) Day 3-7, Top panel: Early stages in MNGC formation shown in THPs infected with *gfpH37Rv* (arrow) top panel; 485ex/530 em) Bottom panel: Nuclei were stained using Diamidinophenyl –indole (DAPI; 380 nm ex/480 nm em) and the cell fusion triggered by *Mtb* infected macrophage is indicated by an arrow. The arrowhead shows the cytoplasmic veil. b) Days 7-20. Merged fluorescent images acquired at 485 nm-ex/530 nm-em/380 nm-ex/480 nm-em. MNGCs shown over time with *gfpH37Rv* within cells (White bar= 5 μ m). Data representative of 5 separate experiments.

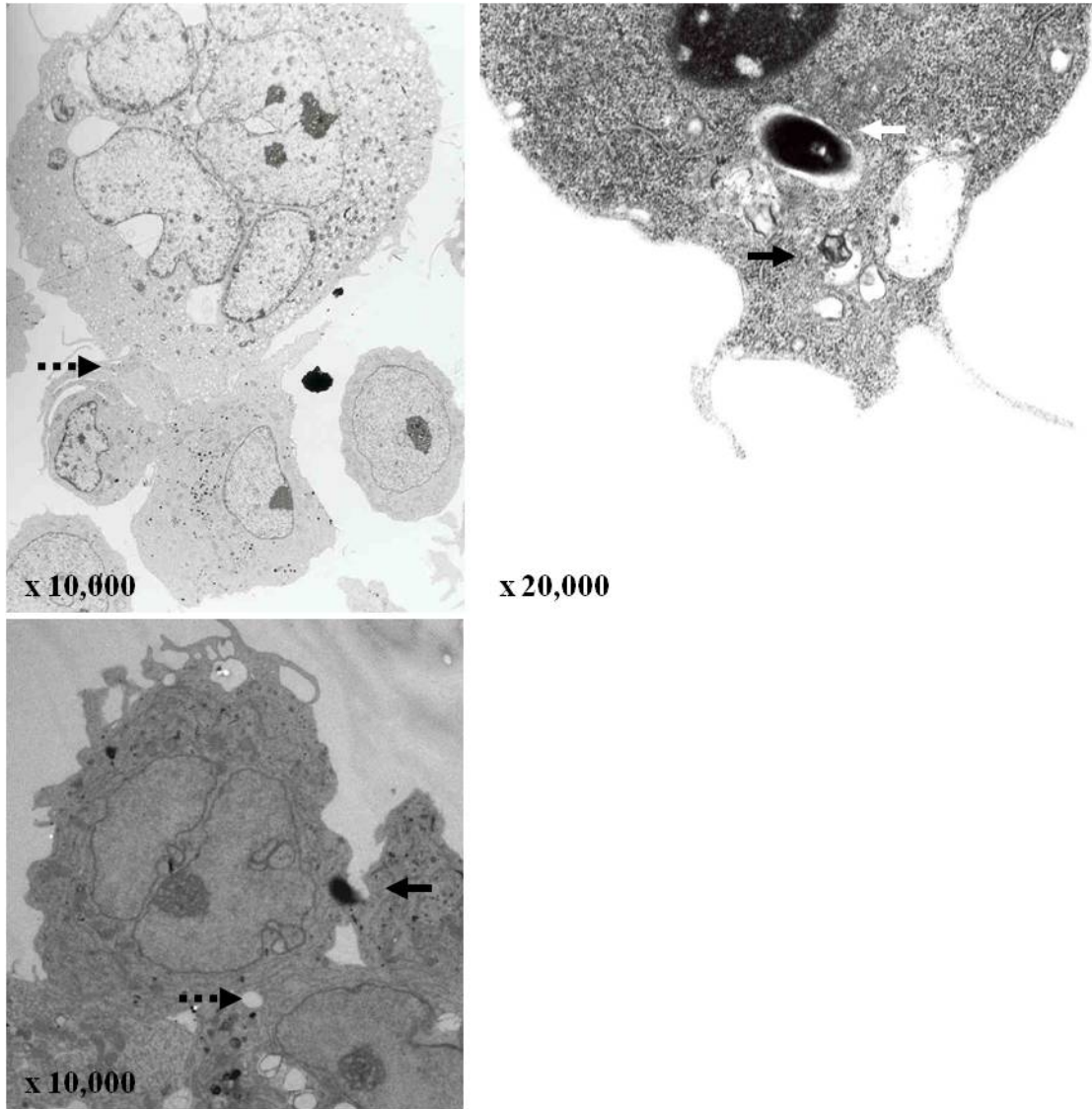


Figure 9D. Electron microscopic (EM) analysis of multi-nucleated giant cell formation of THPs through treatment with RAVD.

RAVD-THPs were infected for 4 hrs (MOI of 1), washed three times to remove non-phagocytosed bacteria, fixed in 0.2% glutaraldehyde, embedded, sectioned and examined a JEOL EM after negative staining with uranyl acetate. Magnification indicated as inset. *Left top and bottom:* Images show that macrophages fuse with adjacent THPs through a zone represented by inter-digitating septae (broken arrow). *Top right:* A single intact Mtb phagosome with tight membrane (white arrow) and bacterial debris in a phagosome (black arrow) in macrophages treated with RAVD are shown. Data representative of 5 separate experiments.

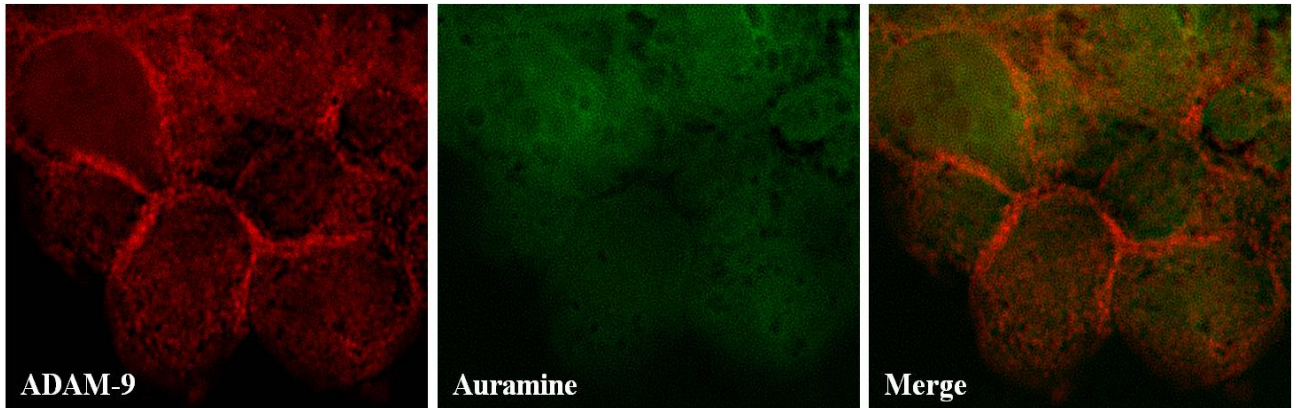


Figure 10. Cell fusion in may involve ADAM-9 present between fusing RAVD-THPs.

RAVD-THPs were infected for 4 hrs with unlabelled Mtb H37Rv (MOI of 1), washed three times and incubated. Every seven days replenishment of RAVD, fresh medium and uninfected THPs to the cell culture was performed. At intervals the cells were fixed, stained with Auramine for the detection of Mtb and probed with Texas Red fluorescent antibodies against ADAM-9. On Day 28, 24 hrs after fresh addition of uninfected RAVD-THPS, adjacent cells show ADAM-9 present on their membranes.

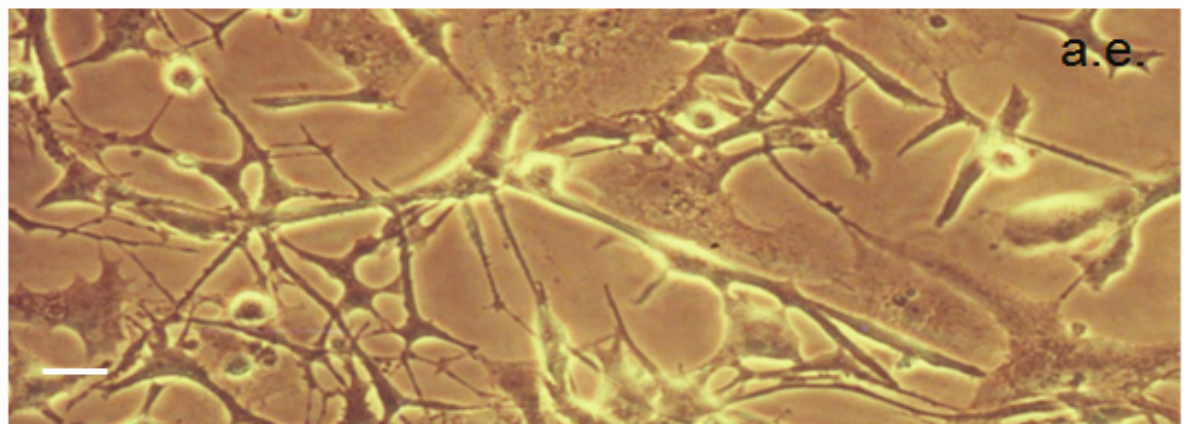
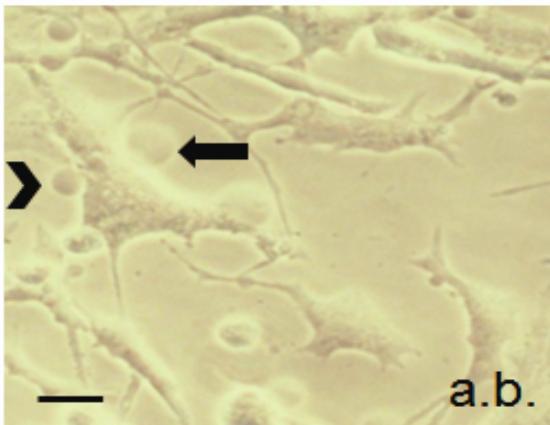
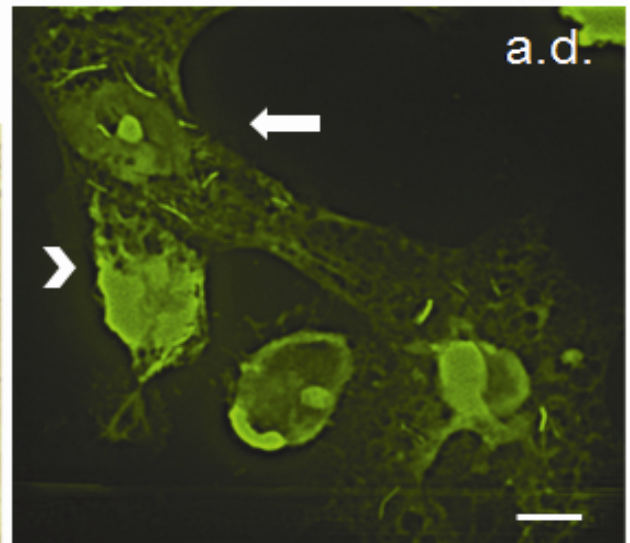
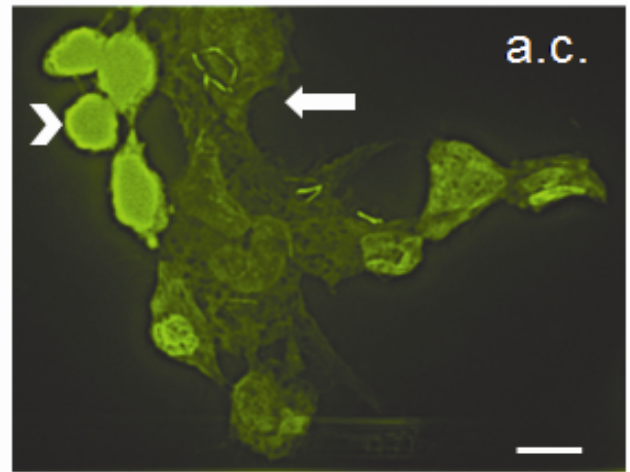
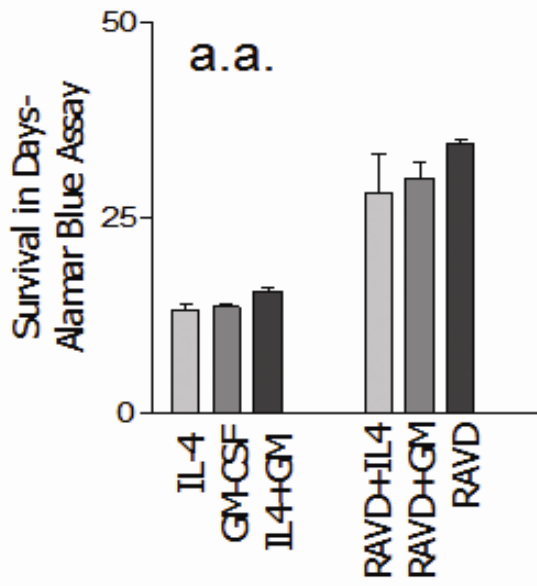


Figure 11A. Activation with RAVD but not cell fusion-inducing cytokines leads to long lived MNGCs containing *M. tuberculosis*.

a.a.) Survival of Mtb infected THPs measured after treatment with either recombinant human IL-4 or GM-CSF or their combination with RAVD. Fluorescent conversion of the vital dye, Alamar blue, was used to monitor viability of THPs (100% viability=100AFUs from 24 well cultures measured at 485/530 nm using Ascent fluoroscan). Only RAVD-THPs showed prolong survival measured up to 40 days in this experiment. Those treated with IL-4 or GM-CSF died because of excess growth of Mtb (not shown). *a.b.*) RAVD cells of panel (a.a.) examined under phase contrast shows a MNGC (arrow) fusing with single THPs (arrowhead) on day 45. *a.c. & a.d.*) Preformed (day 45) adherent MNGCs (pale green; white arrows) that contain multiple *gfpH37Rv* fuse with freshly added uninfected, carboxyfluorescein diacetate (CFSE) stained THPs (arrowheads) to form expanded MNGCs (bar= 5 μ M). *a.e.*) Phase contrast images of MNGCs on day 60 tend to show syncytium formation (bars= 5 μ M).

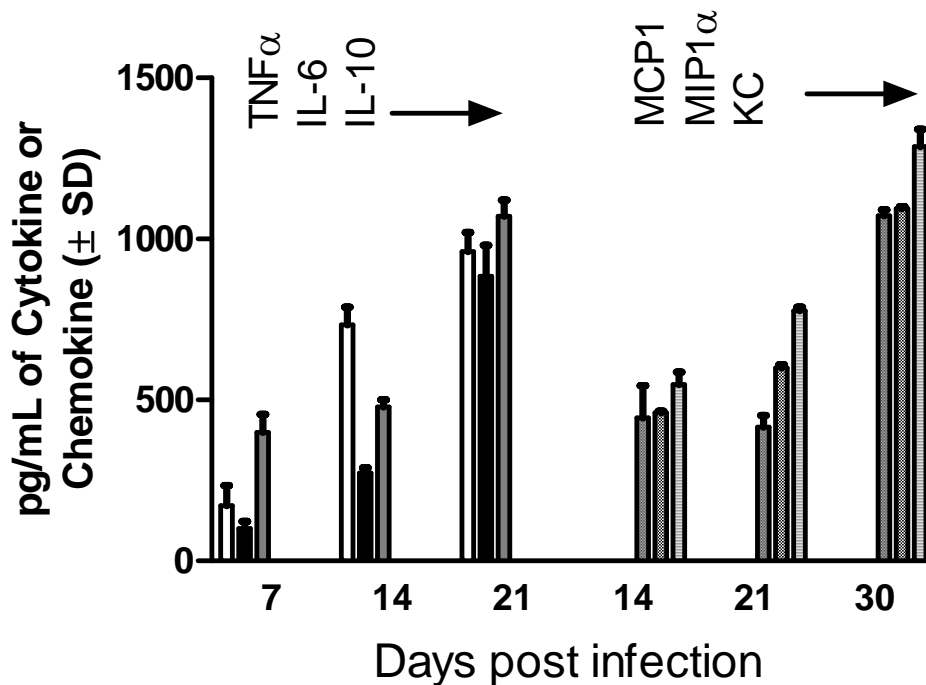


Figure 11B. Cultured *M. tuberculosis* infected MNGCs exhibit biophasic cytokine and chemokine secretion.

RAVD-THPs were infected for 4 hrs (MOI of 1), washed three times to remove non-phagocytosed bacteria, and allowed to incubate. At intervals, supernatants from cell culture were measured for cytokines and chemokines using sandwich ELISA. RAVD-THPs infected with H37Rv show increased cytokine (TNF α , IL6 and IL-10) secretion by Day 21 that decline to baseline level thereafter. Paradoxically, very little chemokines (MCP1, MIP1 α and KC) are observed before day 14 (not shown) but they increase thereafter. Data from three separate experiments in which cytokine supernatants were examined and expressed as mean \pm SEM.

DISCUSSION

During our investigation into the effects of Retinoic acid and Vitamin A on THP maturation, we discovered that the intracellular growth of bacteria was decreased within RAVD-THPs compared to PMA-THPs. The two activators also showed differential expression of receptors on their plasma membrane. One such up-regulated receptor, in RAVD-THPs, was macrophage mannose receptor (MMR). This observation was interesting since MMR has been implicated during macrophage fusion events(71). As vitamin D has also been shown to be involved in cell fusion events(159), we initiated studies to look at phenotypic changes in our RAVD-THPs infection model. It has been suggested that giant cells occurring after cell fusion are better able to degrade intracellular debris and infection. For example, cell fusion leads to osteoclasts that clears and remodels bone. Giant cells occur typically at the center of granulomas. Therefore, we began investigating the possibility of expanding our original concept of using RAVD as a better, more organic and physiological activator of THP cells, to determining if we could produce cell types that are commonly found in TB infections, specifically multi-nucleated giant cells (MNGCs).

We discovered that continuous addition of fresh uninfected RAVD-THPs, every 7-10 days, to cultures of Mtb infected RAVD-THPs led to MNGCs that seemed to control mycobacterial infections. Although the MNGCs harbored mycobacteria, the pathogen did not grow uncontrollably and macrophage cell membrane integrity was maintained. This was in contrast to PMA-THPs, which even after addition of freshly added uninfected THPs were unable to control intracellular Mtb growth eventually leading to cell death and failure to form MNGCs. Higher concentrations (40 nM), PMA has been shown to induce cell fusion but only in human blood monocytes cultured for over 20 days(160). It is possible that infection with Mtb allows for RAVD-THPs to live longer in culture, therefore allowing them to fuse to newly added non-infected RAVD-THPs.

We also observed that RAVD-THPs that formed MNGCs produced copious cytokines at the beginning of the infection then increased in chemokine secretion suggesting that they are capable of recruiting and activating immune cells should they occur *in vivo*. It would have been exciting to test this hypothesis using Dr. Canaday's F9A6 antigen 85b recognizing humanized T-cells. However, as previously stated, we would need to optimize the T-cell overlay assay before we could proceed.

It is interesting to note that MNGC formation in culture has been shown to be dependent on the stage of monocyte to macrophage maturation. Fully matured macrophages are unable to fuse and require addition of monocytes to form MNGCs(161). This may explain our observation that cells treated with monocyte "maturation agents" such as IL-4 and GM-CSF did not exhibit as much MNGC formation as THPs treated with RAVD alone. This leads to the idea that although RAVD-THPs express

a more mature surface receptor profile than PMA-THPs, they still retain a “monocyte-like” phenotype that allows for increased cell fusion. As it still is not clear the mechanism of how monocyte cells fuse or what changes occur during monocyte maturation that inhibits cell fusion, our model could be a good tool to use to probe those interactions.

CHAPTER 6

**LONG TERM ACTIVATION OF *MYCOBACTERIUM TUBERCULOSIS* INFECTED
MACROPHAGES WITH RAVD LEADS TO INCREASED PROTEASE ACTIVITY
AND LYSOSOMAL LOCALIZATION WITH BACTERIA IN THP-1 MACROPHAGES**

INTRODUCTION

Phagosome Maturation

Phagocytosis is a process that enables macrophages to clear out cell debris such as apoptotic cells and to eliminate pathogens. During the phagocytic process, bacterial ligands can bind to macrophage receptors that facilitate the plasma membrane to extend and engulf the pathogen to form a membrane bound structure called the phagosome. Phagosomes can undergo a fairly rapid maturation process (5-15 min)(162) in order for its contents to be digested and degraded. This is a sequential process that involves the maturation of the phagosome, where Rab5⁺ early phagosomes fuse with Rab7⁺ lysosomes to result in a phagolysosome. Phagolysosome formation is marked by the acquisition of lysosome-associated membrane proteins (LAMPs) such as LAMP-1 and LAMP-3 (CD63) and generation of acidic proteases such as cathepsin D and G that are activated through vacuole acidification, in turn, mediated by membrane localization of vacuolar proton ATPase. Mtb is a facultative intracellular parasite entering the host cell via phagocytosis. In order for Mtb to survive, it has several evasion mechanisms that collectively lead to “phagosome maturation arrest.” In this process, that is a hall mark of Mtb, phagosomes containing bacteria avoid fusion with lysosome and prevent degradation. The maturation arrest is however a complex process in which Mtb evades fusion with lysosomes but fuses selectively with other endosomes and plasma membrane-derived fragments to allow intraphagosomal growth(163). A more controversial method that involves escape of Mtb from the phagosome into the macrophage cytosol has also been reported(164).

Phagosomes in MNGCs

It is well documented that when macrophages fuse to form multi-nucleated giant cells (MNGC) they lose the ability to phagocytose extracellular material(165). However, what is less clear is whether MNGCs can process their existing phagosomes into a matured phagolysosome and the precise localization of the phagosomes. We have previously shown that RAVD-THPs infected with Mtb can induce better antimycobacterial processes such as ROS, RNS, autophagy and cathelicidin (**Chapter 4**). We therefore analyzed whether RAVD-induced MNGC formation would lead to an increase in phagosome maturation and therefore better control of intracellular Mtb growth.

RESULTS

RAVD induces generation of active Cathepsin-D protease within the Mtb phagosomes of THP macrophages.

Mtb was recoverable when THP lysates were plated on agar media until Day 30-35 (**Figure 9B**). However, after 28 days, frequently, THPs failed to yield CFUs on agar media even though they were clearly observable in lesser numbers within RAVD-THPs through microscopy. We speculated therefore that Mtb could avoid PL fusion to survive longer while Vitamin D₃ may enhance P-L fusion(166). Thus, phagosomes of Mtb were fractionated using sucrose gradients from RAVD activated, Mtb infected THPs(95). The phagosome pellets and post-nuclear supernatant fractions were then probed with antibodies to Cathepsin-D (Cat-D) and lysosomal proteins indicative of PL fusion. Of these, Cat-D is a major protease that has been to be proteolytic for Mtb in acidic environments and targeted to their phagosomes(95). Cat-D also generates peptide epitopes from Mtb proteins(167). Cat-D breaks down from a 52 kDa immature inactive form to an enzymatically active 32 kDa form in an acidic pH. First, sucrose gradient purified phagosomes of Mtb were analyzed using western blot for Cat-D, an enzyme known to be targeted to Mtb phagosome(168). Phagosomes of *gfpH37Rv* from RAVD-THPs contained the inactive Cat-D when they were examined 24 hrs after infection while by 48 to 72 hrs, active components of Cat-D appeared within the phagosomes (**Figure 12A**). Interestingly, at early times points (less than 7 days) Cat-G was absent in Mtb phagosomes harvested from RAVD THPs (not shown).

RAVD induces Cat-D, Cat-G and lysosomal markers in THP macrophages that colocalize with Mtb phagosomes

In the foregoing studies, we used western blot to document Cat-D since the active and inactive forms of Cat-D are only observable using blots and molecular weight standards(95). As Mtb persisted in smaller numbers in MNGCs, over time, it became difficult to purify phagosomes in sufficient numbers using sucrose gradients. Therefore, immunofluorescence (IF) analysis was performed to localize Cathepsins and lysosomal markers using *gfpH37Rv* within MNGCs. This is an accepted procedure to determine lysosomal fusion of Mtb phagosomes.

In addition to the well characterized Cat-D, Cat-G enzyme has been reported to be bactericidal for Mtb(169). **Figure 12B** illustrates that *gfpH37Rv* within RAVD-THPs stained for these markers suggesting that Mtb localized to protease rich compartments after RAVD activation. Finally, colocalization of phagosomes containing Mtb with lysosomal markers, LAMP1 and CD63, were also scored in RAVD-THPs. CD63 is present in abundance in activated macrophages and is speculated to play a role in phagocytic and P-L fusion events(70). It is a definitive marker of lysosomes. Likewise,

LAMP1 is involved in maintaining lysosome acidity and protecting the lysosomal membranes from autodigestion. RAVD-THP phagosomes containing Mtb showed extensive colocalization with CD63 and LAMP1, suggesting that after RAVD activation, internalized Mtb are located in lysosomal compartments (**Figure 12C**). In these two studies, we used inert latex bead controls to ensure that the antibodies also stained the latex beads after RAVD activation. Together, these studies strongly suggest that RAVD markedly enhances the localization of Mtb into protease rich compartments within THPs that are presumably degradative in nature.

Long term activation with RAVD leads to MNGCs that contain persistent and virulent *M. tuberculosis*

We noted an unusual observation that irrespective of the day of examination some *gfp*Mtb remained completely unstained by either protease or lysosomal markers with THPs. **Figure 12D** illustrates such Mtb that are apparently viable since they maintain *gfp*- fluorescence even after 20 days in culture but do not stain with LAMP1, a phagolysosomal marker. We speculate that such Mtb were cytosolic and thus did not stain with membrane markers such as LAMP1.

To further define the status of persistent Mtb, additional experiments were carried out. THPs were cultured in 8 well slide chambers and at different time intervals, intracellular *gfp*Mtb were scored per 100 macrophages and correlated to viable counts by plating whole cell lysates of replicate chamber THPs. **Figure 13A** illustrates that even when viable Mtb were not culturable on agar plates, *gfp*Mtb were observable within THPs in slide chambers. Finally, THPs were tested over time for the expression of mRNA for antigen85B which is a specific marker for viability of Mtb. **Figure 13B** shows that even when viable Mtb were not recovered from THPs on day 30, mRNA for antigen 85B was observed indicating that viable Mtb persisted within THPs. We therefore suggest that treatment of THPs with RAVD leads, over time, to a decline in the viability of Mtb and that some of bacteria appear to enter a persistent state.

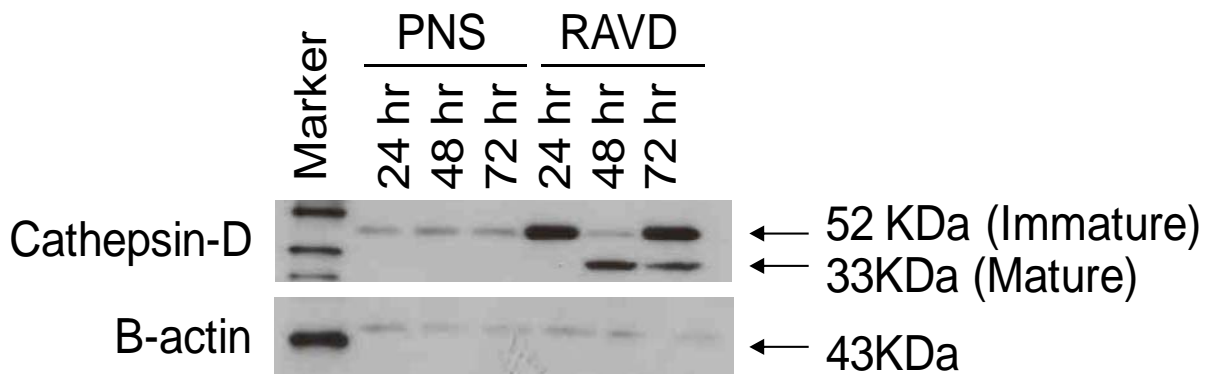


Figure 12A. Sucrose–gradient purified phagosomes of *M. tuberculosis* H37Rv from RAVD-THP are enriched with cathepsin-D.

Phagosomes containing Mtb H37Rv were purified from RAVD-THPs at intervals as indicated using sucrose gradients. Phagosome pellets and phagosome free-post-nuclear supernatants (cytosol or PNS) were analyzed using Western blot using antibodies against Cathepsin-D (Cat-D), an aspartyl protease. This antibody detects the immature 52 kDa form as well as the mature 33 kDa form of Cat-D. Western blot shows that immature form of Cat-D at 24 hrs. and mature, active form at 48 hrs compared to the enrichment of Cat-D in the PNS. Bottom lane shows loading control β -actin. Western blot is representative of 4 separate similar experiments.

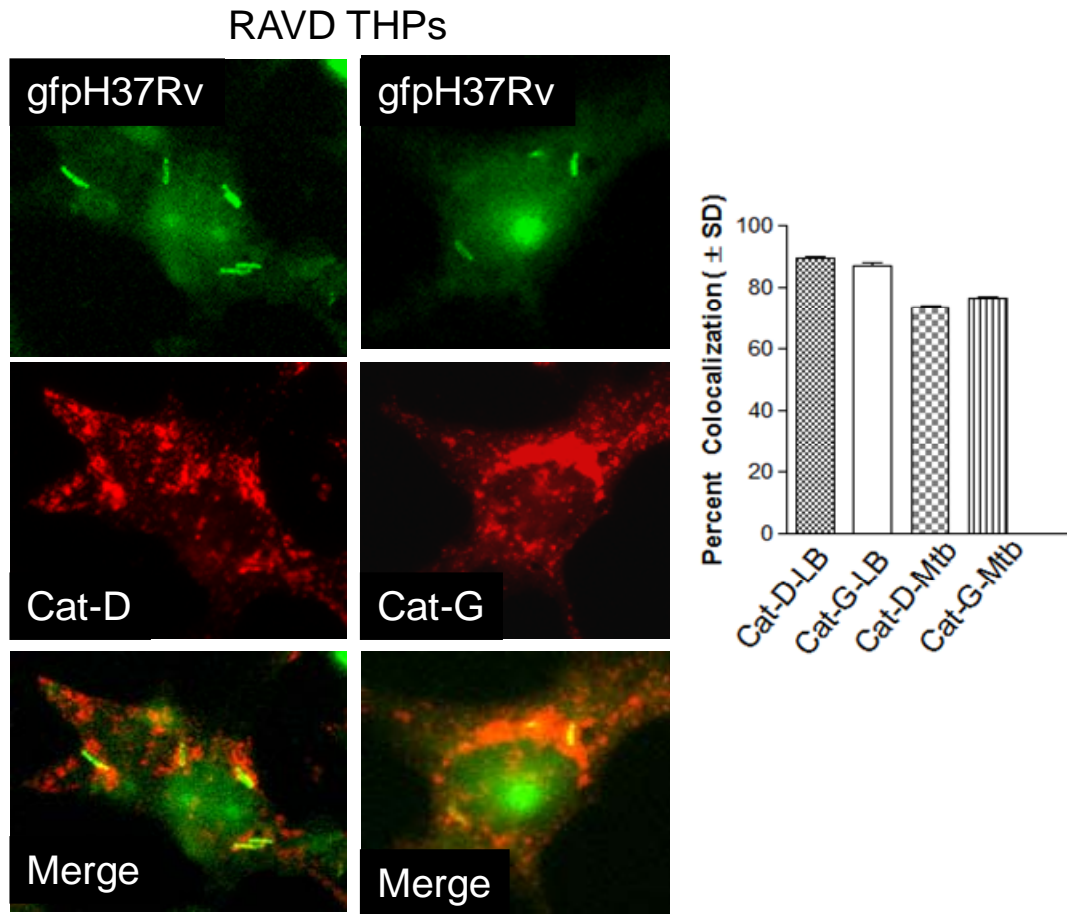


Figure 12B. RAVD induce co-localization of *M. tuberculosis gfpH37Rv* with Cathepsin-D and Cathepsin-G proteases in THP macrophages.

RAVD-THPs were infected with *gfpH37Rv* and stained for Cathepsin D (Cat-D; aspartyl protease) and Cathepsin G (Cat-G; serine protease) using specific antibodies and counterstained with Texas red labeled conjugates. Mtb phagosomes strongly colocalize with Cat-D and Cat-G after 21 days in culture. Approximately 75% of phagosomes containing *gfpH37Rv* stained for these markers. Inert latex beads also stain for these markers as they mature into lysosomes (not shown). Data from 5 separate experiments are summarized in the bar graph (± SD).

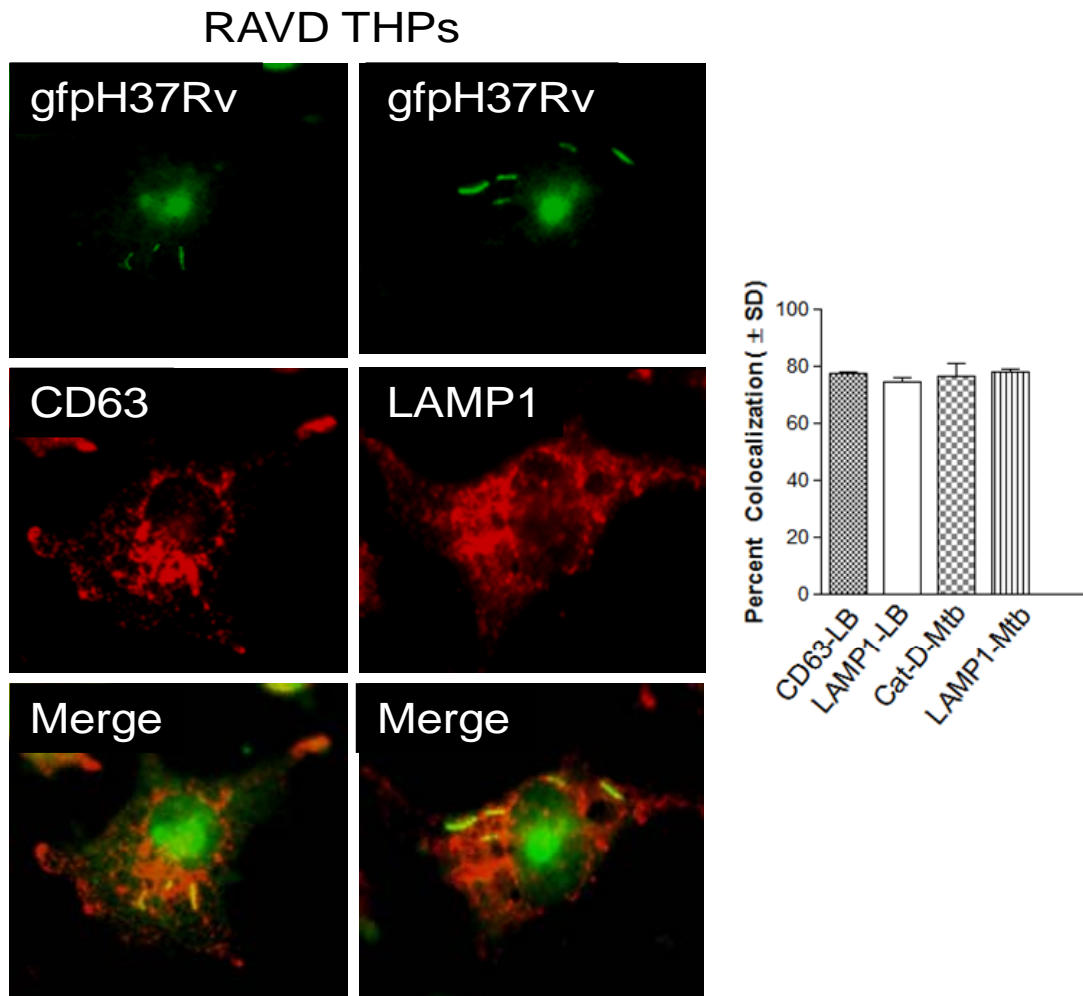


Figure 12C. RAVD induces co-localization of *M. tuberculosis* *gfpH37Rv* with lysosomal markers, CD63 and LAMP-1 within THP macrophages.

RAVD-THPs were infected with *gfpH37Rv* and stained for LAMP-1 and CD63 (LAMP-3) using specific antibodies and counterstained with Texas red labeled conjugates. RAVD-THPs stained strongly for the lysosomal markers CD63 and LAMP-1 after 21 days in culture. Approximately 80% of phagosomes containing *gfpH37Rv* stained for these markers. Inert latex beads also stain for lysosomal markers as they mature into lysosomes rapidly (not shown). Data from 5 separate experiments are summarized in the bar graph (± SD).

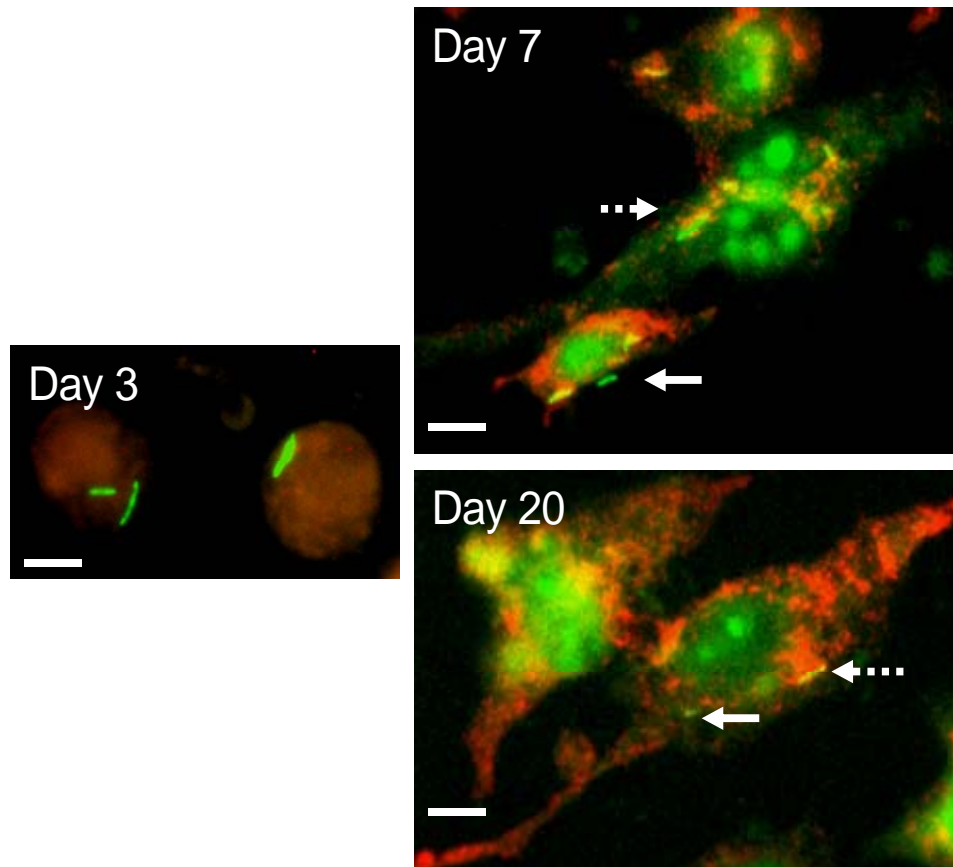
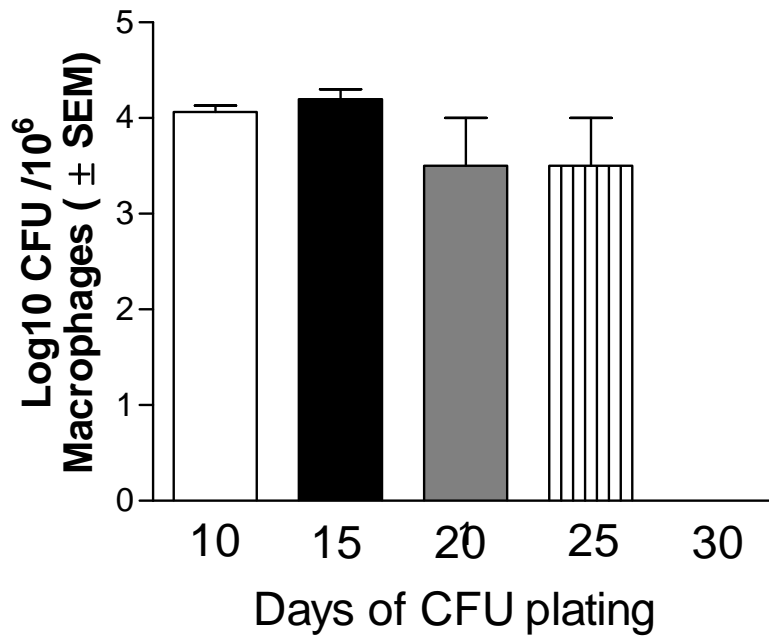


Figure 12D. Some *M. tuberculosis* *gfpH37Rv* phagosomes avoid labeling with LAMP1, a known marker for Mtb phagosomes.

RAVD-THPs were infected with *gfpH37Rv*, maintained as MNGCs over 30 days in 8-well slide chambers and at intervals, stained for LAMP-1 and then counterstained with Texas red labeled conjugates. RAVD-THPs contained many *gfpH37Rv* that co-localized with LAMP-1 from day 7 through day 20 (broken arrow) but some remain unstained (solid arrow). Data from one of 5 separate but similar experiments shown.

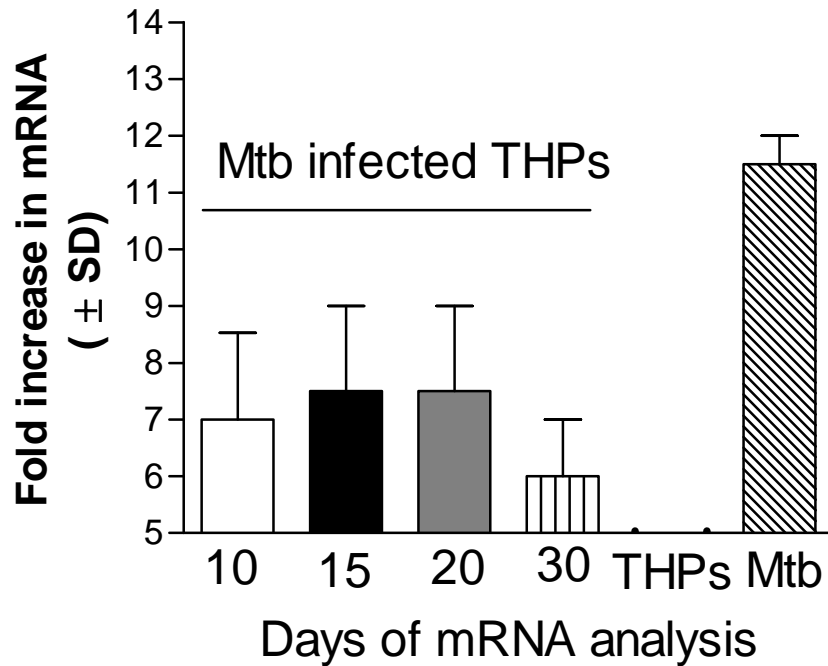


Microscopic *gfpH37Rv* Counts per 100 Macrophages per chamber

Slide Chamber	Days of CFU Plating				
	10	15	20	25	30
1	45	46	23	13	12
2	34	34	34	23	11
3	54	56	23	12	18

Figure 13A. Mycobacterial growth cannot be consistently detected after 30 days in infected RAVD-THPs.

RAVD-THPs were infected with *gfpH37Rv* and maintained as MNGCs over 30 days in 8-well slide chambers. At intervals, *gfpH37Rv* were enumerated per 100 THPs through microscopy in triplicate chambers of slide culture and replicate chamber THPs were lysed and plated for CFUs *as a whole* to recover CFUs on 7H11 agar. RAVD-THPs with persisting Mtb showed no growth in agar plates by day 30 (mean ± SEM of 3 experiments).



	Days of mRNA Analysis			
	10	15	20	30
Log₁₀ CFU Counts per 10⁶ MΦs	4.4	4.2	4.1	0

Figure 13B. Mycobacterial growth cannot be consistently detected after 30 days in infected RAVD-THPs, but mRNA for Antigen 85B remain positive.

RAVD-THPs were infected with Mtb H37Rv and maintained as MNGCs over 30 days in 24-well culture plates. RAVD-THPs were analyzed at time intervals for mRNA specific for Antigen 85B of Mtb using RT-PCR. Plated cell lysates and CFU counts were correlated with mRNA analysis. On day 30, mRNA messages were detected even when Mtb were not recoverable on agar media from lysates of THPs (mean ± SD of 3 experiments).

DISCUSSION

When we initiated this part of the study, we were interested in the ability of MNGCs to control intracellular MTB infection by permitting the Mtb phagosomes to fuse with the lysosomes. We found that MNGCs did permit more localization of Mtb phagosomes with lysosomes and that there was a progressive reduction in bacterial viability. However, when we evaluated the persistence of mycobacteria within the MNGCs we were surprised to find that a small population of non-culturable bacteria was viable within the cells, emitting green fluorescence (*gfpH37Rv*) and producing mRNA for Antigen-85b, even after 30 days of culture. There are some genes of Mtb that are expressed more by bacteria entering into a latent phase. An example is the α -crystallin. However, our attempts at determining if Mtb were in a latent state by evaluating α -crystallin (*acr*) expression proved unproductive as we were unable to detect any mRNA for this antigen. However, we do believe that the bacteria are persistent in these cultures as mRNA for Antigen 85B indicates viable bacteria(170). Gene signatures associated with persistence and dormancy may allow us to develop better methods to detect and treat latent tuberculosis in humans and RAVD THPs may provide a novel long term model to study persistence of Mtb.

CHAPTER 7

**OVERALL GENERAL
DISCUSSION AND CONCLUSIONS**

DISCUSSION

Monocytes and monocytoïd cell lines generally express reduced numbers of receptors and are less efficient in phagocytosing pathogens(86). However, differentiated macrophages express abundant receptors, are more phagocytic and have enhanced intracellular mechanisms of bactericidal activity mediated by phagocyte oxidase (phox), inducible nitric oxide synthase (iNOS), increased targeting of proteolytic enzymes such as Cathepsins and enhanced phagosome-lysosome fusion(86). Monocyte to macrophage differentiation occurs after binding of pathogens to monocytes via their receptors in combination with the release of self-activating cytokines such as TNF- α , G-CSF and GM-CSF. Differentiation can be induced *in vitro* by phorbol esters(46), VD(47) and RA(48). However, following mycobacterial infection *in vivo* macrophages transform into Langhans type of MNGCs that are surrounded by immune cells of granulomas and contain Mtb thought to be non-replicating or dormant. Classic histological studies show that such bacilli reactivate to cause active infection while MNGCs can revert into macrophage phenotype and spread infection in rabbits and guinea pigs(171). To the best of our knowledge, an *in vitro* model of human macrophages that undergoes phenotypic changes closely associated with a transition between replicating Mtb into persistent Mtb has not been reported before. We suggest therefore that RAVD induced MNGC model is more similar to events that occur within humans. We observed that RA and VD were separately able to activate THPs although, maximal differentiation occurred in the presence of the two vitamins (**Figure 1A-C, 2A-B; Table 1A-C, 2A**). Subsequently, RAVD exerted more effective bactericidal effects compared to RA or VD alone (**Figure 5**). These effects were due in part to the induction of NADPH oxidase (**Figure 6A-E**) although there was evidence that modest induction of iNOS also occurred (**Figure 6E**). Significantly, RAVD induced macrophage mediated killing of most Mtb organisms but few were left to survive within the macrophages that remarkably transformed into MNGCs (**Figure 5, Figure 9B**). Such MNGCs produced copious cytokines and chemokines (**Figure 11B**) suggesting that they are capable of recruiting and activating immune cells should they occur *in vivo*. This is the first report of the induction of long living MNGCs with Mtb infection using activation with physiologically compatible macrophage modulators such as RA and VD. Addition of cytokines such as GM-CSF and IL-4 did not markedly alter the RAVD induced transformation of MNGCs (**Figure 11A-a.a.**). This suggested that RA and VD₃ mediated biochemical processes separate from those induced by the cytokines.

The induction of MNGCs by RAVD correlated and clarified previously reported observations. VD was found to enhance DC-SIGN levels in THPs earlier (**Figure 1D**) and the well documented role of DC-SIGN in mycobacterial recognition confirmed the increased efficacy of RAVD-THPs during phagocytosis (**Figure 3**). Likewise, increased expression of Mannose receptor (MMR) in RAVD-THPs

(**Figure 2B**) correlated with the finding that inhibition of MMR prevented MNGC formation(172). Clearly, RAVD transformed THPs and we suggest that, by inference, they regulate differentiation of human monocytes to a more efficient macrophage phenotype.

The bactericidal function of RAVD in THPs was partly due to the induction of ROS since the ROS inhibitor DPI enhanced survival of Mtb (**Figure 6E**). Although other pathways cannot be ruled out, this was similar to the previously reported induction of ROS by RA(128). Recently, a study showed that Vitamin D₃ alone can induce autophagosome formation to kill internalized Mtb(123). Knock-down of beclin-1, a key protein involved in targeting vesicles for autophagy, demonstrated that RAVD can also activate autophagy in order to keep intracellular Mtb growth in check (**Figure 7B**). It should be noted here that we tested the dual effects of RAVD, whereas the individual effects of RA and VD were measured in cells with slightly different phenotype in earlier studies. RA and VD are ingested by humans together and we further propose that it is the dual effect of RA and VD that is likely to be important *in vivo*.

Our initial studies indicated that inhibition of iNOS with NMMA enhanced the survival of intracellular Mtb in RAVD-THPs (**Figure 6E**) although, curiously, we did not find significant levels of nitrate, an indicator of NO synthesis in the medium. It is possible that NO is induced but at such low levels not detectable by Greiss reagent. VD has been reported to induce iNOS in murine and human macrophages(126) and it remains to be determined whether it does induce sustained iNOS in THPs.

Among the spectrum of effects of RAVD on THPs, we observed a striking change in the morphology that led to the formation of MNGCs containing persistent Mtb (**Figure 9C**). Since persistence of Mtb in humans is the leading cause of reactivation tuberculosis, these findings need additional elaboration. Neither RA nor VD alone led to long living THP derived MNGCs but their combination was very effective. Since VD induced or suppressed giant cell formation depending upon the cell phenotype and RA only transformed trophoblasts and osteoclasts(173), we propose that their combination is more effective in inducing MNGC formation in THPs. In addition, we found that RAVD induced cell fusion through the induction of the matrix metalloproteinase (ADAM-9) that was detectable only as a transient staining between the cell junctions (**Figure 10**). Finally, RAVD induced MNGCs could be kept *in vitro* for observation for over 60 days yielding the longest living giant cell phenotype in culture.

A more interesting observation was the persistence of Mtb in MNGCs in a non-replicating stage for as long as 60 days *in vitro*. First, microscopy showed more fluorescent-Mtb per MNGC than recoverable colony counts from lysates of MNGCs (**Figure 13A**). Second, MNGCs positive for *gfp*Mtb but negative for CFU growth on plate media still expressed mRNA for Antigen-85B which is a marker for viable Mtb (**Figure 13B**). This was reminiscent of our previous observation that persistent, non

replicating Mtb in mice treated with antibiotics still expressed abundant mRNA for Antigen 85B. These studies together indicate that RAVD eliminate most replicating Mtb through inducing bactericidal functions but few surviving Mtb are driven into a non-replicating persistence. Thus, we successfully developed a novel macrophage model to study the long term persistence of Mtb. The availability of a cell culture model that reflects the natural niche for Mtb *in vivo* is important from several directions. It may be possible to study the dynamics of persistence over time and devise methods to eliminate persistent Mtb. Analysis of MNGCs may reveal mechanisms that keep replicating Mtb contained and unable to spread disease. Preliminary studies were performed to neutralize both ROS and NO in MNGCs to determine whether persistent Mtb could be revived with unsuccessful results. However, we propose that reactivation of Mtb within macrophages is dependent upon multiple, perhaps time-dependent, factors that need to be carefully dissected out. These include the blockade of multiple mechanisms of bactericidal activity and cytokine mediated modulation of MNGCs in conjunction with stimulation of intracellular Mtb through growth stimulatory 'quorum sensing factors'. The availability of persistent Mtb within a macrophage niche is an attractive model to address these issues.

CHAPTER 8

MATERIALS AND METHODS

Materials and Methods

Activation of THPs and mycobacteria. Human THP-1 monocytoid cell line (TIB#3456, ATCC, MD) was maintained at 37°C and 5% CO₂ in HEPES buffered RPMI-1640 (Sigma Aldrich, St. Louis, MO) medium with 10% heat inactivated FBS, 50 µg/mL gentamicin and 100U /mL penicillin /mL (pH 7.2). THPs were genotyped by ATCC to exclude contamination with other cell lines. Cells were passed so that cell counts did not exceed 10⁶/mL. When needed, cells were expanded into 75 mL flasks and were activated with retinoic acid (1 µM) and vitamin D₃ (1 µM) or phorbol myristyl acetate (10 ng/mL = 16 nM; all from Sigma Aldrich, St Louis MO) for 3 days. RAVD concentrations were selected based on the physiological levels that occur in the fluids of humans(174, 175). It is noted here that the cholecalciferol version of Vitamin D was used in this study. Vitamin D is predominantly metabolised to 1,25 Dihydroxyvitamin D₃ in the liver and kidneys. However, during infection, macrophages and dendritic cells have been shown to metabolize cholecalciferol for use in their antimicrobial processes(10). *Mycobacterium tuberculosis* (Mtb) H37Rv were obtained from ATCC repository and *gfp*- strains of Mtb were prepared as described before (176). They were cultured in 7H9 broth with (*gfp* expressing Mtb H37Rv or Mtb H37Ra strains) or without (Mtb H37Rv and Mtb H37Ra) 25 µg/mL kanamycin for 10 days and highly viable suspension aliquots frozen stored at -80°C.

Surface receptor analysis. Cells were activated for 3 days using varying doses of PMA (1, 10 and 50 ng/mL) and RAVD (10, 100 and 1000 nM) and infected with H37Rv for 24 hrs. The infected cells were washed once with PBS, Fc blocked and stained, on ice for 30 min, with FITC or PE conjugated anti-CD1d, CD14, CD44, CD80, CD86, CD184, CD195, DC-SIGN and HLA-DR (all from BD Pharmingen, San Jose, CA) antibodies. The cells were post-fixed with 2.7% paraformaldehyde before analysis in BD Facscan. PMA and RAVD activated and infected THPs were analyzed for mannose receptor expression by incubation with FITC-tagged mannosylated MBSA (FITC-MBSA) (Sigma Aldrich, St Louis MO) for 30 min at 37°C after which the cells were washed and fixed for cytometric analysis (177). In this assay, uptake of into THPs was performed incubated at both 4°C and 37°C. At, 4°C minimal uptake occurs compared to active uptake at 37°C.

Infection of THPs with Mtb and short term growth curves. Mtb suspensions were subjected to gentle sonication at 4 watts, matched to McFarland standard #1 and spun at 500 rpm for 2 mins. The supernatant contained single colony forming unit (CFU) of Mtb without clumps and were used for infection. Activated THP cells were infected with an MOI of 1-10 with Mtb for 4-24 hrs at 37°C and 5% CO₂ with gentle mixing to ensure uniform infection. Cells were washed three times with sterile medium

to remove non-phagocytosed bacteria, counted and dispensed to 24-well plates (CFU counts, MNGC cultures) or 8-well chamber slides (Mtb uptake, immunostains) at 10^6 cells/mL medium containing antibiotics (50 μ g/mL gentamicin and 100U /mL penicillin /mL) in replicates. For growth curves between days 1-10, cells from 24-well plates were aspirated, pelleted, and lysed in 0.05% SDS within the same well thus accounting for adherent as well as some floating macrophages. When macrophages were adherent both floater cells as well as adherent macrophages were pooled for preparing lysates, which were then were plated at ten-fold dilutions on 7H11 agar (Remel, Lenexa, KS) for colony forming unit (CFU) counts. PMA-THPs generally die between days 7-10 due to an excess growth of Mtb while RAVD-THPs control growth of Mtb and cells remain viable. Viability of THPs during Mtb infection was determined by adding 10% by volume of alamar blue vital stain that turns pink within 4 hrs when macrophages are fully viable. The dye conversion was quantitated using an Asecnt fluorometer; it is also readable using an ELISA reader (Invitrogen, USA).

Growth and maintenance in slide chambers: Cells plated onto 8-well chamber slides (Permanox plastic chamber slides, Nalge Nunc International, Rochester, NY), became adherent after Mtb infection and were fixed either with absolute alcohol for Ziehl-Neelsen stain and scored by microscopy for Mtb uptake into the macrophages or with 2.7% paraformaldehyde for immunostaining with antibodies. THPs in slide chambers were kept alive for several weeks or months with medium replenishment as described below.

Long term cultures of THPs and induction of Multi-Nucleated Giant Cells (MNGCs). THPs infected with Mtb as above for short term infection were continued into long term cultures of MNGCs as follows. Only RAVD-THPs were viable beyond 10 days of Mtb infection. On day 3 post infection, when RAVD-THPs begin to adhere to 24-well plates, cells were aspirated and fresh culture media containing RAVD (1 μ M) and antibiotics (50 μ g/mL gentamicin and 100U /mL penicillin /mL) were added to the culture plates. On day 10, when the cells had differentiated and most adhered to the plastic surface, fresh media with RAVD supplement was added along with freshly activated but uninfected RAVD-THP cells to a final concentration not exceeding 10^6 cells/mL. Thus, the only time Mtb was added to long term cultures of THPs was during an initial infection. Thereafter, fresh media supplemented with RAVD was added every 3 days and freshly activated cells every 7 days. Pre-formed giant cells on monolayers fused with freshly added THP cells yielding increasingly larger MNGC. Control cultures of THP-1 cells activated with RAVD and without Mtb infection did not survive beyond 10 days. a) *Growth curve of Mtb.* During long term infection lasting 10-60 days, Mtb infected THPs were adherent but some floaters were present. Thus, during this time interval cells were aspirated,

pelleted and lysed along with adherent cells on monolayers to determine CFU counts. b) *Cell fusion to expand MNGCs*: To demonstrate cell fusion, preformed MNGCs adherent to tissue culture wells were added with Carboxyfluorescein diacetate (CFSE; Molecular Probes, Eugene OR) stained, RAVD-THPs. Cells were stained with CFSE as per manufacturer's instructions. Cell fusion was visible between MNGCs fusing with CFSE stained single THPs. c) *Cytokine effects*: RAVD and cytokines were compared for their ability to induce MNGCs by infecting THPs with Mtb and addition of either RAVD or recombinant human IL-4 and GM-CSF separately or in combination (R & D Sciences; 20 ng/ml/10⁶ macrophages each). THPs were re-incubated with fresh IL-4 or GM-CSF, replenished daily. To determine synergistic effects, RAVD- THPs were also added with the cytokines. d) *Viability analysis*: Alamar blue was used as vital stain to determine viability of MNGCs. e). *Cytokines and chemokine secretion from MNGCs*: Cytokines and chemokines secreted from MNGCs were quantitated using sandwich ELISA with paired antibodies (R & D Sciences, USA). Long term cultures for MNGCs were performed over 20 times with reproducible results within a 2 year time frame. d) *Phagosome analysis for proteases*. Mtb phagosomes were purified from RAVD-THPs on day 12 using sucrose gradients and analyzed for Cathepsin-D using western blot. These methods have been optimized in our laboratory(95) (178) (179).

Phagosome Isolation. For the isolation of Mtb-containing phagosomes, macrophages were infected as previously described. Phagosomes were fractionated as per the procedures described by Ullrich et al.(180, 181) Briefly, as per our modified protocol, macrophages were scraped, washed three times in fractionation buffer (PFB) with 10mM HEPES, 5 mM EDTA, 5 mM EGTA (pH 7.0), and suspended in PFB with homogenization buffer (25 mM Tris-HCl (pH 7.4), 0.25 M sucrose, 2.5 mM dithiothreitol (DTT), 2.5 mM EDTA, and the following inhibitors: 5 mM benzamidine, 50 µg/ml leupeptin, 50 µg/ml aprotinin, 50 µg/ml trypsin inhibitor, 5 µg/ml pepstatin, 1 mM PMSF, and 20 mM NaF). Pellets were then homogenized in a glass tissue homogenizer 10 times and passed 10 times through a 28-gauge needle. Lysates were centrifuged at 500 x g for 5 min to sediment nuclei and the postnuclear supernatant was layered on a step gradient of 50% and 12% sucrose in PFB. After centrifugation at 1000 x g for 60 min, the interphase of phagosome fraction was collected and further purified by passing through two successive cushions of 70- and 400-kDa Ficoll in PFB as described before. The final purified phagosomal pellet was collected by centrifugation at 10,000 x g for 15 min and suspended in SDS sample buffer for use in Western Blot analysis.

Antigen processing and presentation assays. THP-1 or human MonoMac macrophages cell lines were cultured in 25mL flasks infected with either H37Rv or BCG-14 at an MOI of 10. After infection, the

cells were aliquoted into microcentrifuge tubes (1.5×10^5 cells/tube) and washed by centrifugation three times to remove any non-phagocytosed bacteria. Antigen 85b (F9A6) or α -crystallin (5MB) specific T-cell hybridoma cells (graciously donated by Dr. David Canaday) were pelleted and resuspended in 0.5 mL of DMEM. T-cell hybridoma cells were combined with infected THPs or MonoMac cells and allowed to incubate for the specified times. Supernatants were collected at 4 or 24 hrs and analyzed using ELISA for IL-2 production.

Immunofluorescent Labeling. Activated THPs infected with *gfpH37Rv* were grown in an 8-well chamber slides were washed once with PBS, fixed in 2.7% paraformaldehyde and permeabilized for 30 min with a staining buffer containing 1% saponin, 0.1% glycine, and 2% heat-inactivated autologous human serum in PBS. The slides were washed and stained overnight at 4°C with 1/250 dilution of antibodies against p47/67^{phox}, CD63, LAMP-1, Cathepsin-D and Cathepsin-G. Antibody dilutions were arrived at using preliminary dose-titrations. The slides were washed three times with staining buffer and then a 1:2500 dilution of the appropriate secondary Texas-Red conjugated antibody (Santa Cruz Biotechnology, Santa Cruz, CA) was added and incubated at room temperature for one hour. After further washing, the slides were mounted in Fluorsave (Calbiochem, Gibbstown, NJ) with or without DAPI stain and examined using a Nikon fluorescence microscope equipped with deconvolution software followed by analysis in a laser confocal microscope. Negative controls consisted of naïve THPs (no activation) and uninfected activated THPs. In addition, isotype controls used were *gfpH37Rv* infected cells stained with normal goat or mouse IgG followed by a secondary antibody conjugated with Texas Red. All uninfected and unactivated THPs presented a uniform low background fluorescence using this procedure. Phagosomes staining for distinct antibodies were scored for colocalization as described before in our previous studies using mouse macrophages(124). For colocalization experiments, bacteria of over 100 macrophages in each chamber of triplicate well slides were counted and averaged for three separate experiments. The colocalization percentage was plotted and Student's *t* test was used to determine significance between the groups.

Detection of Reactive Oxygen Species (ROS) and Nitric Oxide. Activated THPs were treated with 2,7-Dichlorodihydrofluorescein diacetate (H_2DCFDA , Invitrogen, Carlsbad CA) as per the manufacturer's instructions to measure internal ROS production in pre and post Mtb infected macrophages. Basal levels of ROS in activated THPs were analyzed for a three day period by flow cytometry. Mtb infected cells were incubated for 5 days and tested for intracellular fluorescence as above using fluorometry (Ascent Fluoroscanner) instead of flow cytometry because of contamination issues and infectious risk with virulent Mtb. The specificity of ROS mediated conversion of DCF was

confirmed by using the ROS inhibitor, 10mM diphenyleneiodonium (DPI; Sigma Aldrich, St. Louis, MO). The contribution of inducible nitric oxide synthase (iNOS) to the killing of internalized Mtb was determined by the addition of 10 μ M of N(G)-monomethyl-L-arginine (L-NMMA; Alexis Biochemicals, San Diego, CA; an inhibitor of nitric oxide response) to the cultures and the supernatants were titrated using diaminonaphthalene (DAN) fluorescent dye and Ascent Fluoroscan instrument.

siRNA Knock-down of Beclin-1 to determine induction of autophagy. THP-1 cells were seeded 2×10^6 cells per well onto a 6-well plate and rested for 24 hrs in media without antibiotics. They were then activated with RAVD as above and three days later, the knock-down of beclin-1 was performed as per manufacturer's instructions (Lonza AG, Walkersville MD) where the beclin-1 siRNA (Sigma Aldrich, St Louis MO) was nucleofected into the cells and allowed to rest for 24 hrs. Infection with Mtb was then performed for 4 hrs, washed cells were re-incubated and lysates of macrophages were plated for CFU counts of Mtb. Just before infection, western blot analysis with an antibody to beclin1 (Santa Cruz Biotechnology, USA) was conducted to determine knock-down. The fluid phase autophagosome marker monodansyl-cadaverine (MDC) was used to label Mtb phagosomes of beclin1 knockdown and control THPs as described before(116).

Western blot Analysis. Whole cell lysates or phagosome fractionations were collected then heated at 98°C for 5 min. Samples were electrophoresed using either 7–15% or 10-15% gradient SDS gel, electroblotted and membranes were probed with cathepsins, autophagy etc. Bands were visualized using an ECL chemiluminescence kit from Amersham Biosciences.

Electron Microscopy. Infected RAVD activated THP cells were prepared for examination by transmission electron microscopy. After the indicated incubation periods, the glutaraldehyde-fixed (2% in PBS, pH 7.6) cells were washed in Millonig's buffer, post-fixed in 50/50 osmium tetroxide/Millonig's, dehydrated through graded ethanol solutions and embedded in 50/50 LX-112 resin/propylene oxide. 500nm sections are cut from each block using a glass knife on a Leica Ultracut R microtome and stained with 0.5% Toluidine Blue. The blocks were trimmed and thin sections (80nm & 100nm) are cut using a DiATOME diamond knife, one each of the two thicknesses are floated on either 100 or 150 mesh copper grids (Electron Microscopy Sciences) and heat fixed in a 70°C oven for at least one hour. The grids are stained for 15 mins using 2% uranyl acetate, rinsed with double distilled water, stained 5 mins in Renold's lead citrate, rinsed and dried in a 70°C oven. The specimen grids are imaged in a JEOL 1200 transmission electron microscope at 60kV with digital images collected using a 1k X 1k Gatan BioScan camera, Model 792.

Analysis of persisting and non-replicating Mtb in THPs. RAVD-THPs were activated and infected with *gfpH37Rv* as above and maintained as MNGCs in 8 well slide chambers or 24 well TC plates up to 30 days or more. At time intervals- a) THPs of the 8 well slide chambers in triplicates were lysed with 200 μ L per chamber of 0.01% SDS and the entire lysate was plated on 7H11 agar plates for CFUs expressed per 10^6 macrophages, b) replicate chambers macrophages were washed at the same time, fixed and examined for *gfpH37Rv* through microscopic evaluation and expressed as number of Mtb per 100 macrophages per chamber in triplicates, and c) THPs in parallel cultures of 24 well plates were lysed with RNazol and mRNA obtained was analyzed using real-time PCR as described using the following primers for antigen 85B(170, 182). The primers were; Forward primer: 5'-TCAGGGGATGGGGCCTAGCC-3' Reverse primer: 5'- GCTTGGGGATCTGCTGCGTA-3' RT primer: 5'- GCCGGCGCCTAACGAACTCTGC-3' Taqman Probe: 85B-TP 5'-FAM-TCGAGTGACCCGGCATGGGAGCGT-BHQ-1 – 3'. Fold-expression of mRNA from macrophage lysates was compared to mRNA messages from a 7 day viable culture of Mtb that was adjusted to contain 10^6 CFU/mL diluted from a suspension matched to McFarland #1 turbidity standard (10^8 CFU/mL).

REFERENCES

1. WHO. 2006. Global Tuberculosis Control. In *WHO Report*.
2. Toossi, Z. 2000. The inflammatory response in Mycobacterium tuberculosis infection. *Arch Immunol Ther Exp (Warsz)* 48:513-519.
3. Ulrichs, T., and Kaufmann, S.H. 2006. New insights into the function of granulomas in human tuberculosis. *J Pathol* 208:261-269.
4. Saunders, B.M., Frank, A.A., and Orme, I.M. 1999. Granuloma formation is required to contain bacillus growth and delay mortality in mice chronically infected with Mycobacterium tuberculosis. *Immunology* 98:324-328.
5. Williams, C.J.B. 1849. Cod liver oil in phthisis. *London Journal of Medicine* 1:1-18.
6. Nnoaham, K.E., and Clarke, A. 2008. Low serum vitamin D levels and tuberculosis: a systematic review and meta-analysis. *Int J Epidemiol* 37:113-119.
7. Chan, T.Y. 2000. Vitamin D deficiency and susceptibility to tuberculosis. *Calcif Tissue Int* 66:476-478.
8. Wilkinson, R.J., Llewelyn, M., Toossi, Z., Patel, P., Pasvol, G., Lalvani, A., Wright, D., Latif, M., and Davidson, R.N. 2000. Influence of vitamin D deficiency and vitamin D receptor polymorphisms on tuberculosis among Gujarati Asians in west London: a case-control study. *Lancet* 355:618-621.
9. Gao, L., Tao, Y., Zhang, L., and Jin, Q. Vitamin D receptor genetic polymorphisms and tuberculosis: updated systematic review and meta-analysis. *Int J Tuberc Lung Dis* 14:15-23.
10. Mora, J.R., Iwata, M., and von Andrian, U.H. 2008. Vitamin effects on the immune system: vitamins A and D take centre stage. *Nat Rev Immunol*. 2008 Sep;8(9):685-98
11. van Etten, E., and Mathieu, C. 2005. Immunoregulation by 1,25-dihydroxyvitamin D₃: basic concepts. *The Journal of steroid biochemistry and molecular biology* 97:93-101.
12. Barnes, P.F., Modlin, R.L., Bikle, D.D., and Adams, J.S. 1989. Transpleural gradient of 1,25-dihydroxyvitamin D in tuberculous pleuritis. *J Clin Invest* 83:1527-1532.
13. Wientroub, S., Winter, C.C., Wahl, S.M., and Wahl, L.M. 1989. Effect of vitamin D deficiency on macrophage and lymphocyte function in the rat. *Calcif Tissue Int* 44:125-130.

14. Cohen, M.S., Mesler, D.E., Snipes, R.G., and Gray, T.K. 1986. 1,25-Dihydroxyvitamin D3 activates secretion of hydrogen peroxide by human monocytes. *J Immunol* 136:1049-1053.
15. Rigby, W.F., Shen, L., Ball, E.D., Guyre, P.M., and Fanger, M.W. 1984. Differentiation of a human monocytic cell line by 1,25-dihydroxyvitamin D3 (calcitriol): a morphologic, phenotypic, and functional analysis. *Blood* 64:1110-1115.
16. Roux-Lombard, P., Cruchaud, A., and Dayer, J.M. 1986. Effect of interferon-gamma and 1 alpha,25-dihydroxyvitamin D3 on superoxide anion, prostaglandins E2, and mononuclear cell factor production by U937 cells. *Cell Immunol* 97:286-296.
17. Fagan, D.L., Prehn, J.L., Adams, J.S., and Jordan, S.C. 1991. The human myelomonocytic cell line U-937 as a model for studying alterations in steroid-induced monokine gene expression: marked enhancement of lipopolysaccharide-stimulated interleukin-1 beta messenger RNA levels by 1,25-dihydroxyvitamin D3. *Mol Endocrinol* 5:179-186.
18. Prehn, J.L., Fagan, D.L., Jordan, S.C., and Adams, J.S. 1992. Potentiation of lipopolysaccharide-induced tumor necrosis factor-alpha expression by 1,25-dihydroxyvitamin D3. *Blood* 80:2811-2816.
19. Liu, P.T., Stenger, S., Li, H., Wenzel, L., Tan, B.H., Krutzik, S.R., Ochoa, M.T., Schaubert, J., Wu, K., Meinken, C., et al. 2006. Toll-like receptor triggering of a vitamin D-mediated human antimicrobial response. *Science* 311:1770-1773.
20. Martineau, A.R., Honecker, F.U., Wilkinson, R.J., and Griffiths, C.J. 2007. Vitamin D in the treatment of pulmonary tuberculosis. *J Steroid Biochem Mol Biol* 103:793-798.
21. Provvedini, D.M., Tsoukas, C.D., Deftos, L.J., and Manolagas, S.C. 1983. 1,25-dihydroxyvitamin D3 receptors in human leukocytes. *Science* 221:1181-1183.
22. Lemire, J.M., Adams, J.S., Sakai, R., and Jordan, S.C. 1984. 1 alpha,25-dihydroxyvitamin D3 suppresses proliferation and immunoglobulin production by normal human peripheral blood mononuclear cells. *J Clin Invest* 74:657-661.
23. Helming, L., Bose, J., Ehrchen, J., Schiebe, S., Frahm, T., Geffers, R., Probst-Kepper, M., Balling, R., and Lengeling, A. 2005. 1alpha,25-Dihydroxyvitamin D3 is a potent suppressor of interferon gamma-mediated macrophage activation. *Blood* 106:4351-4358.

24. Gollnick, H., Ehlert, R., Rinck, G., and Orfanos, C.E. 1990. Retinoids: an overview of pharmacokinetics and therapeutic value. *Methods Enzymol* 190:291-304.
25. Blomhoff, R., and Blomhoff, H.K. 2006. Overview of retinoid metabolism and function. *J Neurobiol* 66:606-630.
26. Moise, A.R., Noy, N., Palczewski, K., and Blaner, W.S. 2007. Delivery of retinoid-based therapies to target tissues. *Biochemistry* 46:4449-4458.
27. Iwata, M. 2009. Retinoic acid production by intestinal dendritic cells and its role in T-cell trafficking. *Semin Immunol* 21:8-13.
28. Saurer, L., McCullough, K.C., and Summerfield, A. 2007. In vitro induction of mucosa-type dendritic cells by all-trans retinoic acid. *J Immunol* 179:3504-3514.
29. Semba, R.D. 1999. Vitamin A as "anti-infective" therapy, 1920-1940. *J Nutr* 129:783-791.
30. Evans, D.I., and Attock, B. 1971. Folate deficiency in pulmonary tuberculosis: relationship to treatment and to serum vitamin A and beta-carotene. *Tubercle* 52:288-294.
31. Crowle, A.J., Ross, E.J., and May, M.H. 1987. Inhibition by 1,25(OH)₂-vitamin D₃ of the multiplication of virulent tubercle bacilli in cultured human macrophages. *Infect Immun* 55:2945-2950.
32. Frolik, C.A., and J. A. Olson. 1984. *Extraction, separation, and chemical analysis of retinoids*. New York: Academic Press, Inc. 182-233 pp.
33. Yamada, H., Mizuno, S., Ross, A.C., and Sugawara, I. 2007. Retinoic acid therapy attenuates the severity of tuberculosis while altering lymphocyte and macrophage numbers and cytokine expression in rats infected with *Mycobacterium tuberculosis*. *J Nutr* 137:2696-2700.
34. Crowle, A.J., and Ross, E.J. 1989. Inhibition by retinoic acid of multiplication of virulent tubercle bacilli in cultured human macrophages. *Infect Immun* 57:840-844.
35. Takeshita, F., Kobiyama, K., Miyawaki, A., Jounai, N., and Okuda, K. 2008. The non-canonical role of Atg family members as suppressors of innate antiviral immune signaling. *Autophagy* 4:67-69.
36. Gutierrez, M.G., Master, S.S., Singh, S.B., Taylor, G.A., Colombo, M.I., and Deretic, V. 2004. Autophagy is a defense mechanism inhibiting BCG and *Mycobacterium tuberculosis* survival in infected macrophages. *Cell* 119:753-766.

37. Holmes, A.D.A., H.L. 1930. The value of cod liver oil for underpar children of school age. *N. Engl. J. Med* 202:470-476.
38. Pattison, C.L. 1930. Treatment of bone tuberculosis by large amounts of vitamins A and D. *Brit. Med. J.* 2.
39. Abba, K., Sudarsanam, T.D., Grobler, L., and Volmink, J. 2008. Nutritional supplements for people being treated for active tuberculosis. *Cochrane Database Syst Rev*:CD006086.
40. Tavera-Mendoza, L., Wang, T.T., Lallemand, B., Zhang, R., Nagai, Y., Bourdeau, V., Ramirez-Calderon, M., Desbarats, J., Mader, S., and White, J.H. 2006. Convergence of vitamin D and retinoic acid signalling at a common hormone response element. *EMBO Rep* 7:180-185.
41. Anand, P.K., Kaul, D., and Sharma, M. 2008. Synergistic action of vitamin D and retinoic acid restricts invasion of macrophages by pathogenic mycobacteria. *J Microbiol Immunol Infect* 41:17-25.
42. Bastie, J.N., Balitrand, N., Guidez, F., Guillemot, I., Larghero, J., Calabresse, C., Chomienne, C., and Delva, L. 2004. 1 alpha,25-dihydroxyvitamin D3 transrepresses retinoic acid transcriptional activity via vitamin D receptor in myeloid cells. *Mol Endocrinol* 18:2685-2699.
43. Anand, P.K., and Kaul, D. 2003. Vitamin D3-dependent pathway regulates TACO gene transcription. *Biochem Biophys Res Commun* 310:876-877.
44. Tsuchiya, S., Yamabe, M., Yamaguchi, Y., Kobayashi, Y., Konno, T., and Tada, K. 1980. Establishment and characterization of a human acute monocytic leukemia cell line (THP-1). *Int J Cancer* 26:171-176.
45. Theus, S.A., Cave, M.D., and Eisenach, K.D. 2004. Activated THP-1 cells: an attractive model for the assessment of intracellular growth rates of Mycobacterium tuberculosis isolates. *Infect Immun* 72:1169-1173.
46. Tsuchiya, S., Kobayashi, Y., Goto, Y., Okumura, H., Nakae, S., Konno, T., and Tada, K. 1982. Induction of maturation in cultured human monocytic leukemia cells by a phorbol diester. *Cancer Res* 42:1530-1536.
47. Kim, K.J., Kim, H.H., Kim, J.H., Choi, Y.H., Kim, Y.H., and Cheong, J.H. 2007. Chemokine stromal cell-derived factor-1 induction by C/EBPbeta activation is

- associated with all-trans-retinoic acid-induced leukemic cell differentiation. *J Leukoc Biol* 82:1332-1339.
48. McCarthy, D.M., San Miguel, J.F., Freake, H.C., Green, P.M., Zola, H., Catovsky, D., and Goldman, J.M. 1983. 1,25-dihydroxyvitamin D₃ inhibits proliferation of human promyelocytic leukaemia (HL60) cells and induces monocyte-macrophage differentiation in HL60 and normal human bone marrow cells. *Leuk Res* 7:51-55.
 49. Crowle, A.J., and Ross, E.J. 1990. Comparative abilities of various metabolites of vitamin D to protect cultured human macrophages against tubercle bacilli. *J Leukoc Biol* 47:545-550.
 50. Taylor, P.R., Martinez-Pomares, L., Stacey, M., Lin, H.H., Brown, G.D., and Gordon, S. 2005. Macrophage receptors and immune recognition. *Annu Rev Immunol* 23:901-944.
 51. Zhang, Y., Doerfler, M., Lee, T.C., Guillemin, B., and Rom, W.N. 1993. Mechanisms of stimulation of interleukin-1 beta and tumor necrosis factor-alpha by Mycobacterium tuberculosis components. *J Clin Invest* 91:2076-2083.
 52. Bowdish, D.M., Sakamoto, K., Kim, M.J., Kroos, M., Mukhopadhyay, S., Leifer, C.A., Tryggvason, K., Gordon, S., and Russell, D.G. 2009. MARCO, TLR2, and CD14 are required for macrophage cytokine responses to mycobacterial trehalose dimycolate and Mycobacterium tuberculosis. *PLoS Pathog* 5:e1000474.
 53. Drage, M.G., Pecora, N.D., Hise, A.G., Febbraio, M., Silverstein, R.L., Golenbock, D.T., Boom, W.H., and Harding, C.V. 2009. TLR2 and its co-receptors determine responses of macrophages and dendritic cells to lipoproteins of Mycobacterium tuberculosis. *Cell Immunol* 258:29-37.
 54. Rosas-Taraco, A.G., Revol, A., Salinas-Carmona, M.C., Rendon, A., Caballero-Olin, G., and Arce-Mendoza, A.Y. 2007. CD14 C(-159)T polymorphism is a risk factor for development of pulmonary tuberculosis. *J Infect Dis* 196:1698-1706.
 55. Kang, Y.A., Lee, H.W., Kim, Y.W., Han, S.K., Shim, Y.S., and Yim, J.J. 2009. Association between the -159C/T CD14 gene polymorphism and tuberculosis in a Korean population. *FEMS Immunol Med Microbiol* 57:229-235.
 56. Leemans, J.C., Florquin, S., Heikens, M., Pals, S.T., van der Neut, R., and Van Der Poll, T. 2003. CD44 is a macrophage binding site for Mycobacterium tuberculosis that

- mediates macrophage recruitment and protective immunity against tuberculosis. *J Clin Invest* 111:681-689.
57. Ponta, H., Sherman, L., and Herrlich, P.A. 2003. CD44: from adhesion molecules to signalling regulators. *Nat Rev Mol Cell Biol* 4:33-45.
 58. Puig-Kroger, A., Serrano-Gomez, D., Caparros, E., Dominguez-Soto, A., Relloso, M., Colmenares, M., Martinez-Munoz, L., Longo, N., Sanchez-Sanchez, N., Rincon, M., et al. 2004. Regulated expression of the pathogen receptor dendritic cell-specific intercellular adhesion molecule 3 (ICAM-3)-grabbing nonintegrin in THP-1 human leukemic cells, monocytes, and macrophages. *J Biol Chem* 279:25680-25688.
 59. Geijtenbeek, T.B., Van Vliet, S.J., Koppel, E.A., Sanchez-Hernandez, M., Vandenbroucke-Grauls, C.M., Appelmelk, B., and Van Kooyk, Y. 2003. Mycobacteria target DC-SIGN to suppress dendritic cell function. *J Exp Med* 197:7-17.
 60. Tailleux, L., Schwartz, O., Herrmann, J.L., Pivert, E., Jackson, M., Amara, A., Legres, L., Dreher, D., Nicod, L.P., Gluckman, J.C., et al. 2003. DC-SIGN is the major Mycobacterium tuberculosis receptor on human dendritic cells. *J Exp Med* 197:121-127.
 61. Geijtenbeek, T.B., Kwon, D.S., Torensma, R., van Vliet, S.J., van Duijnhoven, G.C., Middel, J., Cornelissen, I.L., Nottet, H.S., KewalRamani, V.N., Littman, D.R., et al. 2000. DC-SIGN, a dendritic cell-specific HIV-1-binding protein that enhances trans-infection of T cells. *Cell* 100:587-597.
 62. Appelmelk, B.J., van Die, I., van Vliet, S.J., Vandenbroucke-Grauls, C.M., Geijtenbeek, T.B., and van Kooyk, Y. 2003. Cutting edge: carbohydrate profiling identifies new pathogens that interact with dendritic cell-specific ICAM-3-grabbing nonintegrin on dendritic cells. *J Immunol* 170:1635-1639.
 63. Cambi, A., Gijzen, K., de Vries, J.M., Torensma, R., Joosten, B., Adema, G.J., Netea, M.G., Kullberg, B.J., Romani, L., and Figdor, C.G. 2003. The C-type lectin DC-SIGN (CD209) is an antigen-uptake receptor for *Candida albicans* on dendritic cells. *Eur J Immunol* 33:532-538.
 64. Alvarez, C.P., Lasala, F., Carrillo, J., Muniz, O., Corbi, A.L., and Delgado, R. 2002. C-type lectins DC-SIGN and L-SIGN mediate cellular entry by Ebola virus in cis and in trans. *J Virol* 76:6841-6844.

65. Colmenares, M., Puig-Kroger, A., Pello, O.M., Corbi, A.L., and Rivas, L. 2002. Dendritic cell (DC)-specific intercellular adhesion molecule 3 (ICAM-3)-grabbing nonintegrin (DC-SIGN, CD209), a C-type surface lectin in human DCs, is a receptor for *Leishmania* amastigotes. *J Biol Chem* 277:36766-36769.
66. Koppel, E.A., Ludwig, I.S., Hernandez, M.S., Lowary, T.L., Gadikota, R.R., Tuzikov, A.B., Vandenbroucke-Grauls, C.M., van Kooyk, Y., Appelmelk, B.J., and Geijtenbeek, T.B. 2004. Identification of the mycobacterial carbohydrate structure that binds the C-type lectins DC-SIGN, L-SIGN and SIGNR1. *Immunobiology* 209:117-127.
67. Barreiro, L.B., Neyrolles, O., Babb, C.L., Tailleux, L., Quach, H., McElreavey, K., Helden, P.D., Hoal, E.G., Gicquel, B., and Quintana-Murci, L. 2006. Promoter variation in the DC-SIGN-encoding gene CD209 is associated with tuberculosis. *PLoS Med* 3:e20.
68. Schlesinger, L.S. 1993. Macrophage phagocytosis of virulent but not attenuated strains of *Mycobacterium tuberculosis* is mediated by mannose receptors in addition to complement receptors. *J Immunol* 150:2920-2930.
69. Prigozy, T.I., Sieling, P.A., Clemens, D., Stewart, P.L., Behar, S.M., Porcelli, S.A., Brenner, M.B., Modlin, R.L., and Kronenberg, M. 1997. The mannose receptor delivers lipoglycan antigens to endosomes for presentation to T cells by CD1b molecules. *Immunity* 6:187-197.
70. Astarie-Dequeker, C., N'Diaye, E.N., Le Cabec, V., Rittig, M.G., Prandi, J., and Maridonneau-Parini, I. 1999. The mannose receptor mediates uptake of pathogenic and nonpathogenic mycobacteria and bypasses bactericidal responses in human macrophages. *Infect Immun* 67:469-477.
71. DeFife, K.M., Jenney, C.R., McNally, A.K., Colton, E., and Anderson, J.M. 1997. Interleukin-13 induces human monocyte/macrophage fusion and macrophage mannose receptor expression. *J Immunol* 158:3385-3390.
72. Linehan, S.A., Martinez-Pomares, L., and Gordon, S. 2000. Mannose receptor and scavenger receptor: two macrophage pattern recognition receptors with diverse functions in tissue homeostasis and host defense. *Adv Exp Med Biol* 479:1-14.
73. Baena, A., and Porcelli, S.A. 2009. Evasion and subversion of antigen presentation by *Mycobacterium tuberculosis*. *Tissue Antigens* 74:189-204.

74. Wang, Y., Curry, H.M., Zwilling, B.S., and Lafuse, W.P. 2005. Mycobacteria inhibition of IFN-gamma induced HLA-DR gene expression by up-regulating histone deacetylation at the promoter region in human THP-1 monocytic cells. *J Immunol* 174:5687-5694.
75. Hmama, Z., Gabathuler, R., Jefferies, W.A., de Jong, G., and Reiner, N.E. 1998. Attenuation of HLA-DR expression by mononuclear phagocytes infected with Mycobacterium tuberculosis is related to intracellular sequestration of immature class II heterodimers. *J Immunol* 161:4882-4893.
76. Remus, N., Alcais, A., and Abel, L. 2003. Human genetics of common mycobacterial infections. *Immunol Res* 28:109-129.
77. Cohen, N.R., Garg, S., and Brenner, M.B. 2009. Antigen Presentation by CD1 Lipids, T Cells, and NKT Cells in Microbial Immunity. *Adv Immunol* 102:1-94.
78. Gagliardi, M.C., Teloni, R., Giannoni, F., Mariotti, S., Remoli, M.E., Sargentini, V., Videtta, M., Pardini, M., De Libero, G., Coccia, E.M., et al. 2009. Mycobacteria exploit p38 signaling to affect CD1 expression and lipid antigen presentation by human dendritic cells. *Infect Immun* 77:4947-4952.
79. Bhatt, K., Uzelac, A., Mathur, S., McBride, A., Potian, J., and Salgame, P. 2009. B7 costimulation is critical for host control of chronic Mycobacterium tuberculosis infection. *J Immunol* 182:3793-3800.
80. Xu, Y., Liu, W., Shen, H., Yan, J., Yang, E., and Wang, H. Recombinant Mycobacterium bovis BCG expressing chimaeric protein of Ag85B and ESAT-6 enhances immunostimulatory activity of human macrophages. *Microbes Infect* 12:683-689.
81. Kan-Sutton, C., Jagannath, C., and Hunter, R.L., Jr. 2009. Trehalose 6,6'-dimycolate on the surface of Mycobacterium tuberculosis modulates surface marker expression for antigen presentation and costimulation in murine macrophages. *Microbes Infect* 11:40-48.
82. Hwang, S.A., Wilk, K.M., Budnicka, M., Olsen, M., Bangale, Y.A., Hunter, R.L., Kruzel, M.L., and Actor, J.K. 2007. Lactoferrin enhanced efficacy of the BCG vaccine to generate host protective responses against challenge with virulent Mycobacterium tuberculosis. *Vaccine* 25:6730-6743.

83. Pollok-Kopp, B., Schwarze, K., Baradari, V.K., and Oppermann, M. 2003. Analysis of ligand-stimulated CC chemokine receptor 5 (CCR5) phosphorylation in intact cells using phosphosite-specific antibodies. *J Biol Chem* 278:2190-2198.
84. Hoshino, Y., Tse, D.B., Rochford, G., Prabhakar, S., Hoshino, S., Chitkara, N., Kuwabara, K., Ching, E., Raju, B., Gold, J.A., et al. 2004. Mycobacterium tuberculosis-induced CXCR4 and chemokine expression leads to preferential X4 HIV-1 replication in human macrophages. *J Immunol* 172:6251-6258.
85. Kang, P.B., Azad, A.K., Torrelles, J.B., Kaufman, T.M., Beharka, A., Tibesar, E., DesJardin, L.E., and Schlesinger, L.S. 2005. The human macrophage mannose receptor directs Mycobacterium tuberculosis lipoarabinomannan-mediated phagosome biogenesis. *J Exp Med* 202:987-999.
86. Schwende, H., Fitzke, E., Ambs, P., and Dieter, P. 1996. Differences in the state of differentiation of THP-1 cells induced by phorbol ester and 1,25-dihydroxyvitamin D3. *J Leukoc Biol* 59:555-561.
87. Harding, C.V., and Boom, W.H. Regulation of antigen presentation by Mycobacterium tuberculosis: a role for Toll-like receptors. *Nat Rev Microbiol* 8:296-307.
88. Leddon, S.A., and Sant, A.J. Generation of MHC class II-peptide ligands for CD4 T-cell allorecognition of MHC class II molecules. *Curr Opin Organ Transplant* 15:505-511.
89. Fulton, S.A., Reba, S.M., Pai, R.K., Pennini, M., Torres, M., Harding, C.V., and Boom, W.H. 2004. Inhibition of major histocompatibility complex II expression and antigen processing in murine alveolar macrophages by Mycobacterium bovis BCG and the 19-kilodalton mycobacterial lipoprotein. *Infect Immun* 72:2101-2110.
90. Noss, E.H., Pai, R.K., Sellati, T.J., Radolf, J.D., Belisle, J., Golenbock, D.T., Boom, W.H., and Harding, C.V. 2001. Toll-like receptor 2-dependent inhibition of macrophage class II MHC expression and antigen processing by 19-kDa lipoprotein of Mycobacterium tuberculosis. *J Immunol* 167:910-918.
91. Torres, M., Ramachandra, L., Rojas, R.E., Bobadilla, K., Thomas, J., Canaday, D.H., Harding, C.V., and Boom, W.H. 2006. Role of phagosomes and major histocompatibility complex class II (MHC-II) compartment in MHC-II antigen processing of Mycobacterium tuberculosis in human macrophages. *Infect Immun* 74:1621-1630.

92. Kincaid, E.Z., Wolf, A.J., Desvignes, L., Mahapatra, S., Crick, D.C., Brennan, P.J., Pavelka, M.S., Jr., and Ernst, J.D. 2007. Codominance of TLR2-dependent and TLR2-independent modulation of MHC class II in *Mycobacterium tuberculosis* infection in vivo. *J Immunol* 179:3187-3195.
93. Pecora, N.D., Fulton, S.A., Reba, S.M., Drage, M.G., Simmons, D.P., Urankar-Nagy, N.J., Boom, W.H., and Harding, C.V. 2009. *Mycobacterium bovis* BCG decreases MHC-II expression in vivo on murine lung macrophages and dendritic cells during aerosol infection. *Cell Immunol* 254:94-104.
94. Ramachandra, L., Noss, E., Boom, W.H., and Harding, C.V. 2001. Processing of *Mycobacterium tuberculosis* antigen 85B involves intraphagosomal formation of peptide-major histocompatibility complex II complexes and is inhibited by live bacilli that decrease phagosome maturation. *J Exp Med* 194:1421-1432.
95. Singh, C.R., Moulton, R.A., Armitige, L.Y., Bidani, A., Snuggs, M., Dhandayuthapani, S., Hunter, R.L., and Jagannath, C. 2006. Processing and presentation of a mycobacterial antigen 85B epitope by murine macrophages is dependent on the phagosomal acquisition of vacuolar proton ATPase and in situ activation of cathepsin D. *J Immunol* 177:3250-3259.
96. Driessen, C., Bryant, R.A., Lennon-Dumenil, A.M., Villadangos, J.A., Bryant, P.W., Shi, G.P., Chapman, H.A., and Ploegh, H.L. 1999. Cathepsin S controls the trafficking and maturation of MHC class II molecules in dendritic cells. *J Cell Biol* 147:775-790.
97. Sendide, K., Deghmane, A.E., Pechkovsky, D., Av-Gay, Y., Talal, A., and Hmama, Z. 2005. *Mycobacterium bovis* BCG attenuates surface expression of mature class II molecules through IL-10-dependent inhibition of cathepsin S. *J Immunol* 175:5324-5332.
98. Soualhine, H., Deghmane, A.E., Sun, J., Mak, K., Talal, A., Av-Gay, Y., and Hmama, Z. 2007. *Mycobacterium bovis* bacillus Calmette-Guerin secreting active cathepsin S stimulates expression of mature MHC class II molecules and antigen presentation in human macrophages. *J Immunol* 179:5137-5145.
99. Sendide, K., Deghmane, A.E., Reyrat, J.M., Talal, A., and Hmama, Z. 2004. *Mycobacterium bovis* BCG urease attenuates major histocompatibility complex class II trafficking to the macrophage cell surface. *Infect Immun* 72:4200-4209.

100. Sturgill-Koszycki, S., Schlesinger, P.H., Chakraborty, P., Haddix, P.L., Collins, H.L., Fok, A.K., Allen, R.D., Gluck, S.L., Heuser, J., and Russell, D.G. 1994. Lack of acidification in Mycobacterium phagosomes produced by exclusion of the vesicular proton-ATPase. *Science* 263:678-681.
101. Wiker, H.G., and Harboe, M. 1992. The antigen 85 complex: a major secretion product of Mycobacterium tuberculosis. *Microbiol Rev* 56:648-661.
102. Shimonkevitz, R., Kappler, J., Marrack, P., and Grey, H. 1983. Antigen recognition by H-2-restricted T cells. I. Cell-free antigen processing. *J Exp Med* 158:303-316.
103. Noss, E.H., Harding, C.V., and Boom, W.H. 2000. Mycobacterium tuberculosis inhibits MHC class II antigen processing in murine bone marrow macrophages. *Cell Immunol* 201:63-74.
104. Ziegler-Heitbrock, H.W., Thiel, E., Futterer, A., Herzog, V., Wirtz, A., and Riethmuller, G. 1988. Establishment of a human cell line (Mono Mac 6) with characteristics of mature monocytes. *Int J Cancer* 41:456-461.
105. El-Benna, J., Dang, P.M., and Perianin, A. Peptide-based inhibitors of the phagocyte NADPH oxidase. *Biochem Pharmacol* 80:778-785.
106. Segal, B.H., Leto, T.L., Gallin, J.I., Malech, H.L., and Holland, S.M. 2000. Genetic, biochemical, and clinical features of chronic granulomatous disease. *Medicine (Baltimore)* 79:170-200.
107. Lau, Y.L., Chan, G.C., Ha, S.Y., Hui, Y.F., and Yuen, K.Y. 1998. The role of phagocytic respiratory burst in host defense against Mycobacterium tuberculosis. *Clin Infect Dis* 26:226-227.
108. Lee, P.P., Chan, K.W., Jiang, L., Chen, T., Li, C., Lee, T.L., Mak, P.H., Fok, S.F., Yang, X., and Lau, Y.L. 2008. Susceptibility to mycobacterial infections in children with X-linked chronic granulomatous disease: a review of 17 patients living in a region endemic for tuberculosis. *Pediatr Infect Dis J* 27:224-230.
109. Nathan, C., and Shiloh, M.U. 2000. Reactive oxygen and nitrogen intermediates in the relationship between mammalian hosts and microbial pathogens. *Proc Natl Acad Sci U S A* 97:8841-8848.
110. Beckman, J.S., Beckman, T.W., Chen, J., Marshall, P.A., and Freeman, B.A. 1990. Apparent hydroxyl radical production by peroxynitrite: implications for endothelial injury from nitric oxide and superoxide. *Proc Natl Acad Sci U S A* 87:1620-1624.

111. Long, R., Light, B., and Talbot, J.A. 1999. Mycobacteriocidal action of exogenous nitric oxide. *Antimicrob Agents Chemother* 43:403-405.
112. Chan, E.D., Chan, J., and Schluger, N.W. 2001. What is the role of nitric oxide in murine and human host defense against tuberculosis? Current knowledge. *Am J Respir Cell Mol Biol* 25:606-612.
113. Nims, R.W., Cook, J.C., Krishna, M.C., Christodoulou, D., Poore, C.M., Miles, A.M., Grisham, M.B., and Wink, D.A. 1996. Colorimetric assays for nitric oxide and nitrogen oxide species formed from nitric oxide stock solutions and donor compounds. *Methods Enzymol* 268:93-105.
114. Jagannath, C., Actor, J.K., and Hunter, R.L., Jr. 1998. Induction of nitric oxide in human monocytes and monocyte cell lines by *Mycobacterium tuberculosis*. *Nitric Oxide* 2:174-186.
115. Stromhaug, P.E., and Klionsky, D.J. 2001. Approaching the molecular mechanism of autophagy. *Traffic* 2:524-531.
116. Jagannath, C., Lindsey, D.R., Dhandayuthapani, S., Xu, Y., Hunter, R.L., Jr., and Eissa, N.T. 2009. Autophagy enhances the efficacy of BCG vaccine by increasing peptide presentation in mouse dendritic cells. *Nat Med* 15:267-276.
117. Hoyer-Hansen, M., Bastholm, L., Mathiasen, I.S., Elling, F., and Jaattela, M. 2005. Vitamin D analog EB1089 triggers dramatic lysosomal changes and Beclin 1-mediated autophagic cell death. *Cell Death Differ* 12:1297-1309.
118. Shin, D.M., Yuk, J.M., Lee, H.M., Lee, S.H., Son, J.W., Harding, C.V., Kim, J.M., Modlin, R.L., and Jo, E.K. Mycobacterial Lipoprotein Activates Autophagy via TLR2/1/CD14 and a Functional Vitamin D Receptor Signaling. *Cell Microbiol*.
119. Rivas-Santiago, B., Hernandez-Pando, R., Carranza, C., Juarez, E., Contreras, J.L., Aguilar-Leon, D., Torres, M., and Sada, E. 2008. Expression of cathelicidin LL-37 during *Mycobacterium tuberculosis* infection in human alveolar macrophages, monocytes, neutrophils, and epithelial cells. *Infect Immun* 76:935-941.
120. Liu, P.T., Stenger, S., Tang, D.H., and Modlin, R.L. 2007. Cutting edge: vitamin D-mediated human antimicrobial activity against *Mycobacterium tuberculosis* is dependent on the induction of cathelicidin. *J Immunol* 179:2060-2063.
121. Wu, H., Zhang, G., Minton, J.E., Ross, C.R., and Blecha, F. 2000. Regulation of cathelicidin gene expression: induction by lipopolysaccharide, interleukin-6, retinoic

- acid, and Salmonella enterica serovar typhimurium infection. *Infect Immun* 68:5552-5558.
122. Morizane, S., Yamasaki, K., Kabigting, F.D., and Gallo, R.L. Kallikrein expression and cathelicidin processing are independently controlled in keratinocytes by calcium, vitamin D(3), and retinoic acid. *J Invest Dermatol* 130:1297-1306.
 123. Yuk, J.M., Shin, D.M., Lee, H.M., Yang, C.S., Jin, H.S., Kim, K.K., Lee, Z.W., Lee, S.H., Kim, J.M., and Jo, E.K. 2009. Vitamin D3 induces autophagy in human monocytes/macrophages via cathelicidin. *Cell Host Microbe* 6:231-243.
 124. Daniel, D.S., Dai, G., Singh, C.R., Lindsey, D.R., Smith, A.K., Dhandayuthapani, S., Hunter, R.L., Jr., and Jagannath, C. 2006. The reduced bactericidal function of complement C5-deficient murine macrophages is associated with defects in the synthesis and delivery of reactive oxygen radicals to mycobacterial phagosomes. *J Immunol* 177:4688-4698.
 125. Dugas, N., Mossalayi, M.D., Calenda, A., Leotard, A., Becherel, P., Mentz, F., Ouaz, F., Arock, M., Debre, P., Dornand, J., et al. 1996. Role of nitric oxide in the anti-tumoral effect of retinoic acid and 1,25-dihydroxyvitamin D3 on human promonocytic leukemic cells. *Blood* 88:3528-3534.
 126. Rockett, K.A., Brookes, R., Udalova, I., Vidal, V., Hill, A.V., and Kwiatkowski, D. 1998. 1,25-Dihydroxyvitamin D3 induces nitric oxide synthase and suppresses growth of Mycobacterium tuberculosis in a human macrophage-like cell line. *Infect Immun* 66:5314-5321.
 127. Yang, C.S., Shin, D.M., Kim, K.H., Lee, Z.W., Lee, C.H., Park, S.G., Bae, Y.S., and Jo, E.K. 2009. NADPH oxidase 2 interaction with TLR2 is required for efficient innate immune responses to mycobacteria via cathelicidin expression. *J Immunol* 182:3696-3705.
 128. N'Diaye, E.N., Vaissiere, C., Gonzalez-Christen, J., Gregoire, C., Le Cabec, V., and Maridonneau-Parini, I. 1997. Expression of NADPH oxidase is induced by all-trans retinoic acid but not by phorbol myristate acetate and 1,25 dihydroxyvitamin D3 in the human promyelocytic cell line NB4. *Leukemia* 11:2131-2136.
 129. Nishida, Y., Arakawa, S., Fujitani, K., Yamaguchi, H., Mizuta, T., Kanaseki, T., Komatsu, M., Otsu, K., Tsujimoto, Y., and Shimizu, S. 2009. Discovery of Atg5/Atg7-independent alternative macroautophagy. *Nature* 461:654-658.

130. Saunders, B.M., Frank, A.A., Orme, I.M., and Cooper, A.M. 2002. CD4 is required for the development of a protective granulomatous response to pulmonary tuberculosis. *Cell Immunol* 216:65-72.
131. Bouley, D.M., Ghori, N., Mercer, K.L., Falkow, S., and Ramakrishnan, L. 2001. Dynamic nature of host-pathogen interactions in *Mycobacterium marinum* granulomas. *Infect Immun* 69:7820-7831.
132. Via, L.E., Lin, P.L., Ray, S.M., Carrillo, J., Allen, S.S., Eum, S.Y., Taylor, K., Klein, E., Manjunatha, U., Gonzales, J., et al. 2008. Tuberculous granulomas are hypoxic in guinea pigs, rabbits, and nonhuman primates. *Infect Immun* 76:2333-2340.
133. Im, J.G., Itoh, H., Shim, Y.S., Lee, J.H., Ahn, J., Han, M.C., and Noma, S. 1993. Pulmonary tuberculosis: CT findings--early active disease and sequential change with antituberculous therapy. *Radiology* 186:653-660.
134. Long, R., Maycher, B., Dhar, A., Manfreda, J., Hershfield, E., and Anthonisen, N. 1998. Pulmonary tuberculosis treated with directly observed therapy: serial changes in lung structure and function. *Chest* 113:933-943.
135. Poey, C., Verhaegen, F., Giron, J., Lavayssiere, J., Fajadet, P., and Duparc, B. 1997. High resolution chest CT in tuberculosis: evolutive patterns and signs of activity. *J Comput Assist Tomogr* 21:601-607.
136. Ulrichs, T., Kosmiadi, G.A., Trusov, V., Jorg, S., Pradl, L., Titukhina, M., Mishenko, V., Gushina, N., and Kaufmann, S.H. 2004. Human tuberculous granulomas induce peripheral lymphoid follicle-like structures to orchestrate local host defence in the lung. *J Pathol* 204:217-228.
137. Tsai, M.C., Chakravarty, S., Zhu, G., Xu, J., Tanaka, K., Koch, C., Tufariello, J., Flynn, J., and Chan, J. 2006. Characterization of the tuberculous granuloma in murine and human lungs: cellular composition and relative tissue oxygen tension. *Cell Microbiol* 8:218-232.
138. Kaplan, G., Post, F.A., Moreira, A.L., Wainwright, H., Kreiswirth, B.N., Tanverdi, M., Mathema, B., Ramaswamy, S.V., Walther, G., Steyn, L.M., et al. 2003. *Mycobacterium tuberculosis* growth at the cavity surface: a microenvironment with failed immunity. *Infect Immun* 71:7099-7108.

139. Puissegur, M.P., Botanch, C., Duteyrat, J.L., Delsol, G., Caratero, C., and Altare, F. 2004. An in vitro dual model of mycobacterial granulomas to investigate the molecular interactions between mycobacteria and human host cells. *Cell Microbiol* 6:423-433.
140. Enelow, R.I., Sullivan, G.W., Carper, H.T., and Mandell, G.L. 1992. Induction of multinucleated giant cell formation from in vitro culture of human monocytes with interleukin-3 and interferon-gamma: comparison with other stimulating factors. *Am J Respir Cell Mol Biol* 6:57-62.
141. Lemaire, I., Yang, H., Lauzon, W., and Gendron, N. 1996. M-CSF and GM-CSF promote alveolar macrophage differentiation into multinucleated giant cells with distinct phenotypes. *J Leukoc Biol* 60:509-518.
142. McInnes, A., and Rennick, D.M. 1988. Interleukin 4 induces cultured monocytes/macrophages to form giant multinucleated cells. *J Exp Med* 167:598-611.
143. Weinberg, J.B., Hobbs, M.M., and Misukonis, M.A. 1984. Recombinant human gamma-interferon induces human monocyte polykaryon formation. *Proc Natl Acad Sci U S A* 81:4554-4557.
144. Chambers, T.J. 1977. Fusion of hamster macrophages induced by lectins. *J Pathol* 123:53-61.
145. Takashima, T., Ohnishi, K., Tsuyuguchi, I., and Kishimoto, S. 1993. Differential regulation of formation of multinucleated giant cells from concanavalin A-stimulated human blood monocytes by IFN-gamma and IL-4. *J Immunol* 150:3002-3010.
146. Lazarus, D., Yamin, M., McCarthy, K., Schneeberger, E.E., and Kradin, R. 1990. Anti-RMA, a murine monoclonal antibody, activates rat macrophages: II. Induction of DNA synthesis and formation of multinucleated giant cells. *Am J Respir Cell Mol Biol* 3:103-111.
147. Orentas, R.J., Reinlib, L., and Hildreth, J.E. 1992. Anti-class II MHC antibody induces multinucleated giant cell formation from peripheral blood monocytes. *J Leukoc Biol* 51:199-209.
148. Tabata, N., Ito, M., Shimokata, K., Suga, S., Ohgimoto, S., Tsurudome, M., Kawano, M., Matsumura, H., Komada, H., Nishio, M., et al. 1994. Expression of fusion regulatory proteins (FRPs) on human peripheral blood monocytes. Induction of homotypic cell aggregation and formation of multinucleated giant cells by anti-FRP-1 monoclonal antibodies. *J Immunol* 153:3256-3266.

149. Abe, E., Ishimi, Y., Jin, C.H., Hong, M.H., Sato, T., and Suda, T. 1991. Granulocyte-macrophage colony-stimulating factor is a major macrophage fusion factor present in conditioned medium of concanavalin A-stimulated spleen cell cultures. *J Immunol* 147:1810-1815.
150. Kreipe, H., Radzun, H.J., Rudolph, P., Barth, J., Hansmann, M.L., Heidorn, K., and Parwaresch, M.R. 1988. Multinucleated giant cells generated in vitro. Terminally differentiated macrophages with down-regulated c-fms expression. *Am J Pathol* 130:232-243.
151. Postlethwaite, A.E., Jackson, B.K., Beachey, E.H., and Kang, A.H. 1982. Formation of multinucleated giant cells from human monocyte precursors. Mediation by a soluble protein from antigen-and mitogen-stimulated lymphocytes. *J Exp Med* 155:168-178.
152. Sone, S., Bucana, C., Hoyer, L.C., and Fidler, I.J. 1981. Kinetics and ultrastructural studies of the induction of rat alveolar macrophage fusion by mediators released from mitogen-stimulated lymphocytes. *Am J Pathol* 103:234-246.
153. Parks, D.E., and Weiser, R.S. 1975. The role of phagocytosis and natural lymphokines in the fusion of alveolar macrophages to form Langhans giant cells. *J Reticuloendothel Soc* 17:219-228.
154. Cain, H., and Kraus, B. 1982. Cellular aspects of granulomas. *Pathol Res Pract* 175:13-37.
155. Kraus, B. 1982. Formation of giant cells in vivo. *Immunobiology* 161:290-297.
156. Puissegur, M.P., Lay, G., Gilleron, M., Botella, L., Nigou, J., Marrakchi, H., Mari, B., Duteyrat, J.L., Guerardel, Y., Kremer, L., et al. 2007. Mycobacterial lipomannan induces granuloma macrophage fusion via a TLR2-dependent, ADAM9- and beta1 integrin-mediated pathway. *J Immunol* 178:3161-3169.
157. Purton, L.E., Lee, M.Y., and Torok-Storb, B. 1996. Normal human peripheral blood mononuclear cells mobilized with granulocyte colony-stimulating factor have increased osteoclastogenic potential compared to nonmobilized blood. *Blood* 87:1802-1808.
158. Sorokin, S.P., McNelly, N.A., and Hoyt, R.F., Jr. 1992. Macrophage development: IV. Effects of blood factors on macrophages from prenatal rat lung cultures. *Anat Rec* 233:415-428.
159. Tanaka, H., Shinki, T., Hayashi, T., Jin, C.H., Miyaura, C., Abe, E., and Suda, T. 1989. Spermidine-dependent proteins are involved in the fusion of mouse alveolar

- macrophages induced by 1 alpha,25-dihydroxyvitamin D3 and interleukin 4. *Exp Cell Res* 180:72-83.
160. Hassan, N.F., Kamani, N., Meszaros, M.M., and Douglas, S.D. 1989. Induction of multinucleated giant cell formation from human blood-derived monocytes by phorbol myristate acetate in in vitro culture. *J Immunol* 143:2179-2184.
161. Most, J., Spötl, L., Mayr, G., Gasser, A., Sarti, A., and Dierich, M.P. 1997. Formation of multinucleated giant cells in vitro is dependent on the stage of monocyte to macrophage maturation. *Blood* 89:662-671.
162. Pietersen, R., Thilo, L., and de Chastellier, C. 2004. Mycobacterium tuberculosis and Mycobacterium avium modify the composition of the phagosomal membrane in infected macrophages by selective depletion of cell surface-derived glycoconjugates. *Eur J Cell Biol* 83:153-158.
163. Rohde, K., Yates, R.M., Purdy, G.E., and Russell, D.G. 2007. Mycobacterium tuberculosis and the environment within the phagosome. *Immunol Rev* 219:37-54.
164. van der Wel, N., Hava, D., Houben, D., Fluittsma, D., van Zon, M., Pierson, J., Brenner, M., and Peters, P.J. 2007. M. tuberculosis and M. leprae translocate from the phagolysosome to the cytosol in myeloid cells. *Cell* 129:1287-1298.
165. Lay, G., Poquet, Y., Salek-Peyron, P., Puissegur, M.P., Botanch, C., Bon, H., Levillain, F., Duteyrat, J.L., Emile, J.F., and Altare, F. 2007. Langhans giant cells from M. tuberculosis-induced human granulomas cannot mediate mycobacterial uptake. *J Pathol* 211:76-85.
166. Hmama, Z., Sendide, K., Talal, A., Garcia, R., Dobos, K., and Reiner, N.E. 2004. Quantitative analysis of phagolysosome fusion in intact cells: inhibition by mycobacterial lipoarabinomannan and rescue by an 1alpha,25-dihydroxyvitamin D3-phosphoinositide 3-kinase pathway. *J Cell Sci* 117:2131-2140.
167. Boog, C.J., Wagenaar, J.P., van Holten, C., Wauben, M.H., and van Noort, J.M. 1993. Differential T-cell recognition of cathepsin D-released mycobacterial Hsp65 fragments by arthritic versus healthy Lewis rats. *Transplant Proc* 25:2840-2841.
168. Kondo, E., and Kanai, K. 1973. Degradation of tuberculoproteins by cathepsin D-type proteinase of alveolar and peritoneal macrophages of mice. *Jpn J Med Sci Biol* 26:213-227.

169. Rivera-Marrero, C.A., Stewart, J., Shafer, W.M., and Roman, J. 2004. The down-regulation of cathepsin G in THP-1 monocytes after infection with *Mycobacterium tuberculosis* is associated with increased intracellular survival of bacilli. *Infect Immun* 72:5712-5721.
170. Pai, S.R., Actor, J.K., Sepulveda, E., Hunter, R.L., Jr., and Jagannath, C. 2000. Identification of viable and non-viable *Mycobacterium tuberculosis* in mouse organs by directed RT-PCR for antigen 85B mRNA. *Microb Pathog* 28:335-342.
171. Hektoen, L. 1898. The Fate of the Giant Cells in Healing Tuberculous Tissue, as Observed in a Case of Healing Tuberculous Meningitis. *J Exp Med* 3:21-52.
172. McNally, A.K., DeFife, K.M., and Anderson, J.M. 1996. Interleukin-4-induced macrophage fusion is prevented by inhibitors of mannose receptor activity. *Am J Pathol* 149:975-985.
173. Kaji, Y., Ikeda, K., Ikeda, T., Kawakami, K., Sasaki, K., Shindo, M., Hatake, K., Harada, M., Motoyoshi, K., Mori, S., et al. 2000. IL-4, but not vitamin D(3), induces monoblastic cell line UG3 to differentiate into multinucleated giant cells on osteoclast lineage. *J Cell Physiol* 182:214-221.
174. Moan, J., Lagunova, Z., Lindberg, F.A., and Porojnicu, A.C. 2009. Seasonal variation of 1,25-dihydroxyvitamin D and its association with body mass index and age. *J Steroid Biochem Mol Biol* 113:217-221.
175. Hollis, B.W. 2005. Circulating 25-hydroxyvitamin D levels indicative of vitamin D sufficiency: implications for establishing a new effective dietary intake recommendation for vitamin D. *J Nutr* 135:317-322.
176. Dhandayuthapani, S., Via, L.E., Thomas, C.A., Horowitz, P.M., Deretic, D., and Deretic, V. 1995. Green fluorescent protein as a marker for gene expression and cell biology of mycobacterial interactions with macrophages. *Mol Microbiol* 17:901-912.
177. Takahara, K., Yashima, Y., Omatsu, Y., Yoshida, H., Kimura, Y., Kang, Y.S., Steinman, R.M., Park, C.G., and Inaba, K. 2004. Functional comparison of the mouse DC-SIGN, SIGNR1, SIGNR3 and Langerin, C-type lectins. *Int Immunol* 16:819-829.
178. Katti, M.K., Dai, G., Armitige, L.Y., Rivera Marrero, C., Daniel, S., Singh, C.R., Lindsey, D.R., Dhandayuthapani, S., Hunter, R.L., and Jagannath, C. 2008. The Delta *fbpA* mutant derived from *Mycobacterium tuberculosis* H37Rv has an enhanced susceptibility to intracellular antimicrobial oxidative mechanisms, undergoes limited

- phagosome maturation and activates macrophages and dendritic cells. *Cell Microbiol* 10:1286-1303.
179. Rao, P.K., Singh, C.R., Jagannath, C., and Li, Q. 2009. A systems biology approach to study the phagosomal proteome modulated by mycobacterial infections. *Int J Clin Exp Med* 2:233-247.
 180. Ullrich, H.J., Beatty, W.L., and Russell, D.G. 2000. Interaction of Mycobacterium avium-containing phagosomes with the antigen presentation pathway. *J Immunol* 165:6073-6080.
 181. Ullrich, H.J., Beatty, W.L., and Russell, D.G. 1999. Direct delivery of procathepsin D to phagosomes: implications for phagosome biogenesis and parasitism by Mycobacterium. *Eur J Cell Biol* 78:739-748.
 182. Hu, Y., Mangan, J.A., Dhillon, J., Sole, K.M., Mitchison, D.A., Butcher, P.D., and Coates, A.R. 2000. Detection of mRNA transcripts and active transcription in persistent Mycobacterium tuberculosis induced by exposure to rifampin or pyrazinamide. *J Bacteriol* 182:6358-6365.

VITA

Jaymie L. Estrella was born in Hawaii as the fourth of five children to parents Jesus C. Estrella and Lillian B. Estrella. She graduated from California State University, San Bernardino with both a Bachelor of Science in Chemistry and a Bachelor of Arts in Biology. She began her graduate studies in pathology with the Graduate School of Biomedical Sciences at the University of Texas Health Science Center at Houston in August 2004.